

The superconductivity of Sr_2RuO_4 and the physics of spin-triplet pairing

Andrew Peter Mackenzie

School of Physics and Astronomy, University of St. Andrews, North Haugh, St. Andrews, Fife KY16 9SS, Scotland

Yoshiteru Maeno

*Department of Physics, Kyoto University, Kyoto 606-8502, Japan
and International Innovation Center, Kyoto University, Kyoto 606-8501, Japan*

(Published 1 May 2003)

This review presents a summary and evaluation of the experimental properties of unconventional superconductivity in Sr_2RuO_4 as they were known in the spring of 2002. At the same time, the paper is intended to be useful as an introduction to the physics of spin-triplet superconductivity. First, the authors show how the normal-state properties of Sr_2RuO_4 are quantitatively described in terms of a quasi-two-dimensional Fermi liquid. Then they summarize its phenomenological superconducting parameters in the framework of the Ginzburg-Landau model, and discuss the existing evidence for spin-triplet pairing. After a brief introduction to the vector order parameter, they examine the most likely symmetry of the triplet state. The structure of the superconducting energy gap is discussed, as is the effect of symmetry-breaking magnetic fields on the phase diagram. The article concludes with a discussion of some outstanding issues and desirable future work. Appendixes on additional details of the normal state, difficulty in observing the bulk Fermi surface by angle-resolved photoemission, and the enhancement of superconducting transition temperature in a two-phase Sr_2RuO_4 -Ru system are included.

CONTENTS

I. Introduction	658	E. Experimental evidence for triplet pairing	674
A. Aim and context of the article	658	1. Spin susceptibility by the NMR Knight shift	674
B. Outline	658	2. Spin susceptibility by polarized neutron scattering	676
C. Unconventional superconductivity	659	F. Summary and conclusions	677
D. Spin-triplet Cooper pairing	660	IV. Most Likely Symmetry of the Sr_2RuO_4 Triplet State	677
E. The discovery of superconductivity in Sr_2RuO_4 and the suggestion of triplet pairing	661	A. Introduction to the d vector	677
II. Normal-State Properties	662	1. The elegance of d -vector formalism	677
A. Bulk normal-state properties of Sr_2RuO_4	663	2. Deducing details of the superconducting state from \mathbf{d}	678
1. Crystal structure, chemical stability, and phonon spectra	663	3. Allowed states for Sr_2RuO_4 and spin-orbit coupling as a degeneracy breaking mechanism	679
2. Electronic structure calculations	663	B. The spin part of the pair wave function of Sr_2RuO_4 from the Knight shift and spin-polarized neutron scattering	680
3. Anisotropic electrical conductivity	664	C. Time-reversal symmetry breaking probed by muon spin rotation and neutron studies of the flux lattice	681
4. Electronic specific heat	665	1. Muon spin rotation	681
5. Static susceptibility	665	2. Magnetic-field distribution of the vortex lattice	682
B. "Microscopic" knowledge of the metallic state from quantum oscillations	665	3. Implications of TRS breaking at T_c	683
1. The Fermi-surface topography	665	V. Structure of the Superconducting Gap	683
2. Quasiparticle masses	667	A. Evidence for a T -linear quasiparticle density deep in the superconducting state	683
3. Basic quasiparticle parameters of Sr_2RuO_4	667	1. Specific heat	684
C. Normal-state parameters of Sr_2RuO_4 compared to those of other materials	667	2. NMR/NQR relaxation rate	685
D. Normal-state spin dynamics	668	3. Penetration depth	685
III. Basic Properties of the Superconducting State	669	4. Thermal conductivity in zero applied magnetic field	686
A. Early measurements	669	B. The issue of gap nodes and their position	687
B. The effects of impurities	670	1. In-plane quasiparticle thermal conductivity in applied magnetic fields	687
1. Impurity suppression of the transition temperature	670	2. Out-of-plane phonon thermal conductivity combined with in-plane magnetic fields	688
2. Impurity effects on other properties of the superconducting state	671		
C. Ginzburg-Landau parameters of clean limit Sr_2RuO_4	672		
D. Tunneling and proximity-effect studies	673		

3. Ultrasound attenuation	689
C. Summary	691
VI. Towards a Theory	692
A. Summary of the main experimental constraints on the symmetry of the Sr_2RuO_4 order parameter	692
B. Promising theoretical scenarios	692
1. Horizontal line nodes and orbital-dependent superconductivity	692
2. Symmetry-conserving gap minima as an alternative to vertical line nodes	694
C. Remarks on the mechanism	694
VII. Multiple Superconducting Phases	695
A. The existence of a second phase in a symmetry-breaking magnetic field	695
B. Unusual upper critical-field limiting	696
C. Summary	696
VIII. Conclusions and Future Work	697
A. Main conclusions and their strength	697
B. Outstanding issues and desirable future work	697
C. Sr_2RuO_4 in a broader context	698
Acknowledgments	699
Appendix A: Additional Details of the Normal-State Physics of Sr_2RuO_4	699
1. Hall effect and magnetoresistance	699
2. Calculation of bulk properties using quantum oscillation parameters	700
3. Luttinger volume	700
4. Electronic specific heat	700
5. In-plane transport	700
6. Resistive anisotropy	701
7. Other quantum oscillation work on Sr_2RuO_4	701
8. High-temperature and high-pressure normal-state transport	701
Appendix B: Issues Concerning Angle-Resolved Photoemission Spectroscopy in Sr_2RuO_4	702
Appendix C: The “3-K” Phase of Sr_2RuO_4 -Ru	703
Appendix D: Further Examples of Vector Order Parameters	705
1. An example of the nonunitary state—the two-dimensional analog of the A1 phase of superfluid ^3He	706
2. The two-dimensional analog of the B phase of superfluid ^3He	706
3. A final example, of possible relevance to Sr_2RuO_4 in symmetry-breaking fields	707
References	707

I. INTRODUCTION

A. Aim and context of the article

The aim of this article is to review the fascinating superconducting properties of the layered perovskite oxide Sr_2RuO_4 . The main theme will be a discussion of the evidence that has built over the past eight years that the superconducting condensate consists of Cooper pairs bound in an unusual spin-triplet state. Our goal is to present the evidence and discussion in as transparent a way as possible, to produce an article that will serve several purposes. First and foremost, we will try to give as comprehensive a review of the existing experimental

literature as is practical. This does not mean that we will reference and discuss every paper that has been published on Sr_2RuO_4 ; constraint of space alone will prevent us from doing that. When we first began thinking about a review article in 1998, the literature consisted of some 50 papers. We have paid for the delay, since at the time of writing (early spring, 2002), the figure has risen to over 400 papers. Our article is principally concerned with experiment, and we have not attempted to produce a complete review of the theoretical work on the subject. Some of the theoretical papers that have particularly influenced our thinking are discussed, but we have been unable to cover nearly as many as we would have liked. We ask for our colleagues' understanding on this issue, and very much hope that a comprehensive review of the theoretical situation will be written in the future.

To try to avoid becoming dated too quickly by developments in a fast-moving field, we will also try to explain the context and concepts that underlie the subject. Ideally, we would like the committed student to find this article a useful introduction to unconventional superconductivity in general, if he or she is prepared to invest a certain amount of time reading some of the classic texts that we summarize and cite.

Over the course of the past few years we have authored or co-authored a number of short reviews on various aspects of the physics of Sr_2RuO_4 .¹ Those papers could in some ways be seen as precursors of some of the sections treated in this more comprehensive review. Other articles (e.g., Maeno *et al.*, 2001 and Mackenzie *et al.*, 2002) have also been written for less specialized publications; those are designed to be at a more elementary level than the present treatment. Finally, Bergemann *et al.* (2002) have reviewed the normal-state physics of Sr_2RuO_4 in much more detail than we will give here. We therefore refer to that article at various stages of this one.

B. Outline

In the remainder of the opening section we will first introduce the concept of unconventional superconductivity and its intimate relationship with the broader correlated electron problem. Then we will discuss examples of spin-triplet pairing, and the reasons that Sr_2RuO_4 is considered to be an important material in the context. We close the section with a brief historical account of the discovery of superconductivity and the events that led to the suggestion that it may be triplet. The remainder of the article is concerned primarily with reviewing a fairly large body of evidence consistent with this suggestion, but we will also try to explain the outstanding puzzles and any results that appear to contradict the triplet scenario.

¹For example, see Maeno (1997, 2000); Forgan *et al.* (1999); Mackenzie (1999); Maeno, Nakatsuji, and Ikeda (1999); Maeno, Nishizaki, and Mao (1999); Mackenzie and Maeno (2000).

A key feature of the physics behind the superconductivity of Sr_2RuO_4 is the metallic state from which the superconductivity condenses. For that reason, the focus of Sec. II is the way in which the normal state can be described quantitatively as a quasi-two-dimensional Fermi liquid. In Sec. III, we summarize the phenomenological superconducting parameters of Sr_2RuO_4 in the framework of the Ginzburg-Landau model, give an introductory description of the properties that demonstrate the existence of an unconventional superconducting state, and discuss the key results that strongly favor triplet pairing. In Sec. IV, we first introduce the theoretical description of the order parameters of spin-triplet superconductors in terms of the d vector, and then discuss the constraints that several key experiments place on the order parameter in Sr_2RuO_4 .

The two years preceding the writing of this article have seen a concentrated effort to understand the nodal structure of the superconducting energy gap in Sr_2RuO_4 . This important subfield warrants its own section, so in Sec. V we describe the measurements and discuss the extent to which a consensus has been reached. By this stage we will have laid out the main important experimental facts as we see them. Although we make no attempt at a comprehensive theoretical review, in Sec. VI we discuss one of the theoretical scenarios that has been proposed to describe Sr_2RuO_4 , and the extent to which it matches the facts laid out in the first five sections. We believe that this is worthwhile, because even if this theory is not correct in full detail, its development has raised several theoretical points that have to be taken into account in any realistic treatment of the physics of Sr_2RuO_4 . In Sec. VII we briefly discuss the observation of multiple superconducting phases, a topic that is presently the subject of active research. We close with summaries of conclusions that may be drawn at present, outstanding issues, and our ideas of important experiments for the future.

While writing the article, we have become aware of the need to retain a strong focus on superconductivity. However, that is certainly not the only interesting physics to have emerged from Sr_2RuO_4 . We wanted to include some discussion of these topics, but avoid interrupting the flow of the article. For this reason we have opted for some fairly long Appendixes. Appendix A describes aspects of work on the metallic state not directly relevant to the superconductivity, but of interest in their own right. This includes the way in which bulk metallic properties can be calculated using the microscopic parameters deduced from quantum oscillation studies. The analysis also gives emphasis to the assertion made in Sec. II that the low-temperature metallic state can be understood in detail using the predictions of Fermi-liquid theory. Appendix B describes the difficulties encountered in obtaining the correct bulk Fermi surface of Sr_2RuO_4 by angle-resolved photoemission spectroscopy (ARPES). The experience with Sr_2RuO_4 shows how far ARPES has progressed, but also serves as a warning regarding the potential for misinterpretation of its re-

sults in other systems. Appendix C covers the intriguing observation that the controlled introduction of inclusions of pure Ru metal in Sr_2RuO_4 leads to T_c enhancement by nearly a factor of 2. In Appendix D we give examples of the properties of some vector order parameters that are not covered in depth in the main text.

An important by-product of the interest generated by Sr_2RuO_4 has been the detailed investigation of the broader family of metallic ruthenates. Recent years have seen a wealth of interesting discoveries, notably from the study of SrRuO_3 , CaRuO_3 , $\text{Ca}_{2-x}\text{Sr}_x\text{RuO}_4$, $\text{Sr}_3\text{Ru}_2\text{O}_7$, $\text{Ca}_3\text{Ru}_2\text{O}_7$, and $\text{La}_4\text{Ru}_6\text{O}_{19}$. We had originally intended to include a fifth Appendix on this issue, but the need to maintain the focus of the present article, combined with constraints of space and time, caused us to change our mind. A more general treatment of ruthenate physics might well be the subject of a self-standing review article sometime in the future.

C. Unconventional superconductivity

The most important advances in superconductivity research over the past two decades have been the discovery and study of superconductors in which strong electronic correlations play an important role in both the normal-state physics and the superconductivity itself. Examples include heavy-fermion intermetallic compounds, organics, and copper oxides (cuprates). Superconductivity research has thus become intimately related with other important fields of strongly correlated physics, such as metallic behavior in the vicinity of metal-insulator transitions and/or quantum critical points. For this reason, unconventional superconductivity has become one of the most actively studied topics of modern-day condensed-matter physics.

Superconductivity involves the formation of a quantum condensate state by pairing conduction electrons. The condensation may be considered as a kind of Bose-Einstein condensation, because in a very broad sense each pair of the electrons acts like a Bose particle. The pair of electrons, called the Cooper pair, can be in a state of either total spin $S=0$ (spin singlet) or 1 (spin triplet). Because of the anticommuting properties of the electron as a fermion, the antisymmetric spin-singlet state is accompanied by a symmetric orbital wave function (even parity) with orbital angular momentum $L=0$ (s wave), 2 (d wave), etc. The symmetric spin-triplet state is accompanied by an antisymmetric orbital wave function (odd parity) with orbital angular momentum $L=1$ (p wave), 3 (f wave), etc.²

²Strictly speaking, L and S are not good quantum numbers in a crystalline solid, so the “ s -, p -, d -, and f -wave” nomenclature is not accurate. In most superconductors of interest this is a reasonable approximation, however, and it is in widespread use. For that reason, we adopt it in this article. The issue is discussed again in Sec. IV.

Conventional superconductivity is characterized by s -wave Cooper pairs, formed by a net attraction originating from the electron-phonon interaction, as described by the theory of Bardeen, Cooper, and Schrieffer (BCS theory, 1957). S -wave superconductivity is often termed conventional, for several reasons. First, the s state is in some senses the simplest pairing state. There is a relationship between the binding state of the Cooper pairs and the symmetry-breaking properties of the condensate. The order parameter of superconductivity is in general represented by the gap function $\Delta(\mathbf{k})$.³ For an s -wave superconductor the phase of $\Delta(\mathbf{k})$ is constant irrespective of the direction of \mathbf{k} , although there may be some anisotropy in the magnitude of Δ depending on \mathbf{k} . This reflects the fact that the condensate breaks only gauge symmetry at the superconducting transition temperature T_c . Condensates of pairs bound with finite orbital angular momentum usually break additional symmetries (Annett, 1990, 1995; Sigrist and Ueda, 1991). Another reason for s -wave superconductors to be called “conventional” is that for approximately the first six decades of research into superconductivity, only s -wave superconductors were discovered.

Under what conditions might one expect to find more complicated superconducting states becoming energetically favorable? An intuitive picture is linked with the existence of a strong on-site Coulomb repulsion. This favors the formation of a Cooper pair with a large amplitude of the wave function at finite distance, rather than at the origin, in order to reduce the Coulomb repulsion energy. This can be achieved by the electrons in the pair having finite relative orbital angular momentum. Since a strong on-site repulsion is a key ingredient in strong electronic correlation, this accounts in a physically intuitive way for the close relationship between strong correlations and unconventional superconductivity. These considerations apply even when the net attraction among the electrons is attained by spin fluctuations.⁴

Although the relationship between Cooper pair angular momentum and additional symmetry breaking is physically appealing, it is not universal. A more precise definition of unconventional superconductivity is the relation

$$\sum_{\mathbf{k}} \Delta(\mathbf{k}) = 0 \quad (1.1)$$

³Throughout this article, \mathbf{k} is a unit vector when used in a gap function or vector order parameter.

⁴This argument is weaker if the superconducting coherence length is long, because the importance of local effects such as on-site repulsion is diminished. However, even long-coherence-length unconventional superconductors have, to date, been found only in strongly correlated systems.

with the summation over the Fermi surface, which holds for all non- s -wave superconductors.⁵ For example, it is easy to verify that this is the case for the recently established d -wave state of the cuprates, namely,

$$\Delta(\mathbf{k}) = \Delta_d(k_x^2 - k_y^2). \quad (1.2)$$

This defining property of unconventional superconductivity also holds the key for understanding the length of time that it took to be discovered. One of the most important features of an s -wave superconducting condensate is its insensitivity to random elastic scattering from disorder (Anderson, 1959). When Eq. (1.1) holds, however, Anderson’s theorem no longer applies, since the order parameter can be averaged to zero by sufficiently strong scattering around the Fermi surface (Abrikosov and Gor’kov, 1960a; Balian and Werthamer, 1963; Larkin, 1965). Roughly speaking, the criterion for “sufficiently strong” is that the scattering rate equals the average gap energy or, equivalently, the elastic mean free path equals the superconducting coherence length. The shorter the coherence length, the less restrictive the constraints on material purity. It is, therefore, not surprising either that unconventional superconductivity took so long to observe, or that short coherence lengths are a feature of many of its best-known examples (e.g., the cuprates, the heavy-fermion superconductors, and some of the organic materials). Only very recently has there been a rush of discoveries of unconventional superconductors with much longer coherence lengths. As we shall see, Sr_2RuO_4 is at the vanguard of this new generation of ultrapure unconventional superconductors.

D. Spin-triplet Cooper pairing

Nearly all the superconductors known to date, either conventional or unconventional, are spin-singlet paired. Even the celebrated $d_{x^2-y^2}$ high- T_c order parameter involves singlet pairing. The best-known example of triplet pairing is not a superconductor at all, but a superfluid, ^3He , in which the condensate consists of spin-triplet atomic Cooper pairs (Leggett, 1975; Wheatley, 1975; Vollhardt and Wölfle, 1990). The question of whether *superconductivity* carried by spin-triplet pairs exists and how its behavior differs from that of spin-singlet superconductivity naturally arises. Sr_2RuO_4 is

⁵This allows an alternative heuristic argument for the relationship between electron correlations and unconventional superconductivity. Consider the gap equation

$$\Delta(\mathbf{k}) = \Sigma - V_{kk'} [\Delta(\mathbf{k}') / 2E_{k'}] [1 - 2n(\mathbf{k}')],$$

in which $V_{kk'}$ is the interaction between the electrons with momenta \mathbf{k} and \mathbf{k}' (the negative sign corresponds to attraction), $E_k = [\varepsilon_k^2 + \Delta(\mathbf{k})\Delta^*(\mathbf{k})]^{1/2}$ with $\varepsilon_k = \hbar^2 k^2 / 2m - \varepsilon_F$ is the energy of a quasiparticle, and $n(\mathbf{k}) = [\exp(\varepsilon_k / k_B T) + 1]^{-1}$ is the Fermi distribution function. It is easy to see that in the presence of dominantly positive interaction V (electron correlation), the sign of $\Delta(\mathbf{k})$ should alter with \mathbf{k} to lead to a nonzero solution for Δ .

prominent among materials that promise to provide the answers. Although it is almost certainly not unique [for example, there is now almost a consensus in favor of triplet superconductivity in UPt_3 ,⁶ evidence for its existence in $(\text{TMTSF})_2\text{PF}_6$,⁷ UGe_2 ,⁸ and URhGe ,⁹ and the likelihood that it is favored in ZrZn_2 (footnote 10) and possibly Fe (footnote 11)], we hope to show that Sr_2RuO_4 offers perhaps the best opportunity for understanding a triplet superconducting state in detail.

E. The discovery of superconductivity in Sr_2RuO_4 and the suggestion of triplet pairing

The discovery by Bednorz and Müller (1986) of high-temperature (high- T_c) superconductivity in copper oxides (cuprates) had an enormous impact on almost all aspects of research in superconductivity. In terms of material physics and crystal structure, it soon became clear that the essential requirement for a high T_c is the existence of quasi-two-dimensional electronic states arising from the planar CuO_2 network of the layered perovskite structure. Since many transition elements in addition to copper are known to form perovskite oxides, including their layered variants, it was natural to look for superconductivity in metals possessing the layered perovskite structure without copper.

It is interesting to note that it took eight years until the first such noncuprate superconductor was finally found in a ruthenium oxide (Maeno *et al.*, 1994). Why had this superconductivity been overlooked for such a long time despite the worldwide search? We believe that there are several reasons. First, the superconducting transition temperature is much lower than that of the cuprates. Second, there are a few important material differences between the high- T_c cuprates and Sr_2RuO_4 , in spite of their close structural similarity (Fig. 1). The tetravalent ruthenium with a $4d^4$ configuration in Sr_2RuO_4 has an even number of electrons, whereas divalent copper in the mother compounds of high- T_c superconductors is in the $3d^9$ (spin $S = \frac{1}{2}$) configuration with an odd number of electrons. Since strong quantum fluctuations arising from the spin- $\frac{1}{2}$ configuration were theoretically emphasized as a prerequisite for high- T_c superconductivity, it is natural that oxides based on an even number of electrons for the transition metal did not attract the attention of many researchers. Furthermore, the mother compounds of high- T_c cuprates are Mott insulators, and they usually need to be doped to become metallic and

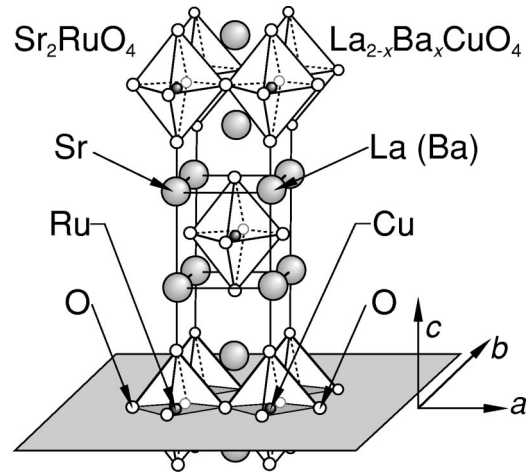


FIG. 1. The layered perovskite structure common to ruthenate and cuprate superconductors.

exhibit superconductivity. In contrast, stoichiometric Sr_2RuO_4 , first reported by Randall and Ward (1959), was known to be a conductor in the absence of chemical doping (Callaghan *et al.*, 1966).

For these reasons, the search for superconductivity in the ruthenates by Maeno and Bednorz at IBM's Zurich laboratory in 1988–1989 initially concentrated on trivalent ruthenates with the $4d^5$ ($S = \frac{1}{2}$) configuration. Later, Lichtenberg joined the group, grew good-quality single crystals of Sr_2RuO_4 , and investigated its transport properties down to 4.2 K (Lichtenberg *et al.*, 1992). At Hiroshima University, continued searches for layered perovskite superconductors in the group of Fujita and Maeno concentrated mainly on ruthenium and rhodium oxides based on the spin- $\frac{1}{2}$ configuration. In the spring of 1994, a first-year graduate student in the group, H. Hashimoto, found a new transition below 2 K in polycrystalline Sr_2RuO_4 , in a measurement of its specific heat (Fig. 2). The ac susceptibility as well as resistivity also showed clear evidence for a transition suggestive

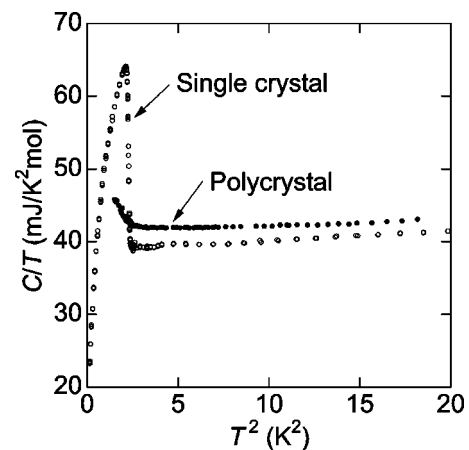


FIG. 2. The first evidence for a transition below 2 K in Sr_2RuO_4 in the measurement of specific heat on a polycrystalline sample (solid circles). Note how small the feature is in comparison to the data that can now be obtained from high-quality single crystals (open circles).

⁶For a review see, for example, Brison *et al.* (2000), and references therein.

⁷For example, see Chashechkina *et al.* (2001); Lee *et al.* (2002), and references therein.

⁸See Saxena *et al.* (2000).

⁹See Aoki *et al.* (2001).

¹⁰See Pfeleiderer *et al.* (2001).

¹¹See Shimizu *et al.* (2001); in this case the high-pressure phase from which the superconductivity forms may not, in fact, have dominantly ferromagnetic correlations.

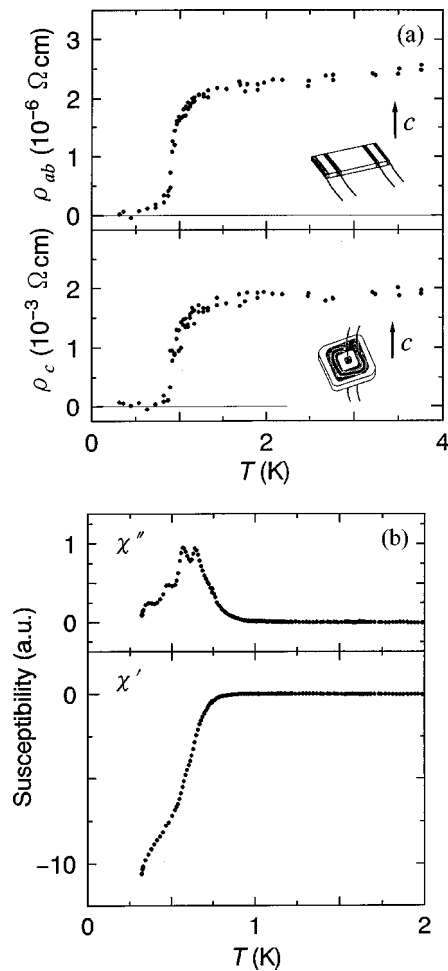


FIG. 3. Resistivity and ac susceptibility of early single crystals of Sr_2RuO_4 , indicating the superconducting transition (Maeno *et al.*, 1994). The depressed value of approximately 0.9 K for T_c and the extra structure in the susceptibility data subsequently proved to be due to the presence of an inhomogeneous distribution of impurities and defects, as discussed in Sec. III.

of superconductivity, but it did not provide conclusive evidence for a superconducting transition, because the poor grain-boundary resistance of the polycrystalline samples hampered the observation of truly zero resistivity. The news was delivered to Bednorz in the summer of 1994 and Lichtenberg's crystals were immediately sent to Hiroshima. In the first measurements at Hiroshima in a ^3He refrigerator, a clear zero resistivity and a strong diamagnetic signal were observed below 1 K, marking definitive evidence of a superconducting transition (Fig. 3).

The low residual resistivity of these early crystals prompted the beginning of the collaboration between the authors of this article, because there seemed to be the hope of performing an experiment that is essentially impossible in less pure oxides, the observation of the de Haas–van Alphen effect. The initial results were obtained in early 1995 by Mackenzie, Julian, *et al.* (1996a, 1996b) at Cambridge, and showed conclusively that the low-temperature metallic state of Sr_2RuO_4 is a Fermi liquid. In combination with bulk magnetic and transport measurements performed in Hiroshima, they allowed an

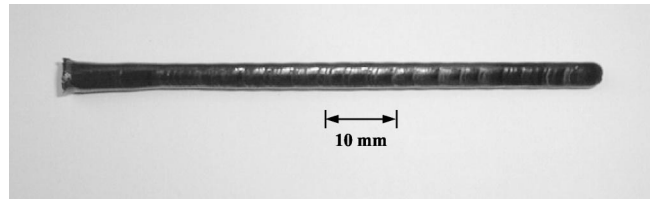


FIG. 4. A single crystal of Sr_2RuO_4 (Mao, Maeno, and Fukuzawa, 2000).

estimate of the Landau parameters. The realization that these bore a strong quantitative similarity to those of ^3He was one of the motivations for Rice and Sigrist (1995) to make the intriguing suggestion that the superconductivity of Sr_2RuO_4 may also be triplet.¹² The bulk of this article might be considered as a review of the work performed to investigate that possibility.

A theme running through the experimental work on Sr_2RuO_4 has been the necessity of growing extremely pure single crystals in order to uncover the underlying physics. All the high-purity crystal growth has been performed by a floating-zone method using “image” furnaces in which melting is achieved crucible-free using focused light. These instruments have been so important to the development of the field that we thought it was appropriate to close this introductory section with a photograph of a crystal grown in an image furnace. Several hundred growth runs of Sr_2RuO_4 have been carried out in image furnaces in Kyoto and a number of other institutions. In Fig. 4 we show an example of the long single-crystal rods that can now be obtained by these techniques.

II. NORMAL-STATE PROPERTIES

Although the main purpose of this review is to discuss the remarkable superconducting state of Sr_2RuO_4 , we begin with a fairly long section on the normal state. This is defined, as usual, as the metallic state that exists above T_c or above the upper critical field (H_{c2}) in the presence of an externally applied magnetic field. We have made this choice because interpretation of many of the experiments pertinent to the superconductivity requires the detailed knowledge that now exists about the metallic state and the underlying electronic structure. Sr_2RuO_4 would be a very interesting correlated electron metal even if no superconducting transition occurred; some fascinating topics that are less directly related to the superconductivity are discussed in Appendixes A and B.

The properties reviewed in this section can be split into two classes. The first include the bulk transport and thermodynamic properties that are generally used to characterize metals. Data falling into this class can be

¹²Triplet pairing in Sr_2RuO_4 was also proposed independently by Baskaran (1996), based on slightly different reasoning from that of Rice and Sigrist.

obtained on almost any metal, in the sense that the experiments can be done even in disordered samples. As will be seen throughout the review, one of the most important features of the physics of Sr_2RuO_4 is that it can be prepared with remarkably *low* disorder. One of the direct consequences is that it has been possible to observe quantum oscillations, which are damped to unobservably small amplitudes by disorder scattering in most multicomponent metals. Analysis of these oscillations gives “microscopic” band-by-band information about the low-energy excitations that determine the low-temperature metallic properties, as will be discussed in Sec. II.B. Electronic structure calculations make accurate predictions of the Fermi-surface topography, but underestimate the effect of strong correlations on the effective masses. In Appendix A we show that the knowledge reviewed in Sec. II.B, combined with the simplicity of the Fermi surface, allows successful quantitative calculations of a number of independently measured bulk properties of Sr_2RuO_4 .

Although we believe that this is the appropriate place to discuss the normal state, we are aware that the section may contain too much detail for the reader principally interested in unconventional superconductivity. The following is a minimal summary for the reader who prefers to begin from Sec. III:

- (i) The superconductivity of Sr_2RuO_4 condenses from a metallic state that is a strongly two-dimensional Fermi liquid.
- (ii) The Fermi surface consists of three weakly corrugated cylindrical sheets, α (which is holelike), and β and γ (which are electronlike). It is shown in Fig. 11 below.
- (iii) There is a significant quasiparticle mass enhancement, summarized in Table II below.
- (iv) Although the dynamical susceptibility is enhanced at $q=0$, the largest peak, due to Fermi-surface nesting, is at $(0.6\pi, 0.6\pi)$.

When other more detailed information from this section is used in the remainder of the article, an effort will be made to back-reference to the specific subsection involved.

A. Bulk normal-state properties of Sr_2RuO_4

1. Crystal structure, chemical stability, and phonon spectra

The starting point for understanding the normal-state properties of any material is knowledge of its crystal structure. That of Sr_2RuO_4 has been studied by a number of groups.¹³ There are some differences of detail, but it is generally agreed that Sr_2RuO_4 has the K_2NiF_4 structure, with $I4/mmm$ body-centered tetragonal

space-group symmetry. In comparison with many compounds that approximately adopt this structure, there is very little evidence for structural distortion in Sr_2RuO_4 , and none for structural phase transitions between room temperature and 100 mK.¹⁴ Since we are concerned with low-temperature properties in this paper, we will use the low-temperature lattice parameters from the precise powder neutron-diffraction study of Chmaissem *et al.* (1998): $a = 0.3862$ and $c = 1.2722$ nm.

It is also known that Sr_2RuO_4 is chemically stable compared to many oxides. Nishizaki *et al.* (1996) reported that T_c is nearly unchanged by high-temperature anneals in oxygen partial pressures ranging from 10^{-2} to 10^2 bars. As described in Sec. III, T_c is an extremely sensitive measure of disorder in Sr_2RuO_4 , so this observation demonstrates both that the oxygen content is stable and that it must be very close to stoichiometry.

Although most discussion (including ours) of the superconducting mechanism for Sr_2RuO_4 concentrates on magnetic fluctuations and Coulomb repulsion, it is very likely that phonons also play a significant role. We will not go into detail here, but we refer the reader to studies of phonon spectra and electron-phonon coupling by neutron scattering (Braden *et al.*, 1998) and Raman scattering (Yamanaka *et al.*, 1996; Udagawa *et al.*, 1998; Sakita *et al.*, 2001). The role played by an anharmonic phonon observed by Braden *et al.* (1998) on the isotope effect in Sr_2RuO_4 is discussed by Mao, Maeno, *et al.* (2001).

2. Electronic structure calculations

To understand the bulk electronic properties of metals it is important to have knowledge of the electronic structure. Soon after the discovery of superconductivity in Sr_2RuO_4 , Oguchi (1995) performed a calculation of the electronic energy band structure within the local-density approximation (LDA), which predicted that the Fermi surface consists of three strongly two-dimensional sheets. The labeling of the three closed surfaces as α , β , and γ is the notation that was introduced later by Mackenzie, Julian, *et al.* (1996a). The calculation showed that α and β dominantly have the character of Ru $4d_{xz,yz}$ orbitals, while γ is dominantly $4d_{xy}$. The α sheet is holelike, while β and γ are electronlike. Since then, the results of a number of other calculations have been published,¹⁵ and while they differ in detail, they all con-

¹³Structural work includes Walz and Lichtenberg (1993); Cava *et al.* (1994); Huang *et al.* (1994); Maeno *et al.* (1994); Neumeier *et al.* (1994); Gardner *et al.* (1995, 1996); Martinez (1995); Vogt and Buttrey (1995); Braden *et al.* (1997); Chmaissem *et al.* (1998).

¹⁴This essentially perfect body-centered tetragonal structure also makes Sr_2RuO_4 unique among the layered perovskite ruthenates. The others in the series all appear to have lower-symmetry orthorhombic structures due, for example, to tilting and/or rotation of the Ru-O octahedra. If Ca is substituted for Ru in the K_2NiF_4 structure, substantial distortions also appear.

¹⁵Electronic structure calculations have also been reported by Singh (1995); Hase and Nishihara (1996); McMullan, Ray, and Needs (1996); Yoshida, Settai, *et al.* (1998); de Boer and de Groot (1999); Noce and Cuoco (1999a, 1999b); Mazin, Papaconstantopoulos, and Singh (2000); Mishonov and Penev (2000); Perez-Navarro, Costa-Quintana, and Lopez-Aguilar (2000).

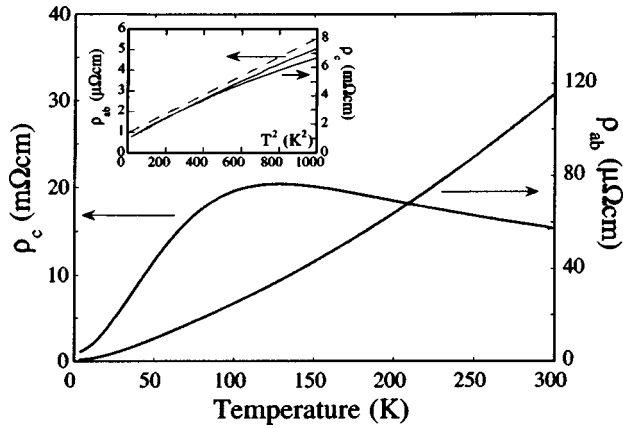


FIG. 5. Anisotropic resistivity in Sr_2RuO_4 , from Hussey *et al.* (1998). The dotted line in the inset, showing the low-temperature T^2 dependence expected of a Fermi liquid, is for comparison with the data.

firm the basic electronic structure of Oguchi. In the absence of experimental data, the calculated electronic structure would undoubtedly have been useful in analyzing subsequent experiments. However, the failure of band-structure calculations to account for some key features of cuprate physics might have led to some skepticism about trusting calculation details on isostructural Sr_2RuO_4 . Fortunately, it has proved to be possible to obtain detailed information about the Fermi surface and quasiparticle spectrum of Sr_2RuO_4 experimentally, by observing quantum oscillations (see Sec. II.B).

3. Anisotropic electrical conductivity

The anisotropic dc resistivity (ρ) of single-crystal Sr_2RuO_4 was first reported by Lichtenberg and collaborators (1992), two years before the discovery of the superconductivity. Their basic results are in agreement with those shown in Fig. 5, which are from a later paper (Hussey *et al.*, 1998). The resistivity is strongly anisotropic, with low-temperature ratios varying between 400 and 4000 reported by several groups.¹⁶ At high temperatures, ρ_c (the interplane resistivity) decreases with increasing temperature, characteristic of an incoherent conduction mechanism. Similar behavior is seen in many cuprate materials (see, e.g., Clarke and Strong, 1997, and references therein). As the temperature is lowered, however, ρ_c goes through a broad maximum at approximately 130 K and then follows a metallic temperature dependence down to T_c . The in-plane resistivity, ρ_{ab} , is metallic from 300 K to low temperatures, and below approximately 20 K, both ρ_{ab} and ρ_c have an approximate T^2 dependence, as shown in the inset. This T^2 dependence of ρ at low temperatures is consistent with the predictions of the Fermi-liquid theory of metals, in which a quadratic temperature dependence of the

¹⁶See Lichtenberg *et al.* (1992); Maeno *et al.* (1994, 1997); Yoshida (1997); Tyler *et al.* (1998); Ohmichi *et al.* (2000).

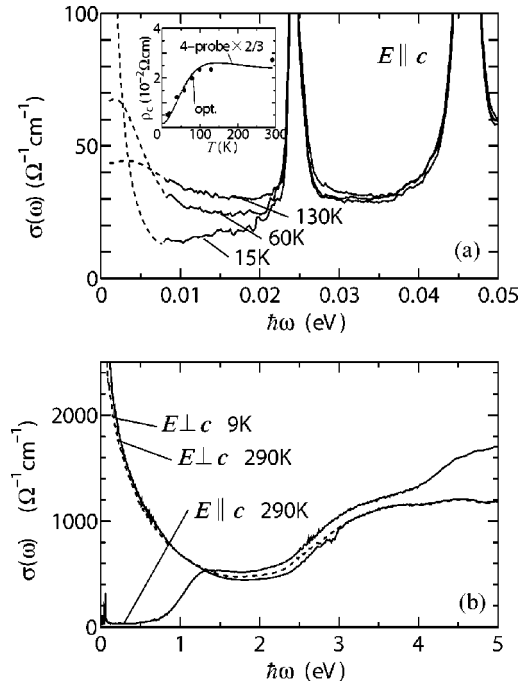


FIG. 6. Optical conductivity data for Sr_2RuO_4 showing that a Drude peak for transport perpendicular to the Ru-O planes only develops at low temperatures (a), while the one for in-plane transport exists up to room temperature (b). The inset to (a) is a comparison between optical and dc transport perpendicular to the planes. From Katsufuji *et al.* (1996).

quasiparticle-quasiparticle scattering rate is imposed by phase-space restrictions on the scattering process (see, e.g., Schofield, 1999). A particularly notable feature is the very low residual resistivity of less than $1 \mu\Omega \text{ cm}$, which gives evidence of the high sample purity.

Another important aspect of the dc transport shown in Fig. 5 is the temperature-independent resistive anisotropy below 20 K, which strongly suggests that a standard anisotropic effective-mass approach is valid for understanding the conduction. This implies highly anisotropic, but basically three-dimensional, conduction at low temperatures, with coherent band formation in the c direction. Although the temperature dependence of ρ_c in the cuprates shows considerable variation with material and doping level, the key feature of the temperature-independent anisotropy has never been observed in a cuprate. The idea of coherent transport in all directions at low temperatures in Sr_2RuO_4 is consistent with a study of ac conductivity by Katsufuji *et al.* (1996), whose main results are summarized in Fig. 6. Below 30 K, a Drude peak is seen with the electric field applied both parallel and perpendicular to the RuO_2 planes. Bulk electrical transport data, then, are consistent with the existence of a Fermi liquid at low temperatures in Sr_2RuO_4 (Maeno *et al.*, 1997). The mechanism of conduction at higher temperatures is an interesting issue, which is mentioned again in Appendix A, along with a discussion of the effects of high pressure on the normal-state transport.

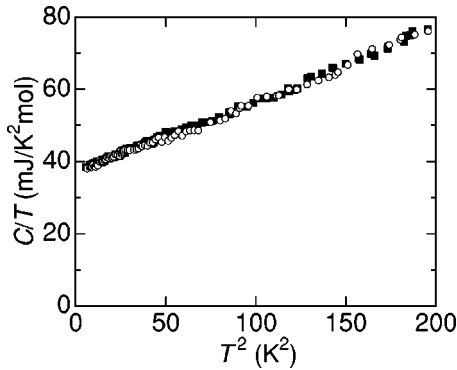


FIG. 7. The total specific heat of Sr_2RuO_4 divided by temperature between T_c and 14 K in zero field (filled squares) and an applied magnetic field of 14 T (open circles) applied parallel to c . From Mackenzie, Ikeda, *et al.* (1998).

4. Electronic specific heat

The normal-state specific heat of Sr_2RuO_4 has been studied at low temperatures by several groups.¹⁷ Early data from polycrystalline material had some variation, but single-crystal experiments at Hiroshima and Kyoto Universities have now given consistent results, an example of which is shown in Fig. 7. Below 15 K, C_p is modeled well by the expression $\gamma_{\text{el}}T + \beta_{\text{ph}}T^3$, with $\gamma_{\text{el}} = 38 \pm 2$ mJ/mol K², and $\beta_{\text{ph}} = 0.2 \pm 0.005$ mJ/mol K⁴. No change is seen in either value to within experimental error (above T_c) in an applied magnetic field of 14 T. Subtracting the phonon term obtained from the fit shown in Fig. 7 gives an electronic term constant to within experimental uncertainty below 15 K, a result that is again consistent with the predictions of Fermi-liquid theory.

The majority of band-structure calculations of the total density of states at E_F in Sr_2RuO_4 yield values for γ_{el} that are smaller than experiment by a factor of 3–4.¹⁸ This is consistent with the presence of strong electron correlations, which are not adequately taken into account in LDA calculations.

5. Static susceptibility

Typical results for the normal-state static susceptibility χ of Sr_2RuO_4 are shown in Fig. 8 (Maeno *et al.*, 1997). The first indication that the raw data are likely to be

¹⁷See Maeno *et al.* (1994); Neumeier *et al.* (1994); Carter *et al.* (1995); Maeno *et al.* (1997); Mackenzie, Ikeda, *et al.* (1998).

¹⁸For example, see Oguchi (1995); Singh (1995); Hase and Nishihara (1996); McMullan, Ray, and Needs (1996); Yoshida, Settai, *et al.* (1998); Mazin, Papaconstantopoulos, and Singh (2000); Mishonov and Penev (2000). An “LDA+ U ” calculation (Perez-Navarro, Costa-Quintana, and Lopez-Aguilar, 2000) reportedly gives good agreement with experiment, but the LDA calculation that these authors use as a starting point already disagrees with most of the other calculations in its prediction of the total density of states, so it would be interesting to see the LDA+ U part confirmed by another group.

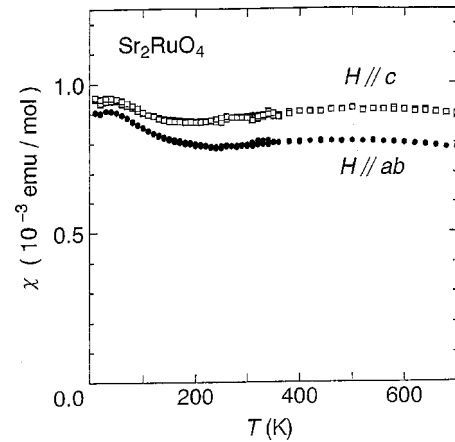


FIG. 8. The static susceptibility of Sr_2RuO_4 for fields of 1 T applied parallel to the ab plane and the c axis, from Maeno *et al.* (1997).

dominated by the spin or Pauli term comes from the striking isotropy of χ in the presence of a very anisotropic electronic structure. The data are only weakly temperature dependent, so extraction of the spin susceptibility can be achieved, in principle, by subtracting two temperature-independent terms, arising from the diamagnetic susceptibility of the core electrons and the orbital, or “Van Vleck” term. The former is estimated to be -0.9×10^{-4} emu/mol, while an estimate of the latter is approximately 1.5×10^{-4} emu/mol (Ishida *et al.*, 1997). Averaging the low-temperature raw data and subtracting these terms then gives a best estimate of 0.9×10^{-3} emu/mol for χ_{spin} .

B. “Microscopic” knowledge of the metallic state from quantum oscillations

The properties described so far in this section are probes of behavior averaged over all the Fermi-surface sheets of Sr_2RuO_4 . An important feature of the work that has been possible on the superconductivity has been the existence of detailed, sheet-by-sheet information about the normal-state quasiparticles. This has come from the observation and analysis of quantum oscillations, which are a consequence of Landau quantization of quasiparticle orbits. A description of the general physics underlying these oscillations and their detection can be found, for example, in Shoenberg (1984), and full details of the work done on Sr_2RuO_4 can be found in Bergemann *et al.* (2002). For this reason only a summary of the salient findings will be given here.

1. The Fermi-surface topography

The extremely high-quality crystals of Sr_2RuO_4 have enabled successful studies of the Shubnikov–de Haas effect, in which oscillations are seen in the electrical resistivity,¹⁹ and of the de Haas–van Alphen (dHvA)

¹⁹See Mackenzie *et al.* (1996a); Ohmichi *et al.* (2000).

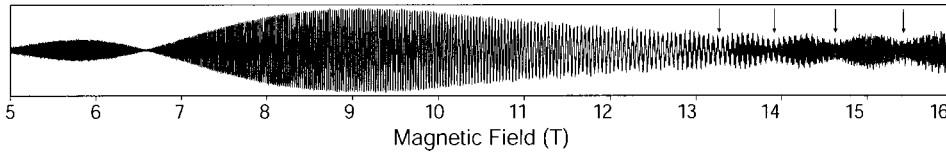


FIG. 9. Typical raw dHvA data from the high-quality crystals of Sr_2RuO_4 that are now available (from Bergemann *et al.*, 2000).

effect, in which the magnetization is studied.²⁰ Typical raw data obtained using a field modulation method to study $\partial^2 M / \partial B^2$ are shown in Fig. 9. The modulation field amplitude has been “tuned” to suppress the amplitude of the otherwise dominant low-frequency oscillation, using a method described by Shoenberg (1984). The Fourier transform of such data contains three fundamental components, labeled α , β , and γ , each corresponding to a closed and approximately cylindrical sheet of the Fermi surface (Fig. 10). By taking data at a closely spaced series of angles for rotations about the (100) and (110) directions, it has been possible to build an extremely detailed picture of the Fermi-surface topography of Sr_2RuO_4 . Even the out-of-plane dispersion is known, with a \mathbf{k} resolution for the α sheet of one part in 10^5 of the Brillouin zone.

The standard way to describe out-of-plane dispersion in low-dimensional metals is through hopping integrals (t_\perp). However, this involves making assumptions about the shape of the Fermi surface that are too simple for Sr_2RuO_4 . Instead, Bergemann *et al.* (2000) parametrized the corrugation of each cylinder through an expansion of the local Fermi wave vector:

$$k_F(\phi, \kappa) = \sum_{\substack{\mu, \nu > 0 \\ \mu \text{ even}}} k_{\mu\nu} \cos \nu \kappa \begin{cases} \cos \mu \phi & (\mu \bmod 4 \equiv 0) \\ \sin \mu \phi & (\mu \bmod 4 \equiv 2) \end{cases}. \quad (2.1)$$

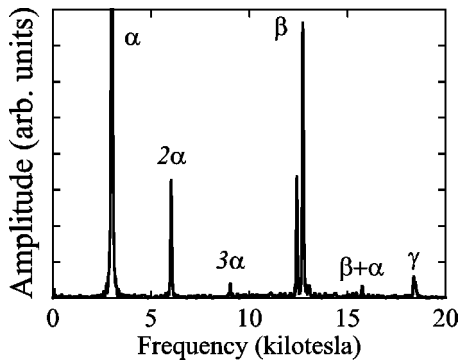


FIG. 10. A typical dHvA spectrum for Sr_2RuO_4 (from Mackenzie, Ikeda, *et al.*, 1998). Both fundamental and harmonic peaks can be seen. The split β peak is due to the more pronounced corrugation of that Fermi-surface sheet (see Fig. 11 below).

²⁰See Mackenzie *et al.* (1996a, 1996b); Yoshida, Settai, *et al.* (1998); Yoshida *et al.* (1999); Bergemann *et al.* (2000, 2001).

In this expression, $\kappa = ck_z/2$, where c is the height of the body-centered tetragonal unit cell, and ϕ is the azimuthal angle of \mathbf{k} in the (k_x, k_y) plane. The average Fermi wave vector is given by $k_{00} \equiv \sqrt{(A_e/\pi)}$, where A_e is the cross-sectional area of the cylindrical Fermi-surface sheet. Symmetry places constraints on the terms that exist in the expansion for a given sheet. For β and γ , which are centered in the Brillouin zone, $k_{\mu\nu}$ is nonzero only for μ divisible by 4. For α , which runs along the zone corners, $k_{\mu\nu}$ is nonzero only for ν even and μ divisible by 4, or for ν odd and $\mu \bmod 4 \equiv 2$. Performing a full fit of the dHvA data to this expansion [which involved a generalization of earlier theoretical treatments of dHvA amplitudes in nearly two-dimensional (2D) materials] led to the Fermi-surface data summarized in Table I and Fig. 11 (Bergemann *et al.*, 2000, 2001, 2002).²¹

It is important to note that the deviations from perfectly two-dimensional, nondispersing cylinders are tiny, so that for many properties, a two-dimensional approximation is adequate. For out-of-plane properties, however, accurate knowledge of the dispersion is crucial and, as we shall see, this is likely to be important in understanding key aspects of the superconductivity. This aspect of the experimental Fermi surface is known in Sr_2RuO_4 to a higher accuracy than can be reliably obtained from band-structure calculations.

TABLE I. Detailed Fermi-surface topography parameters for Sr_2RuO_4 . The warping parameters $k_{\mu\nu}$ are given in units of 10^7 m^{-1} . Entries symbolized by a dash are forbidden by the body-centered tetragonal Brillouin-zone symmetry. From Bergemann *et al.* (2002).

Fermi-surface sheet	k_{00}	k_{40}	k_{01}	k_{02}	k_{21}	k_{41}	k_{42}
α	304	-10	-	0.31	1.3	-	-1.0
β	622	-45	3.8	small	-	-0.6	small
γ	753	small	small	0.53	-	small	0.5

²¹In constructing Fig. 11, dHvA has been combined with probes such as angular magnetoresistance oscillations (Yoshida, Mukai, *et al.*, 1998; Ohmichi, Adachi, *et al.*, 1999) to obtain the cross-sectional shapes. Angle-resolved photoemission spectroscopy (ARPES) ought also to be an ideal tool for the determination of cross-sectional shape. As discussed in Appendix B, ARPES on Sr_2RuO_4 has had a checkered history, but the recent work of Damascelli *et al.* (2000) is in good agreement with a 2D cut through Fig. 11.

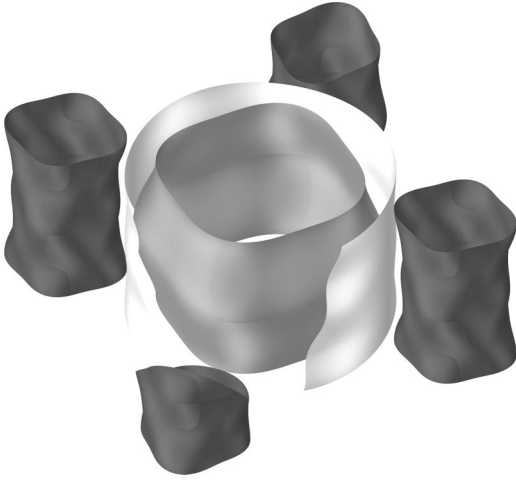


FIG. 11. The experimentally constrained Fermi surface of Sr₂RuO₄, reconstructed from the data of Table I. The ripples due to the out-of-plane dispersion have been exaggerated by a factor of 15. The holelike α sheet is shown by the four dark cylinders. The β sheet is the central cylinder with a nearly square cross section. The γ sheet is the outer central cylinder with a nearly circular cross section. It has been cut out in the bottom left of the drawing to allow the dispersion of β to be seen more clearly. One-quarter of each α sheet is included in the first body-centered tetragonal Brillouin zone. Figure is by C. Bergemann.

2. Quasiparticle masses

The quasiparticle cyclotron effective masses for the α , β , and γ sheets can be determined from the temperature dependence of the amplitudes of their frequency components. The most comprehensive study has been that of Bergemann *et al.* (2001), who checked for systematic field dependence of the masses in fields of up to 33 T. Their values (which the study showed to be accurate to $\pm 10\%$ for β and γ and $\pm 5\%$ for α) are presented in Table II.²² As discussed at more length in Bergemann *et al.* (2002), some forms of non-Fermi-liquid metallic state might lead to unusual field, temperature, and even angular dependencies of the cyclotron effective mass. No such behavior has been reported for Sr₂RuO₄, whose metallic state seems to be a robust Fermi liquid.

3. Basic quasiparticle parameters of Sr₂RuO₄

The notation introduced by Bergemann and co-workers is compact and useful, and enables the calcula-

²²The literature contains some variations from these values. In the original reports of mass analyses (Mackenzie *et al.*, 1996a, 1996b), a simple numerical error in setting up the fit resulted in slightly incorrect masses, notably the report of 12 electron masses for γ . Yoshida, Settai, *et al.* (1998) reported 4.3 electron masses for α , but few details of the procedure used to determine them were given. This value is beyond the limits of the error reported by Bergemann *et al.* (2001, 2002) and also at odds with the findings of Mackenzie *et al.* (1996a, 1996b) and Mackenzie, Ikeda, *et al.* (1998).

TABLE II. Summary of quasiparticle parameters of Sr₂RuO₄.

Fermi-surface sheet	α	β	γ
Character	Holelike	Electronlike	Electronlike
k_F (\AA^{-1}) ^a	0.304	0.622	0.753
m^* (m_e) ^b	3.3	7.0	16.0
m^*/m_{band} ^c	3.0	3.5	5.5
v_F (ms^{-1}) ^d	1.0×10^5	1.0×10^5	5.5×10^4
$\langle v_{\perp}^2 \rangle$ ($\text{m}^2 \text{s}^{-2}$) ^e	7.4×10^5	3.1×10^6	1.0×10^5
t_{\perp} (K) ^f	7.3	15.0	2.7

^a $k_F \equiv k_{00} \equiv \sqrt{(A_e/\pi)}$, where A_e is the cross-sectional area of the sheet. Published band-structure calculations make correct predictions of k_F to an accuracy of approximately 5%.

^bThe masses quoted here are from Bergemann *et al.* (2001), and differ slightly from some other values quoted in the literature. See footnote 22.

^cThe values for m_{band} are taken from McMullan, Ray, and Needs (1996), but are similar for all the published band-structure calculations.

^d $v_F \equiv \hbar k_F / m^*$.

^e $\langle v_{\perp}^2 \rangle \equiv (\hbar^2 k_{00}^2 c^2 / 16 m^{*2}) [\sum_{\mu\nu} k_{\mu\nu}^2 v^2 (1 + \delta_{\mu 0})]$, where c is the body-centered tetragonal lattice parameter of 12.7 and the other symbols are defined as in Eq. (2.7). The $\langle \rangle$ denotes an average through the Brillouin zone.

^fTo parametrize c -axis hopping with a single energy t_{\perp} requires artificial assumptions, as outlined in the text.

tion of a wide range of physical properties. For the purposes of this article, however, we thought that it would be useful to summarize the known quasiparticle parameters using more conventional notation and approximations. This is done in Table II. In this table, $\langle v_{\perp}^2 \rangle$ is the square of the quasiparticle velocity perpendicular to the planes, averaged over a Fermi-surface sheet, which can be calculated directly from the dHvA parameters of Table I (see footnotes to Table II). In converting to average hopping integrals t_{\perp} , however, a somewhat artificial assumption is necessary. We choose the value that would give the observed value of $\langle v_{\perp}^2 \rangle$ if the sheet had a dispersion corresponding to lowest-order tetragonal-type hopping between adjacent layers (i.e., only k_{01} non-zero).

C. Normal-state parameters of Sr₂RuO₄ compared to those of other materials

The normal-state parameters that generated most interest in the superconductivity of Sr₂RuO₄ are the enhancements of the effective mass and susceptibility over the band values. Taking the bulk values for both quantities, one estimates enhancements of approximately 4 and 7, respectively (corresponding to a bulk Wilson ratio of 1.7). As first pointed out by Rice and Sigrist (1995), these are both quantitatively similar to those of ³He at atmospheric pressure, providing one of the main motivations for their suggestion of the possibility of spin-triplet pairing. The mass enhancement is reflected in the Fermi-liquid scattering rate in a fairly standard way for a strongly correlated metal, as reflected by its position on

the empirical Kadowaki-Woods plot (Maeno *et al.*, 1994). The mass enhancement is not the only “bulk” parameter for which there is Fermi-surface specific information in Sr_2RuO_4 . Orbital-specific information on the static susceptibility has been reported by Imai *et al.* (1998) on the basis of ^{101}Ru and ^{17}O NMR and by Mukuda *et al.* (1999b) on the basis of ^{17}O NMR.

D. Normal-state spin dynamics

Among the best candidates for the Cooper pair “glue” in unconventional superconductors are spin fluctuations, because the correlations that tend to favor unconventional order parameters also promote close proximity to magnetism. For that reason, one of the most desirable pieces of information in relation to an unconventional superconductor is knowledge of the spin-fluctuation spectrum. This is particularly so for a material such as Sr_2RuO_4 , because its low T_c , long coherence length, and precisely known electronic structure offer the opportunity for a detailed test of spin-fluctuation theories of superconductivity. Direct information about the spin-fluctuation spectrum is derived from the imaginary part of the dynamical susceptibility, $\chi''(\mathbf{q}, \omega)$.²³ Ideally, one would like to know this quantity over the whole Brillouin zone for all relevant energies, but to achieve that is a formidable task. Although it is far from complete, progress has been made, as we now briefly discuss.

In principle, $\chi''(\mathbf{q}, \omega)$ is a directly measurable quantity, accessible via inelastic neutron scattering. The scattering cross section is so small, however, that very large, high-quality single crystals are needed for the experiments to yield precise information (see, for example, Fig. 4). A technique that can give high precision information on aspects of $\chi''(\mathbf{q}, \omega)$ without the need for such large crystals is nuclear magnetic resonance (NMR). The spin-lattice relaxation time T_1 is related to $\chi''(\mathbf{q}, \omega)$ through

$$\frac{1}{T_1 T} \propto \sum_{\mathbf{q}, \lim \omega \rightarrow 0} \frac{\chi''(\mathbf{q}, \omega)}{\omega}. \quad (2.2)$$

If only one atomic site can be probed, this \mathbf{q} integration is rather restrictive, but if T_1 data are available from more than one site, it is, in principle, possible to extract more information as to whether the fluctuations are predominantly ferromagnetic or antiferromagnetic in character. The relevant analysis is quite involved, however, and experience with Sr_2RuO_4 shows that it can have its pitfalls.

In an early NMR paper, Imai and co-workers (1998) successfully performed difficult ^{101}Ru and ^{17}O T_1 measurements from 4 K to room temperature, and saw very similar temperature dependence from both in-plane sites. They pointed out that this would not be expected if the fluctuations were purely antiferromagnetic, since the

²³For a good introduction to the dynamical susceptibility, see White (1983), Chap. 1.

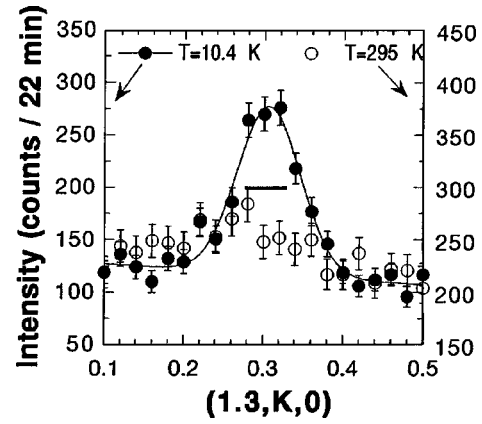


FIG. 12. The inelastic-scattering signal that identified the incommensurate spin fluctuations in Sr_2RuO_4 , from Sidis *et al.* (1999). The x axis is in reciprocal-lattice units, and the peak corresponds to the nesting vector \mathbf{q}_0 of $(0.6\pi, 0.6\pi)$ discussed in the text.

fluctuation amplitude should vanish at the magnetically symmetric O sites. However, they extrapolated this conclusion to an unambiguous statement that the spin fluctuations in Sr_2RuO_4 are predominantly ferromagnetic. The trouble is that the argument really applies to any \mathbf{q}_0 away from (π, π) , and so cannot be used to rule out the possibility of strong fluctuations at some incommensurate nesting vector. In fact, a subsequent inelastic neutron-scattering study by Sidis *et al.* (1999) showed that there is a strong fluctuating amplitude at $\mathbf{q} \approx (0.6\pi, 0.6\pi)$, as shown in Fig. 12. These fluctuations are due to nesting of the α and β sheets of the Fermi surface, and had been predicted in independent theoretical work by Mazin and Singh (1999). Indeed, the close agreement between the band-structure-based prediction and the observation would have been good evidence for the accuracy of such calculations if that evidence had not already been provided by the quantum oscillations described in Sec. II.B. Further inelastic neutron studies of the incommensurate fluctuations have been reported by Servant *et al.* (2000, 2002).

Mukuda and co-workers (1998, 1999a) performed a detailed study of ^{17}O NMR with discrimination between O(1) and O(2) (see Fig. 1), and applied fields parallel and perpendicular to the c axis. Some of the assumptions made in the analysis of these data led them to propose that interlayer spin fluctuations were strongly antiferromagnetic in character. This proposal also turned out to be inconsistent with the results of inelastic neutron scattering, with Servant *et al.* (2000) reporting that no correlated spin fluctuations were observed between the layers. More detailed accounts of the relationship between the neutron scattering and NMR work can be found in Sidis *et al.* (1999) and Ishida *et al.* (2001b). The consensus at present is that there is no fundamental experimental discrepancy, and that the discrepancies of interpretation have been resolved by a reexamination of the earlier analyses.

What, then, is the current status of the experimentally determined $\chi''(\mathbf{q}, \omega)$? The peak at $\mathbf{q}_b \approx (0.6\pi, 0.6\pi)$ is well established, and Sidis *et al.* have measured its energy dependence from 1.5 to 12 meV. This has allowed

them to calculate $\chi'(\mathbf{q}_0, 0)$, and show that it is a factor of ~ 6 larger than $\chi'(0, 0)$, which is obtained from the static susceptibility. That the incommensurate fluctuations are dominant also seems to be supported by the effects of substitution of Ti^{4+} for Ru. This nonmagnetic ion was reported to induce static magnetic order by Minakata and Maeno (2001). Very recently, Braden *et al.* (2002) have shown that the static order is incommensurate, with the same Fermi-surface nesting origin as the peak at \mathbf{q}_0 in the unsubstituted compound.

What is *not* known in any detail is the form of $\chi''(\mathbf{q}, \omega)$ in other regions of (\mathbf{q}, ω) space. It is clearly important that such information be obtained. A further subtlety is the likely need to separate the contributions from the different Fermi-surface (FS) sheets. If the superconductivity is dominated by pairing on γ , for example,²⁴ the effects of nesting resulting from α and β may be of limited relevance to the superconducting mechanism. In resolving this kind of issue, the distinct Ru-orbital characters of the different FS sheets may well prove to be useful. It seems likely that although further inelastic neutron-scattering measurements are of primary importance, their combination with NMR and calculations based on the known electronic structure will be needed to obtain a complete picture.

III. BASIC PROPERTIES OF THE SUPERCONDUCTING STATE

In this section we will begin our review of the superconducting properties and parameters of Sr_2RuO_4 . The contents are organized in approximately chronological order. First, we review the early measurements that gave the initial hints of unconventional superconductivity. We then discuss how the existence of an unconventional state of some kind was essentially established by the observation that the superconductivity can be destroyed by elastic impurity scattering. Understanding the impurity effects enabled the development of techniques for growing clean limit crystals on which a wide variety of further experiments have been carried out; in Sec. III.C we give the basic Ginzburg-Landau parameters of such clean limit material. We then begin our review of experiments that have been performed to investigate the hypothesis of spin-triplet pairing and hence an odd-parity state. We show that while a number of tunneling and proximity-effect experiments are consistent with this hypothesis, none of those performed to date can be regarded as conclusive. We close the section with a discussion of experiments measuring the spin susceptibility in the superconducting state. These fall into a different category, because if they have been correctly performed and interpreted, their results appear to be understandable *only* in terms of triplet pairing.

²⁴See, for example, Agterberg *et al.* (1997); Zhitomirsky and Rice (2001), and the discussion in Sec. VI.

A. Early measurements

In the years immediately following the discovery of superconductivity in Sr_2RuO_4 , some basic features of the superconducting state began to emerge. First, it was shown that T_c is remarkably insensitive to high-temperature annealing in a wide variety of partial pressures of oxygen, in contrast to observations in the cuprates (Nishizaki *et al.*, 1996). It was important that this be established empirically, since it showed that experiments performed in a variety of environments were unlikely to be influenced by chemical instability of the specimens.

The first estimates of the Ginzburg-Landau parameters were attempted using a combination of measurements of H_{c2} and BCS *s*-wave expressions relating the thermodynamic H_c to the normal-state electronic specific heat (Yoshida *et al.*, 1996a). These correctly concluded that Sr_2RuO_4 is only weakly type II when the applied field is parallel to the *c* axis, and that the crystal studied, with $T_c \sim 0.9$ K, was not in the clean limit. Another interesting observation was that of a second dissipation peak in ac susceptibility measurements when dc fields were applied parallel to the Ru-O planes (Yoshida *et al.*, 1996b). Such a dissipation peak is often seen in other superconductors and attributed to vortex synchronization. At low temperatures and at low fields, the flux-line lattice is rigid and not pinned by the randomly distributed pinning centers, resulting in large dissipation due to vortex motion in response to the ac field. As $H_{c2}(T)$ is approached, collective pinning starts when the shear elastic constant of the flux-line lattice diminishes, leading to a decrease in the dissipation (Mao *et al.*, 1999).

Following the suggestions by Rice and Sigrist (1995) and Baskaran (1996) of the possibility of triplet superconductivity in Sr_2RuO_4 , workers in the field were alerted to any signs of unconventional superconducting behavior. Early evidence came from specific-heat measurements on a sample with $T_c = 1.13$ K, which had a substantial residual density of states that could only be understood in a homogeneous *s*-wave superconductor if magnetic impurities were present in the sample (Maeno *et al.*, 1996). At approximately the same time, a combined Ru NMR and nuclear quadrupole resonance study of a sample with $T_c = 0.7$ K yielded even more convincing evidence of unconventional behavior (Ishida *et al.*, 1997). The combination of NMR at relatively high fields in the normal state and NQR in zero applied field in both the normal and superconducting states allowed the nuclear spin-lattice relaxation rate $1/T_1$ to be measured through T_c . In the normal state, $1/T_1$ has the linear temperature dependence expected of a metal, before falling sharply at T_c and then recovering its metalliclike temperature dependence deep into the superconducting state. No coherence peak is seen at T_c . The authors noted that this behavior was qualitatively similar to that seen in some cuprate superconductors, and could be understood in terms of a non-*s*-wave gap state and elastic impurity scattering. They pointed out that it was un-

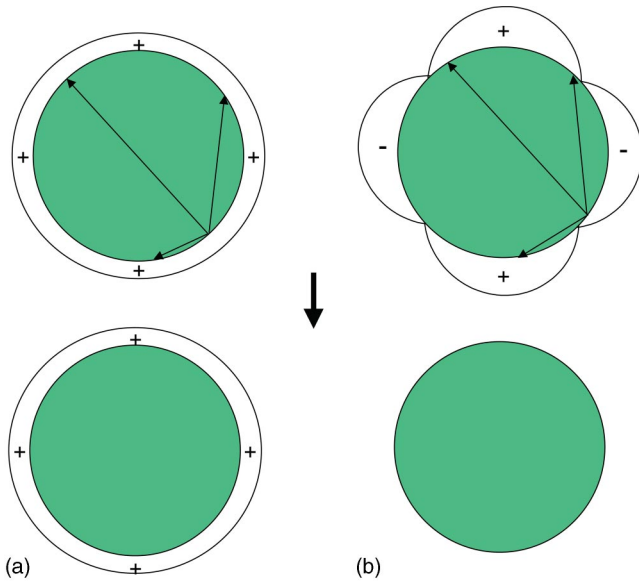


FIG. 13. Sketches showing the effect of strong elastic scattering on two types of superconducting order parameters. In each case the upper sketch represents the \mathbf{k} dependence of the amplitude of the superconducting gap around the Fermi surface, which is shaded. The \mathbf{k} -dependent phase is also shown. Typical elastic-scattering events are denoted by arrows. The lower sketch is the result of strong elastic scattering: (a) isotropic s wave, which is essentially unaffected; (b) $d_{x^2-y^2}$, in which strong scattering averages the gap to zero, destroying the superconductivity. In any p -wave state, the odd parity guarantees that there will also be complete destruction of superconductivity by strong elastic scattering (Color in online edition).

likely to be due to magnetic impurity scattering in an s -wave superconductor, because there were no indications of magnetic impurities from magnetic-susceptibility or NMR measurements. The complete lack of NQR line broadening well below T_c was also good evidence against bulk inhomogeneity (the presence of coexisting metallic and superconducting regions, which could not be ruled out as an interpretation of the specific-heat data in isolation). Although they noted that a dirty d - or p -wave state was the most natural interpretation of the data, the authors estimated that their sample was likely to be in the clean limit, and suggested an intrinsic mechanism for the large residual density of states. In fact, subsequent work showed that T_c had to be much higher before the clean limit could be reached.

B. The effects of impurities

1. Impurity suppression of the transition temperature

The variation of T_c seen in the early work on Sr_2RuO_4 superconductivity motivated a quantitative investigation of impurity effects. Destruction of superconductivity by nonmagnetic impurities is a rather pure test of non- s symmetry, because Anderson's theorem shows that s -wave superconductivity is unaffected by standard elastic impurity scattering (Anderson, 1959). A simplified, intuitive picture is given in Fig. 13. As sketched in

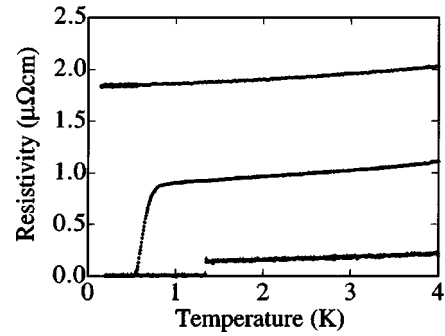


FIG. 14. The low-temperature resistivity of three samples of Sr_2RuO_4 with different levels of elastic scattering. The data in the figure were measured down to 130 mK, but subsequent susceptibility measurements have confirmed that no superconductivity is observed above 20 mK in the sample with a residual resistivity of $1.8 \mu\Omega \text{ cm}$. From Mackenzie, Haselwimmer, *et al.* (1998a, 1998b).

Fig. 13(a), an isotropic s -wave superconductor is characterized by an order parameter with a \mathbf{k} -independent phase. Strong elastic scattering, which mixes all the \mathbf{k} states, does not affect the magnitude of the order parameter. In an s state with an anisotropic gap, the scattering will average the gap, giving a reduction in T_c but not complete suppression of the superconductivity. Only non- s states such as the $d_{x^2-y^2}$ state sketched in Fig. 13(b) have order parameters that completely cancel out under strong \mathbf{k} -space averaging. In a p -wave superconductor, many different forms are possible for the energy gap, as will be discussed in Sec. IV. In all of these, even the ones with no nodes in the gap, the odd spatial parity ensures a full impurity effect and complete suppression of T_c (Balian and Werthamer, 1963; Larkin, 1965).

To investigate the impurity effect in Sr_2RuO_4 , a selection of crystals with T_c ranging from $>1.3 \text{ K}$ to $<20 \text{ mK}$ were selected for detailed investigation by Mackenzie, Haselwimmer, *et al.* (1998a, 1998b). High-precision electron probe microanalysis was used to check for the presence of every element with an atomic number between 11 (Na) and 83 (Bi), with a detection sensitivity typically better than 50 ppm. No magnetic impurities were found in any of the crystals, but the ones with low or zero T_c contained detectable traces of Si and Al at levels (always less than 430 ppm) that showed a correlation with the residual resistivity. Precise measurements of the low-temperature resistivity produced the data shown in Fig. 14. Samples with low residual resistivity showed sharp superconducting transitions, and as the residual scattering increased, T_c dropped and the transitions became broader, until the superconductivity was destroyed altogether. Data from 12 samples are summarized in Fig. 15.

The functional form expected for the behavior of T_c in the presence of pair-breaking scattering was first derived by Abrikosov and Gor'kov (1960a) for magnetic impurities in an s -wave superconductor:

$$\ln\left(\frac{T_c}{T_c^0}\right) = \psi\left(\frac{1}{2} + \frac{\alpha T_c^0}{2\pi T_c}\right) - \psi\left(\frac{1}{2}\right), \quad (3.1)$$

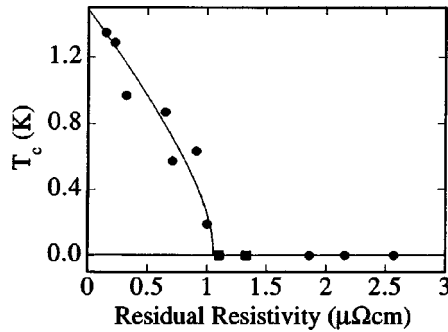


FIG. 15. The dependence of T_c on residual resistivity for Sr₂RuO₄. The squares indicate samples that showed a small drop in resistivity but no sign of bulk superconductivity above 130 mK. The solid line is a fit of the Abrikosov-Gor'kov pair-breaking function to the data as described in the text. Superconductivity is destroyed when the mean free path is approximately equal to the coherence length, and T_c in the clean limit is predicted to be approximately 1.5 K. From Mackenzie, Haselwimmer, *et al.* (1998a, 1998b).

where $\alpha = \hbar / \tau k_B T_{c0}$ is the pair-breaking parameter, $1/\tau$ is the rate of pair-breaking scattering, T_{c0} is the value of T_c in the limit $\alpha \rightarrow 0$, and ψ is the digamma function. For the case of nonmagnetic impurities in unconventional superconductors, the functional form is unchanged, but $\alpha = \hbar / 2\tau k_B T_{c0}$ (Millis *et al.*, 1988; Radtke *et al.*, 1993). The superconductivity is predicted to vanish at a critical value of α , when the lifetime broadening $\hbar\tau^{-1}$ becomes of the same order as the characteristic binding energy $k_B T_{c0}$. Expressed in terms of length, this is roughly equivalent to ℓ becoming of the same order as the superconducting coherence length ξ .

A least-squares fit of the pair-breaking function to the experimental data is shown in Fig. 15. The superconductivity is destroyed when the residual resistivity rises to approximately 1.1 $\mu\Omega$ cm. In this low-temperature limit, the mean free path ℓ can be estimated from the resistivity using the simple formula

$$\ell = \frac{2\pi\hbar d}{e^2 \rho \sum_i k_F^i}, \quad (3.2)$$

where d is the interlayer spacing, and the sum is over the three Fermi-surface sheets whose average radii k_F as measured by quantum oscillations are given in Table II. The value of ℓ at which the superconductivity disappears is approximately 900 Å, comparable to ξ (see Sec. III.C). This semiquantitative agreement is striking, given that the $\ell \sim \xi$ relationship is only an approximate prediction of the theory. Although impurity effects are known in other unconventional superconductors such as the heavy-fermion materials UPt₃ and UPd₂Al₃ (Geibel *et al.*, 1994; Dalichaouch *et al.*, 1995) and the organic salt (TMTSF)₂PF₆ (Choi *et al.*, 1984), it was not possible to make an accurate measurement of ℓ . In the cuprates, interpretation of studies such as those of Fukuzumi and co-workers (1996) is complicated by the influence of inelastic scattering at T_c and the unconventional normal-

state properties. Sr₂RuO₄ has thus provided perhaps the clearest example to date of a nonmagnetic impurity effect in an unconventional superconductor. The effect has subsequently been confirmed in two separate studies (Suderow *et al.*, 1998; Mao *et al.*, 1999).

The fit shown in Fig. 15 also had some predictive power, because it has proved to be possible through improved crystal growth to produce samples with ℓ as long as 3 μ m. The predicted T_c of approximately 1.5 K has been observed, allowing the study of Sr₂RuO₄ to proceed in samples with negligible impurity pair breaking.

2. Impurity effects on other properties of the superconducting state

Since the work on the dependence of T_c on elastic scattering, several studies have been performed on various properties of the superconducting state in Sr₂RuO₄ samples with impurities and defects. In the first of these, the temperature dependence of the upper critical field was studied by ac susceptibility in a series of samples with T_c varying from 0.65 to 1.48 K (Mao *et al.*, 1999). It was shown that T_c could be reduced substantially by changes to growth conditions that introduced defects rather than impurities into the samples. The other main results were that the temperature dependence of H_{c2} shows little dependence on T_c , and that $H_{c2}(0)$ has a $1/(T_c)^2$ dependence. Since $H_{c2} \sim \Phi_0 / 2\pi\xi^2$ and $\xi_0 \sim \hbar v_F / k_B T_c$, the observation is exactly what would be expected for pair breaking in an unconventional superconductor. In a more recent paper, Mao, Maeno, *et al.* (2001) analyzed the impurity dependence of the isotope effect in Sr₂RuO₄ within the Abrikosov-Gor'kov pair-breaking theory.

The other studies were sensitive to the density of pair-broken states below T_c . Although the elastic-scattering dependence of T_c itself is expected to be insensitive to details of the gap state, the number of normal excitations that are produced by the pair breaking will depend on the \mathbf{k} dependence of the gap. Nodes or strong gap anisotropy will lead to more pair-broken states than an isotropic gap for a given scattering rate. Theoretical treatments have recently been given for some p -wave gap states explicitly proposed for Sr₂RuO₄.²⁵ Experimentally, it has been found that if all the Fermi-surface sheets open a gap at T_c , the models in their present form do not account particularly well for the T_c dependence of the residual density of states deduced from specific-heat data (Nishizaki *et al.*, 1998, 1999). Thermal-conductivity measurements have also been reported on strongly pair-broken samples with $T_c = 0.5$ and 0.7 K (Suderow *et al.*, 1998). The results of these studies emphasize the importance of having clean limit samples be-

²⁵See, Agterberg (1999); Maki and Puchkaryov (1999, 2000); Miyake and Narikiyo (1999); Maki *et al.* (2000), and references therein.

fore attempting to deduce gap states from measurements sensitive to normal quasiparticles below T_c (see Sec. V).

C. Ginzburg-Landau parameters of clean limit Sr₂RuO₄

The growth of single crystals with T_c approaching the 1.5-K clean limit value enables the intrinsic superconducting parameters of Sr₂RuO₄ to be derived from experiment. In this section we perform such an analysis, using expressions for a single-component Ginzburg-Landau (G-L) theory. Although it seems that a two-component G-L treatment is more appropriate for Sr₂RuO₄ (see Sec. IV), this would be expected to give relatively small changes in the numerical values of the basic superconducting parameters. We believe that the estimates we give here are a good initial guide to the properties of the superconducting state of Sr₂RuO₄.

The upper critical field for single crystals with $T_c = 1.49$ K has been studied by field-dependent resistivity for $H\parallel ab$ and $H\parallel c$ (Akima *et al.*, 1999), and by ac susceptibility for $H\parallel c$ (Mao *et al.*, 1999). Values of 1.5 and 0.075 T were deduced for $\mu_0 H_{c2}$ for $H\parallel ab$ and $H\parallel c$, respectively. Uncertainties in the choice of criterion to use at low temperatures restrict the accuracy of these values to approximately 5%. The thermodynamic critical field H_c has been derived from specific-heat data by applying standard thermodynamic expressions (see, for example, Tinkham, 1996), with a value of 0.023 T deduced for a sample with $T_c = 1.48$ K (Nishizaki *et al.*, 1999).

These data can be used to estimate the following parameters. The coherence lengths are $\xi_{ab}(0) = [\Phi_0/2\pi\mu_0 H_{c2\parallel c}(0)]^{1/2}$ and $\xi_c(0) = \Phi_0/2\pi\xi_{ab}(0)\mu_0 H_{c2\parallel ab}(0)$, where ξ_{ab} is the coherence length in the ab plane and Φ_0 is the flux quantum.²⁶ Using the relationships $H_{c2}(0) = \sqrt{2}\kappa(0)H_c(0)$ allows values for κ_{ab} and κ_c to be deduced. Here, we adopt the notational convention that $\kappa_{ab} = \lambda_{ab}/\xi_{ab}$ and $\kappa_c = (\lambda_{ab}\lambda_c/\xi_{ab}\xi_c)^{1/2}$, which means that $\kappa_{ab}(0) = H_{c2\parallel c}(0)/\sqrt{2}H_c(0)$, and that λ_{ab} is the penetration depth when the screening currents are flowing in the ab plane. The numerical G-L parameters are listed in Table III. Some of the parameters in Table III have been estimated by other authors. For example, an analysis of the diffracted intensity measured by small-angle neutron scattering from the superconducting flux lattice gave an estimate for λ_{ab} of 1.9×10^3 Å (Riseman *et al.*, 1998), while earlier studies on Sr₂RuO₄ gave $\gamma_s = 26$ (Yoshida *et al.*, 1996a).

In principle, many of the parameters given in Table III can be calculated using the knowledge of the Fermi surface that is summarized in Table II. For instance, the

²⁶It should be noted that the above estimation assumes that H_{c2} is determined by a conventional orbital depairing mechanism. We will discuss later in Sec. VII that $H_{c2\parallel ab}(0)$ appears to be limited more strongly. The estimate given in Table III for $\xi_c(0)$ should therefore be regarded as an upper limit.

TABLE III. Superconducting parameters for Sr₂RuO₄ with negligible impurity pair breaking ($T_c > 1.48$ K). ξ_{ab} is the in-plane coherence length, λ_{ab} is the penetration depth for in-plane screening currents, and $\kappa_{ab} = \lambda_{ab}/\xi_{ab}$, so all these quantities are defined for magnetic fields applied parallel to c . γ_s is the anisotropy parameter of the superconducting state. For other definitions see the main text.

Parameter	ab	c
$\mu_0 H_{c2\parallel c}(0)$ (T)	0.075	
$\mu_0 H_{c2\parallel ab}(0)$ (T)	1.50	
$\mu_0 H_c(0)$ (T)	0.023	
$\xi(0)$ (Å)	660	33
$\lambda(0)$ (Å)	1520	3.0×10^4
$\kappa(0)$	2.3	46
$\gamma_s = \xi_{ab}(0)/\xi_c(0)$	20	

upper critical field in a two-dimensional superconductor with a cylindrical Fermi surface is given by (Schofield, 1995)

$$\mu_0 H_{c2} = 3.53 \Phi_0 \left(\frac{k_B T_c}{\hbar^2} \right)^2 \left(\frac{m_i^*}{k_F^i} \right)^2. \quad (3.3)$$

If there is more than one Fermi-surface sheet, the largest predicted upper critical field would be expected to correspond to observation. For Sr₂RuO₄, the value for the γ sheet is 0.076 T, in remarkably (and possibly fortuitously) good agreement with the observed value. The predictions for α or β are over a factor of 2 less than this, but we note that the estimate ignores any possible in-plane anisotropy of either the Fermi-surface parameters or the superconducting gap.

The penetration depth λ_{ab} is related to the total density of superconducting electrons, and it can be shown that all parts of the Fermi surface that have a gap contribute to the low-temperature value of λ (Rickayzen, 1969). Specifically,

$$\frac{1}{\lambda^2(0)} = \frac{N_A e^2 \mu_0}{V_M m_e} \sum_i \frac{N_i}{m_i^*}, \quad (3.4)$$

where N_i is the number of electrons per formula unit in band i and V_M/N_A is the volume of one formula unit. The specific-heat data of Nishizaki *et al.* (2000) indicate that all three Fermi-surface sheets are essentially fully paired at low temperatures, in which case Eq. (3.4) predicts that $\lambda_{ab} = 980$ Å, in relatively poor agreement with observation. One possibility for the discrepancy is the use of the G-L expressions outside the temperature range of their validity, but this seems unlikely since the temperature dependencies of H_c and H_{c2} are fairly similar.

An even more puzzling discrepancy comes from calculations of the superconducting anisotropy parameter γ_s . Using the BCS-like expression $\xi_0 \sim \hbar v_F/k_B T_c$ leads to the expectation that $\gamma_s = \langle v_F \rangle / \langle v_{\perp} \rangle$, where v_F and v_{\perp} are in-plane and out-of-plane Fermi velocities, and $\langle \rangle$ denotes an appropriate Fermi-surface average. Taking

values for $\langle \nu_{\perp} \rangle$ (defined for simplicity as $\sqrt{\langle \nu_{\perp}^2 \rangle}$) and $\langle \nu_F \rangle$ from Table II gives estimates for γ_s of 117, 57, and 174 for the α , β , and γ Fermi-surface sheets, all of which are larger than the observed value of 20. The latter was obtained experimentally from $H_{c2\parallel ab}/H_{c2\parallel c}$, and might be expected to be determined by the *largest* of the three calculated values if the dominant sheet in determining the pairing were γ , as suggested by the value of $H_{c2\parallel c}$. Although considerable simplifications have been made in parametrizing the complicated c -axis dispersions of Sr_2RuO_4 in one set of $\langle \nu_{\perp} \rangle$, it is hard to see that any of these could account for such a large disagreement. The same considerations apply to the use of a two-component G-L treatment. This discrepancy is discussed again in Sec. VII.

D. Tunneling and proximity-effect studies

In this section we review progress on a broad class of experiments in which unconventional superconductivity is probed by studying the current-voltage characteristics of interfaces of some kind. These could include metal-superconductor, metal-insulator-superconductor, and superconductor-insulator-superconductor junctions. All have been tried on Sr_2RuO_4 , with somewhat mixed results. In some cases, sample quality has been questionable. Even when top quality, well-understood samples have been used, the all-too-common problems of understanding and controlling interfaces have arisen. In this sense, the work on Sr_2RuO_4 has mirrored much of that throughout the history of research on unconventional superconductivity. Interpretation of the work that we will review has usually been made in terms of postulated triplet states, and it is fair to say that while none of the published experiments contradicts the existence of a triplet state, none can be regarded as consistent with *only* such a state. This point is made by most of the authors concerned.

One of the earliest reports in the field came from Jin, Zadorozhny, *et al.* (1999), who studied the temperature dependence of the critical current in what were designed to be Pb- Sr_2RuO_4 -Pb proximity junctions with current injected along the c axis of Sr_2RuO_4 . An interesting effect was seen, but after performing the majority of the experiments, they became aware that the Josephson effect was present only in samples containing significant amounts of Ru inclusions (see Appendix C). As they discuss at some length, this means that the effective geometry was almost certainly Pb-Ru- Sr_2RuO_4 -Ru-Pb, with current injection into the ab planes of Sr_2RuO_4 . In either case, the proximity junction results indicate that an s -wave superconducting wave function penetrating into Sr_2RuO_4 appears to interfere with the superconductivity of Sr_2RuO_4 . An analysis of such a situation based on a first-order process with the assumption of a π -phase shift between the junctions was reported by Honerkamp and Sigrist (1998a), while Yamashiro *et al.* (1998a) made some calculations based on a second-order process in a pure Pb- Sr_2RuO_4 -Pb proximity junction.

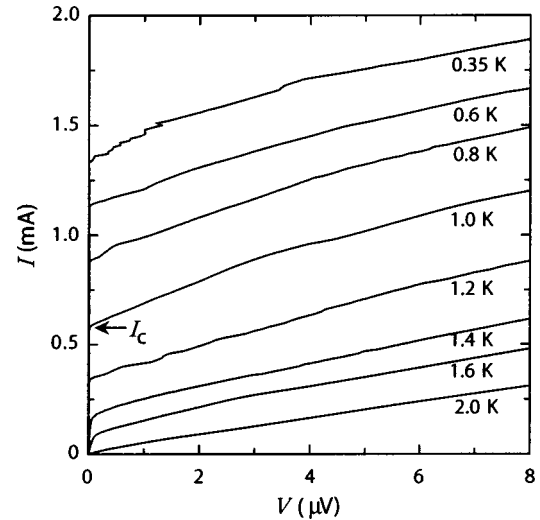


FIG. 16. I - V curves at various temperatures for an in-plane In/ Sr_2RuO_4 junction. The finite critical current I_c is indicated on the figure. From Jin *et al.* (2000).

In later work, Jin *et al.* (2000) reported the results of a study of the Josephson effect between In and Sr_2RuO_4 , this time in high-quality samples in which there was no evidence for Ru inclusions. In c -axis junctions, no Josephson current was seen, in agreement with the group's earlier findings for Pb- Sr_2RuO_4 . For current injection into the ab plane, however, some junctions did give a Josephson current, as shown in Fig. 16. As the authors stress, the junctions are far from perfect. Reproducibility is quite poor, and no Fraunhofer pattern is seen. The form of I - V characteristic suggests the formation of a superconductor-noninsulator-superconductor junction, but it is not clear why this should be the case. As shown in a scanning-tunneling microscopy study by Matzdorf *et al.* (2000), there is an atomic reconstruction of the ab surface layer of Sr_2RuO_4 (which is presumed to be metallic), but no equivalent measurements have been possible on the ac face. This does not cleave well, and Jin *et al.* stressed that surface roughness exists on the polished faces of their sample. More recent work by Sumiyama *et al.* (2002) reported observation of Josephson currents for c -axis Sn- and Nb- Sr_2RuO_4 junctions, in contrast to the report by Jin *et al.* (2000). However, the latter authors warned of the possibility that their observations were due to ab -plane tunneling at steps in their cleaved surfaces.

Notwithstanding these difficulties, the above work raises an important issue. If Sr_2RuO_4 is an odd-parity triplet superconductor, why is a Josephson junction of any kind possible with an even-parity singlet superconductor such as In? Jin *et al.* (2000) give a brief review of calculations that show that first-order Josephson coupling in such cases is possible in the presence of spin-orbit coupling. Under the assumption of a triplet state in Sr_2RuO_4 , their results provide "selection rules" for such coupling. Their observations are, however, equally inter-

pretable in terms of a singlet d -wave state.²⁷

A different consequence of unconventional superconductivity was reported by Laube *et al.* (2000), who investigated Andreev reflection at Pt- Sr_2RuO_4 point-contact junctions in which the current was again injected primarily parallel to the ab planes. The physics of normal-metal- Sr_2RuO_4 junctions has been studied theoretically by Honerkamp and Sigrist (1998b) and other authors.²⁸ Laube *et al.* observed a zero-bias anomaly, and argued that the most likely cause was an Andreev bound state. Such bound states exist only in unconventional superconductors for which the phase is not constant, and so their observation with Sr_2RuO_4 provided more evidence for an unconventional order parameter of some kind. The experiment is not, however, ideal for distinguishing triplet and singlet superconductivity, as the authors themselves emphasized. Another puzzle is that their analysis yielded a value for the superconducting gap that is a factor of 5 higher than that expected for weak coupling.²⁹

In summary, then, considerably more work is likely to take place in the future on tunneling, Andreev scattering, and proximity effects in Sr_2RuO_4 . A long-term goal would be the direct measurement or concrete denial of the existence of odd parity, but reproducible interfaces and junctions will be necessary precursors to this type of experiment. The experience to date suggests that it may take some time before all the relevant difficulties are overcome. As an example of the advances that need to be made, we note that some of the ground-breaking phase-sensitive measurements on the cuprates were made on thin films (e.g., Tsuei *et al.* 1994). The purity requirements for superconductivity in Sr_2RuO_4 are sufficiently stringent that to date, no one has succeeded even in producing a superconducting film, far less a Josephson junction based on one.

E. Experimental evidence for triplet pairing

The experiments described so far provide strong evidence for unconventional superconductivity in Sr_2RuO_4 , but little direct evidence that the superconducting state involves spin-triplet Cooper pairing. In

²⁷Indeed, unpublished work by van Harlingen and collaborators is interpreted by them as evidence against a triplet state in Sr_2RuO_4 . Their observations are qualitatively in agreement with those published by Jin *et al.* (2000), but they argue that the size of the Josephson current that they observe is unlikely to be compatible with the interpretation given by Jin *et al.* Issues of quantitative agreement such as these are likely to be settled only once improved quality junctions become available, and might also require further theoretical input.

²⁸For example, see Yamashiro *et al.* (1997, 1998b, 1999); Hirai, Tanuma, *et al.* (2001); Hirai, Yoshida, *et al.* (2001).

²⁹A value of this magnitude is also at odds with the results of separate unpublished low-temperature scanning-tunneling microscopy studies by Morpurgo and collaborators and the group of J.C.S. Davis, who associate lower-energy features with the opening of the superconducting gap in Sr_2RuO_4 .

principle, this evidence could be determined from a proof of the existence of odd parity or from probes that have a direct sensitivity to the spin part of the pair wave function. As seen in Sec III.D above, no convincing demonstration has yet been made of odd parity. We concentrate, therefore, on spin-sensitive probes. The most precise measurements have been those of the spin susceptibility in the superconducting state by NMR. These experiments and their interpretation are such important aspects of the unfolding story of superconductivity in Sr_2RuO_4 that we think it appropriate to discuss both the technique and the measurements in some detail.

1. Spin susceptibility by the NMR Knight shift

The most direct evidence for triplet pairing so far has come from a study of the spin susceptibility into the superconducting state. In a metal, the origin of Pauli spin susceptibility χ_s is the Zeeman splitting into spin-up and -down Fermi surfaces, accompanied by a lowering of the free energy by $\frac{1}{2}\chi_s H^2$. This Fermi-surface polarization opposes Cooper pair formation in spin singlets, because states $\mathbf{k}\uparrow$ and $\mathbf{k}\downarrow$ no longer exist at the Fermi surface. In weak applied magnetic fields, the free-energy gain from the condensation of superconductivity is dominant, the polarization of the Fermi surface is suppressed, and $\chi_s \rightarrow 0$ as $T \rightarrow 0$. For spin-triplet Cooper pairing, the components of the triplet that involve equal spin pairing are unaffected by the Fermi-surface polarization, so condensation in these channels does not affect the spin susceptibility. For some p -wave order parameters, a partial change in χ_s is predicted for all directions of the applied magnetic field while for others a complete suppression of χ_s is predicted in one direction of the applied field and zero suppression in others (see, for example, Leggett, 1975 and Sec. IV below). The key point of relevance to the following discussion is that an observation of a temperature-independent spin susceptibility deep into the superconducting state can be consistent only with the existence of triplet pairing.

The difficulty of measuring χ_s in superconductors (as opposed to neutral superfluids) is the Meissner effect. Even in strongly type-II materials for which strong field penetration can be achieved, the static susceptibility is dominated by the diamagnetism of the screening currents. This problem can be overcome, in principle, by using the NMR Knight shift to measure the spin susceptibility. The Knight shift is the difference between the NMR frequency of a nucleus when it is in a metal or superconductor rather than an insulator. It has an orbital part (K_{orb}) due to diamagnetism of bound and free electrons, and a spin part (K_{spin}) due to the Pauli paramagnetism of the conduction electrons:

$$\omega = \gamma_{\text{gyr}} B_{\text{int}} (1 + K_{\text{orb}} + K_{\text{spin}}), \quad (3.5)$$

where ω is the NMR frequency, γ_{gyr} is the gyromagnetic ratio of the nucleus being studied, and B_{int} is the average magnetic field in the sample. Typical values for K_{orb} or K_{spin} are below 1%. Only s electrons interact directly with the nucleus, so in the many metals of interest for

which the conduction bands have strongly non- s character, K_{spin} arises from the exchange interaction between the conduction electrons and the s electrons, causing a hyperfine contact interaction between the latter and the nuclei. This effect, called core polarization, is the only way in which the nuclei “see” the spin magnetism of non- s conduction electrons, since their wave functions vanish at the nuclear sites. Negative values of K_{spin} arise when the core polarization contact field is opposite to the applied field, and are fairly common (MacLaughlin, 1976).

In analogy with the above discussion for χ_s , K_{spin} is expected to disappear as $T \rightarrow 0$ in a singlet paired superconductor (Yosida, 1958). In superconductors the Meissner effect means that B_{int} is often suppressed from the value of the applied field when the sample enters the superconducting state. This gives a change to ω that could easily be confused with a change in K_{spin} . In type-I material this problem means that powder samples with very small grain sizes have often been employed, which has in turn led to difficulties of interpretation due to spin-orbit scattering.³⁰

In strongly type-II superconductors, however, the situation is somewhat simpler. The value of κ determines the strength of contributions from the vortex lattice to the observed NMR signal. Both the “Meissner shift” of B_{int} and the broadening due to its inhomogeneity are expected to be of order $\mu_0 M/B_{\text{appl}}$, and M can be estimated using the Abrikosov formula

$$M = \frac{H_{c2} - H}{(2\kappa^2 - 1)\beta}, \quad (3.6)$$

where β is a constant of order 1. For high κ , $\mu_0 M/B_{\text{appl}}$ can be $\sim 10^{-4}$, much smaller than typical Knight shifts. There is then no need to work with grains whose characteristic size is of the order of the penetration depth, as long as the normal-state conductivity is sufficiently low that the rf fields can penetrate significantly into the sample. For example, Knight-shift measurements in $\text{YBa}_2\text{Cu}_3\text{O}_7$ were influential in ruling out the possibility of triplet superconductivity in the cuprates (Takigawa *et al.*, 1989; Barret *et al.*, 1990).

In Sr_2RuO_4 , the conditions are ideal for Knight-shift measurements with the dc field applied in the ab plane. The conductivity along the c axis is relatively low, so the skin depth is tens of microns along the field direction. Also, the material is strongly type II for this configuration (see Table III). For $\kappa = 46$, and $B_{\text{appl}} = B_{c2}/2$, $\mu_0 M/B_{\text{appl}} \sim 2 \times 10^{-4}$, much smaller than typical Knight shifts. It should thus be possible to ignore complications due to the Meissner effect in an NMR experiment on Sr_2RuO_4 , even though this would not be the case for a measurement of the static susceptibility.

³⁰For example, Anderson (1959); Abrikosov and Gorok’v (1960b); Androes and Knight (1961). In some type-I materials, the use of thin-film samples removed the spin-orbit scattering problem and the behavior expected of spin-singlet superconductors was recovered; for a review, see MacLaughlin (1976).

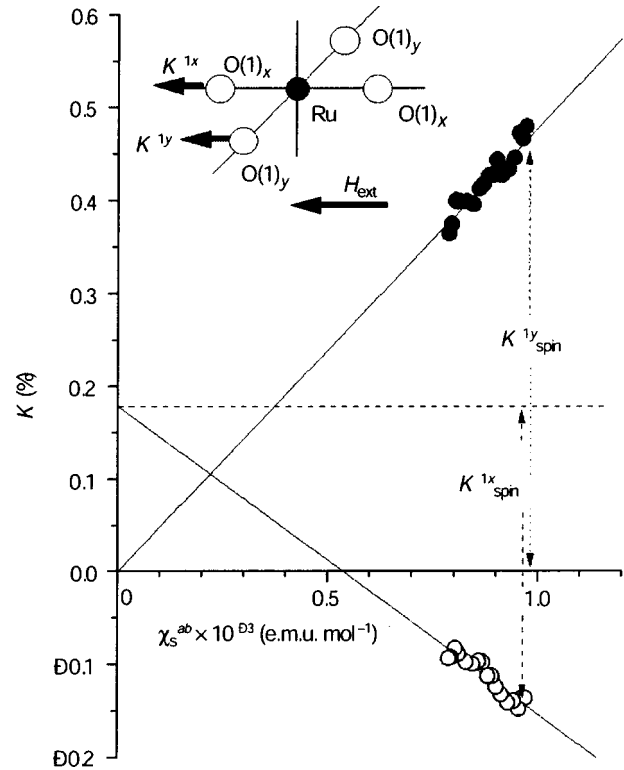


FIG. 17. The Knight shift for the two in-plane oxygen sites $\text{O}(1)_x$ and $\text{O}(1)_y$ (defined in the inset) plotted against the spin part of the static susceptibility χ_s . Values of the orbital Knight shift of 0.2% and 0% are deduced for $\text{O}(1)_x$ and $\text{O}(1)_y$, respectively. From Ishida *et al.* (1998).

This key experiment was performed by Ishida *et al.* (1998), who worked with high-quality samples ($T_c > 1.4$ K) which had been specially enriched with ^{17}O to ensure a favorable value of γ_{gyr} . In the experimental configuration used, there are two inequivalent oxygen sites, $\text{O}(1)_x$ and $\text{O}(1)_y$, which have Knight shifts just above T_c of 0.5% and -0.15% , respectively. In order to separate the contributions of K_{orb} and K_{spin} to the total shift K_{tot} , they used the well-established technique (Clogston *et al.*, 1964) of plotting K_{tot} against the measured normal-state spin susceptibility χ_s (Fig. 17). The rationale behind such “ K - χ ” plots is that any temperature dependence of χ in a narrow band system must come from the spin part. If a parametric plot of K_{tot} versus χ_s shows a linear variation, K_{orb} can be read off from an extrapolation to zero χ_s , allowing the isolation of K_{spin} for any temperature of interest.³¹ For the oxygen NMR in Sr_2RuO_4 , this gives estimates for K_{orb} of 0 and 0.2% for $\text{O}(1)_x$ and $\text{O}(1)_y$, respectively. This analysis is important because it allows a scale to be set for the change in K_{tot} expected in the superconducting

³¹Orbital contributions (assumed to be temperature independent) have been subtracted from χ_{tot} to obtain the χ_s used in Fig. 17, but in Sr_2RuO_4 these are thought to be small (less than 10% of χ_{tot} , as discussed in Sec. II.A.5), and so should not represent a significant source of systematic error in the analysis.

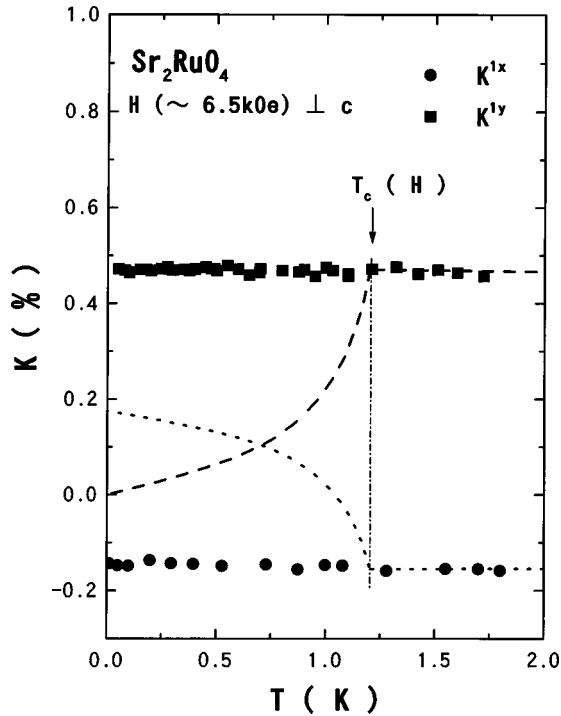


FIG. 18. The temperature dependence of K for the $\text{O}(1)_x$ site (circles) and $\text{O}(1)_y$ site (squares) as Sr_2RuO_4 is cooled through T_c in a magnetic field of 0.65 T applied parallel to the ab planes. Measurements of the spin-lattice relaxation rate were used to confirm by NMR the value of $T_c(H)$, which can also be obtained from susceptibility measurements. If the pairing in Sr_2RuO_4 were spin singlet, K would be expected to be approximately 0.05% and 0.15% in the low-temperature limit for $\text{O}(1)_x$ and $\text{O}(1)_y$, respectively, once the vortex core contribution at 0.65 T had been taken into account. The dotted lines are calculations of the temperature dependence expected for an example of a spin-singlet state, the $d_{x^2-y^2}$ state that exists in the cuprates. The fact that K remains temperature independent in the superconducting state for both sites is strong evidence for triplet pairing. From Ishida *et al.* (1998).

state for each site if $K_{\text{spin}} \rightarrow 0$ as $T \rightarrow 0$ for singlet pairing.

The central observation of Ishida *et al.* is shown in Fig. 18. In contrast to the expectation for singlet superconductivity, no change is resolved in K_{tot} as $T \rightarrow 0$ in an applied field of 0.65 T (just under $B_{c2}/2$). The form of temperature dependence expected for a clean limit d -wave superconductor is shown by the dotted lines. More recently, the Knight-shift experiments have been performed on Ru nuclei, yielding the same conclusion from data with much higher resolution (Ishida *et al.*, 2001a). A fuller analysis of the implications of this result in relation to possible triplet order parameters is given in Sec. IV.B. Here the key point to emphasize is that if this experiment is correctly interpreted, a triplet order parameter of some kind is the only conclusion that can be drawn.

2. Spin susceptibility by polarized neutron scattering

A second measurement that can give information on the magnetic susceptibility into the superconducting

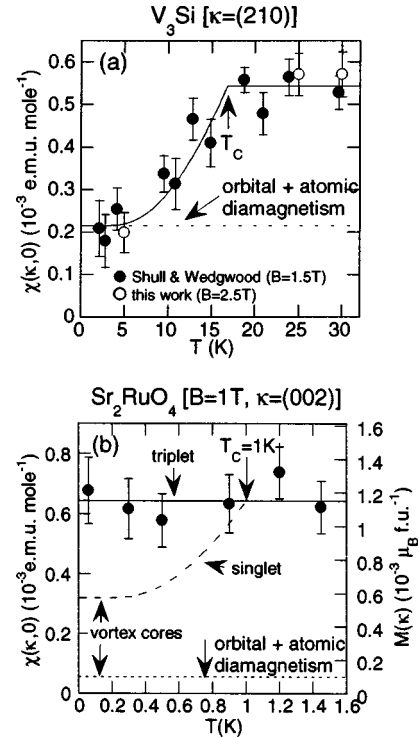


FIG. 19. Spin-polarized neutron-scattering results from an s -wave superconductor (V_3Si) and Sr_2RuO_4 . In (a), the original work of Shull and Wedgwood is confirmed, and the Yosida function is seen to be obeyed. (b) shows that in Sr_2RuO_4 , there is a marked contrast between the observed behavior (temperature independent within experimental error) and that expected if Sr_2RuO_4 had singlet pairing.

state is polarized neutron scattering, a technique first used in the study of s -wave superconductivity by Shull and Wedgwood (1966) and recently applied to Sr_2RuO_4 by Duffy and co-workers (2000). The idea is that in a magnetized material, neutron scattering occurs with Fourier components at reciprocal-lattice vectors because of both the periodicity of the nuclear positions and the microscopic periodicity of the magnetization density. The two scattered waves interfere, and, as described by Duffy *et al.*, the magnetic scattering can be isolated by measuring the flipping ratio R . This is defined as the ratio of scattering cross sections for initial neutron states that are parallel or antiparallel to the applied magnetic field, and with an arbitrary final spin state. For a small induced moment

$$R = 1 + A \frac{M_{\parallel}(\boldsymbol{\kappa})}{F_N(\boldsymbol{\kappa})}, \quad (3.7)$$

where $\boldsymbol{\kappa}$ is the scattering vector, $M_{\parallel}(\boldsymbol{\kappa})$ is the component of magnetization parallel to the applied field, $F_N(\boldsymbol{\kappa})$ is the nuclear structure factor, and $A = 1.16 \times 10^9 \text{ J T m}$.

The findings of Duffy *et al.* (2000) are summarized in Fig. 19. The control measurement on V_3Si shows the expected magnitude of change to the susceptibility due to singlet pairing. In contrast, there is no resolvable change in the measured susceptibility as Sr_2RuO_4 enters the superconducting state, for $B \parallel ab$. This is another key

experiment on Sr₂RuO₄. The basic conclusion is the same as that of Ishida and co-workers (1998), namely, that the behavior of the spin susceptibility into the superconducting state of Sr₂RuO₄ is consistent only with some form of triplet pairing.

F. Summary and conclusions

In this section, we reviewed the basic superconducting parameters of Sr₂RuO₄ and the early experimental work that provided very good evidence for unconventional superconductivity of some kind. We then discussed some of the experiments that have been interpreted explicitly in terms of triplet superconductivity. These undoubtedly fall into two classes: experiments for which a spin-triplet state can be argued to be the “best” interpretation, and experiments for which it seems to be the *only* plausible interpretation. The latter could also be described as experiments whose reported findings would have to be wrong if Sr₂RuO₄ were a spin-singlet superconductor. The NMR and polarized neutron experiments fall into that class, and the fact that they have generated consistent conclusions is strong evidence for the existence of a triplet state of some kind in Sr₂RuO₄. Although we do not wish to state this as a conclusion with 100% certainty, we believe that there is sufficient justification for us to proceed with a more detailed treatment of triplet order parameters, and a closer examination of the experimental data from Sr₂RuO₄ within the triplet framework.

IV. MOST LIKELY SYMMETRY OF THE Sr₂RuO₄ TRIPLET STATE

In this section we discuss the possible *p*-wave order-parameter symmetry of Sr₂RuO₄ in more detail. In order to do this, we first introduce the concept of the *d*-vector order parameter for triplet superconductors. We will try to do this in as simple a way as possible, since our aim is to give a flavor of the concept rather than a detailed derivation. For more complete and rigorous treatments the reader is referred to classic articles such as those by Balian and Werthamer (1963), Leggett (1975), Annett (1990), and Sigrist and Ueda (1991), and the excellent books by Vollhardt and Wölfle (1990), Tsuneto (1998), and Mineev and Samokhin (1999). An elementary discussion of symmetry breaking and unconventional superconductivity can be found in Annett (1995).

In our discussion, we adopt notational and linguistic conventions that were essentially developed for superfluid ³He, in which there is no crystal lattice. Although the lattice in Sr₂RuO₄ clearly plays an important role in many aspects of its electronic structure, this “lattice-free” notation has been widely adopted in the experimental literature, so we believe that it is best to retain it here. The effects of the crystalline environment are then discussed.

In the absence of a crystal lattice, the symmetry of the superconducting state is related simply to the relative

orbital angular momentum of the electrons in each Cooper pair. $L=0$ corresponds to *s* symmetry, $L=2$ to *d*, and $L=1$ to *p*. Even orbital angular momentum corresponds to antisymmetric singlet spin pairing, and odd orbital angular momentum to symmetric spin-triplet pairing with $S=1$. Within this description, which is exact for a superfluid such as ³He, spin space and orbital space are decoupled, so that the direction of *S* has no definite relationship with the direction of *L*.

A. Introduction to the *d* vector

1. The elegance of *d*-vector formalism

The order parameter in a superconductor is expressed in terms of the gap function $\Delta(\mathbf{k})$. Superconductivity is a state of spontaneously broken symmetry, and $\Delta(\mathbf{k})$ has the full symmetry properties of the condensate wave function. Gauge symmetry is always broken at T_c , and in *s* states, no further symmetries are broken. In *d* states, additional symmetry breaking can take place. For the well-known $d_{x^2-y^2}$ state of the cuprates, for example, $\Delta(\mathbf{k})$ breaks the 90° rotation symmetry of the square lattice. In *s*- and *d*-symmetry superconductors, the electrons pair in antisymmetric spin singlets, and a single complex function is sufficient for $\Delta(\mathbf{k})$. In *p*-symmetry superconductors, however, the spatial part of the pair wave function is antisymmetric. The first consequence of this is that the gap function automatically breaks the reflection symmetry of a square lattice in two dimensions. The second consequence is that the spins of the pair form a symmetric triplet state, requiring three independent gap functions to describe the spin dependence of the pairing.

The need to take into account the spin dependence of the pairing motivates the use of a general 2×2 matrix formalism for $\Delta(\mathbf{k})$:

$$\Delta(\mathbf{k}) = \begin{bmatrix} \Delta_{\uparrow\uparrow} & \Delta_{\uparrow\downarrow} \\ \Delta_{\downarrow\uparrow} & \Delta_{\downarrow\downarrow} \end{bmatrix}; \quad (4.1)$$

in which the elements correspond to the spin state of the electrons that constitute the Cooper pair. Here, \mathbf{k} is a unit vector specifying a direction in momentum space. In this formalism, a singlet superconductor is described by setting $\Delta_{\uparrow\uparrow} = \Delta_{\downarrow\downarrow} = 0$ and $\Delta_{\uparrow\downarrow} = -\Delta_{\downarrow\uparrow} = \Delta_s$, while for the triplet case, $\Delta_{\uparrow\downarrow} = \Delta_{\downarrow\uparrow} = \Delta_0$.

Balian and Werthamer (1963) noted that for triplet pairing, the gap matrix can be represented in terms of a three-component complex vector $\mathbf{d}(\mathbf{k}) = [d_x(\mathbf{k}), d_y(\mathbf{k}), d_z(\mathbf{k})]$. If $\mathbf{d}(\mathbf{k})$ is defined such that

$$\Delta(\mathbf{k}) = \begin{bmatrix} \Delta_{\uparrow\uparrow} & \Delta_0 \\ \Delta_0 & \Delta_{\downarrow\downarrow} \end{bmatrix} = \begin{bmatrix} -d_x + id_y & d_z \\ d_z & d_x + id_y \end{bmatrix}, \quad (4.2)$$

then it transforms like a vector under a rotation of spins. The elegance of this formulation has led to the almost universal adoption of the vector representation of the order parameter for triplet superconductors. The *d* vector describes the symmetries of the superconducting state, the spin and orbital angular momentum of the

Cooper pairs, and the nodal structure of the energy gap in a remarkably compact way. In light of the subsequent interest in spin-singlet *d*-wave superconductivity, the choice of \mathbf{d} for the order parameter for spin-triplet superconductors is unfortunate. However, it is in widespread use, and is hence the nomenclature that we adopt in this article.

The gap matrix [Eq. (4.2)] has the same symmetries as the Cooper pair wave function, so the state vector $|\psi\rangle$ of a triplet superconductor can be expressed as

$$|\psi\rangle = \Delta_{\uparrow\uparrow}|\uparrow\uparrow\rangle + \Delta_{\downarrow\downarrow}|\downarrow\downarrow\rangle + \Delta_0(|\uparrow\downarrow\rangle + |\downarrow\uparrow\rangle), \quad (4.3)$$

where the bases $|\uparrow\uparrow\rangle$, $|\downarrow\downarrow\rangle$, and $(1/\sqrt{2})(|\uparrow\downarrow\rangle + |\downarrow\uparrow\rangle)$ correspond to pair spin projections $S_z = 1$, -1 , and 0 , respectively. If a new set of bases \mathbf{x} , \mathbf{y} , and \mathbf{z} is introduced such that

$$\begin{aligned} \mathbf{z} &= |S_z=0\rangle = \frac{1}{\sqrt{2}}(|\uparrow\downarrow\rangle + |\downarrow\uparrow\rangle), \\ \mathbf{x} &= |S_x=0\rangle = \frac{1}{\sqrt{2}}(-|\uparrow\uparrow\rangle + |\downarrow\downarrow\rangle), \\ \mathbf{y} &= |S_y=0\rangle = \frac{1}{\sqrt{2}}(|\uparrow\uparrow\rangle + |\downarrow\downarrow\rangle), \end{aligned} \quad (4.4)$$

the state vector $|\psi\rangle$ can be written

$$|\psi\rangle = \sqrt{2}(d_x\mathbf{x} + d_y\mathbf{y} + d_z\mathbf{z}). \quad (4.5)$$

The energy spectrum of excited quasiparticles with wave vector \mathbf{k} can be expressed in terms of \mathbf{d} as

$$E_k = \sqrt{\varepsilon_k^2 + \mathbf{d} \cdot \mathbf{d}^* \pm |\mathbf{d} \times \mathbf{d}^*|}, \quad (4.6)$$

where E_k is the energy of the quasiparticle, and ε_k is referenced to the chemical potential in the usual way (e.g., see Waldram, 1996 and footnote 4). If $|\mathbf{d} \times \mathbf{d}^*| = 0$, the state is referred to as “unitary,” and $\mathbf{d} \cdot \mathbf{d}^*$ can be simply identified with the square of the superconducting energy gap, $|\Delta(\mathbf{k})|^2$. In contrast, a nonunitary state with $\mathbf{d} \times \mathbf{d}^* \neq 0$ is composed of Cooper pairs with two distinct energy gaps. One of these gaps can even be zero, resulting in a state in which not all the electrons form Cooper pairs, even at $T=0$.

For unitary states,³² all the electrons are paired, and $\mathbf{d}(\mathbf{k})$ has immediate physical meaning. Its direction defines the normal to the plane in which the electrons paired at $(\mathbf{k}, -\mathbf{k})$ are equal spin paired ($|\uparrow\uparrow\rangle$ and $|\downarrow\downarrow\rangle$ relative to any quantization axis in that plane), and its magnitude is proportional to that of the energy gap at $(\mathbf{k}, -\mathbf{k})$.

As we discuss below, the *d* vector that has been discussed most in relation to Sr₂RuO₄ is commonly written

as $\mathbf{d} = \Delta_0 \hat{\mathbf{z}}(k_x \pm ik_y)$, retaining the notation developed for ³He. Here $\hat{\mathbf{z}}$ is a unit vector specifying a direction in spin space, and $(k_x \pm ik_y)$ provides information about the spatial part of the pair wave function. It is important to consider the consequences of a crystal lattice, and hence the extent to which such a notation is useful for Sr₂RuO₄. In the absence of a lattice, spin and orbital angular momenta are good quantum numbers, and spin and orbital spaces are decoupled, with no fixed relative direction. If lattice effects and spin-orbit coupling are too strong, there is little meaning in retaining a classification of superconducting states in terms of the orbital angular momentum of a pair wave function. In Sr₂RuO₄, however, it seems likely that these effects are sufficiently weak that the “lattice-free” nomenclature used here is still a reasonable approximation. Spin-orbit coupling is sufficiently strong to “pin” the spin axes along fixed directions relative to the lattice, but not strong enough to invalidate the idea of a pair wave function with $L=1$.³³

2. Deducing details of the superconducting state from \mathbf{d}

We now give a brief example of deducing details of the pairing state from a *d*-vector order parameter, concentrating on the example of a unitary state given above:

$$\mathbf{d} = \Delta_0 \hat{\mathbf{z}}(k_x \pm ik_y) = \Delta_0 \begin{bmatrix} 0 \\ 0 \\ k_x \pm ik_y \end{bmatrix}. \quad (4.7)$$

In the presence of a weak spin-orbit interaction, it is natural to take the *z* direction of the spin wave function along the crystalline *c* axis. As depicted by the thin arrows in Fig. 20, the $S=1$ paired spins are within the two-dimensional plane (the *ab* plane) and consist of an equally weighted superposition of $|\uparrow\uparrow\rangle$ and $|\downarrow\downarrow\rangle$ states for any quantization axis within that plane.

By definition, the orbital part of a *p*-wave state has angular momentum 1. Since the orbital wave function is expressed by the spherical harmonics

$$Y_{1\pm 1} = \left(\frac{3}{8}\pi\right)^{1/2} \sin\theta \exp(\pm i\phi) = \left(\frac{3}{8}\pi\right)^{1/2} (k_x \pm ik_y), \quad (4.8)$$

$k_x \pm ik_y$ represents the states with $L_z = \pm 1$. Thus the relative orbital motion of the electrons of a Cooper pair is either clockwise or counterclockwise. The fact that *all* the Cooper pairs within a given superconducting domain exercise the same direction of the rotation leads to broken time-reversal symmetry, which we discuss later. The thick arrows in Fig. 20 represent the state with L_z

³²Unitary states are energetically favored in weak-coupled paramagnetic superconductors in the absence of symmetry-breaking fields. A special extra mechanism would be required to produce a nonunitary state. See, for example, Sigrist and Zhitomirsky (1996); their interest and that of Machida *et al.* (1996) in nonunitary states was stimulated by early measurements showing a large residual density of states below T_c . It is now accepted that the best samples have a very small residual density of states (see Sec. V).

³³Strictly speaking, the gap functions should be modified to reflect the lattice symmetry, and $\sin k_x a$ should be used instead of k_x , etc. (see, for example, Miyake and Narikiyo, 1999 or Zhitomirsky and Rice, 2001). Since this convention has not been widely adopted in the literature, we leave it for a more rigorous treatment of the vector order parameters appropriate to Sr₂RuO₄.

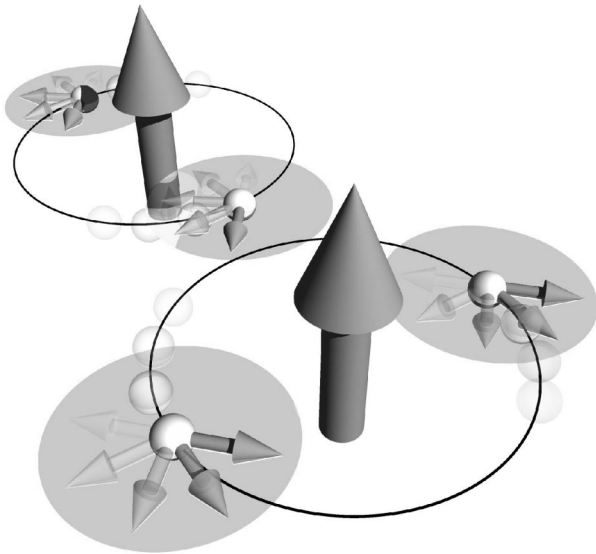


FIG. 20. Sketches of Cooper pair \mathbf{S} and \mathbf{L} vectors for the order parameter $\mathbf{d} = \Delta_0 \hat{z}(k_x \pm ik_y)$. The large arrows denote \mathbf{L} and the small arrows the spins of the electrons in a pair. We assume that weak spin-orbit coupling pins the z direction to the out-of-plane direction of a real, highly anisotropic crystal such as Sr_2RuO_4 . The spins lie in the plane, and all \mathbf{L} vectors are aligned perpendicular to the plane and parallel to one another in any domain. Time-reversal symmetry is therefore broken due to the orbital part of the wave function. In the plane, there is equal spin pairing for any quantization axis, which the series of small arrows aims to depict. This state is the two-dimensional analog of the ABM or A phase of ^3He . Image is by K. Deguchi.

$= +1$; the angular momentum vector is pointing up along the c direction. The energy gap

$$|\Delta(\mathbf{k})| = (k_x^2 + k_y^2)^{1/2} \quad (4.9)$$

is isotropic on a two-dimensional, cylindrical Fermi surface, as shown in Fig. 21. Note the difference between an s -wave gap and that sketched in Fig. 21. Although the magnitude of the gap is isotropic, its phase continuously changes with ϕ , satisfying odd parity.

If the Fermi-surface cross section is not circular, the gap is not isotropic (and functions such as those described in footnote 33 should be used). However, the simple notation of Eq. (4.7) correctly captures two of the key aspects of the superconducting state—its basic symmetries, and the fact that it is nodeless in two dimensions.

The A phase of superfluid ^3He (the ABM state) has the same \mathbf{d} vector as Eq. (4.7). We note once more, however, that superfluid ^3He does not have any crystal to fix the directions of the orbital and spin-wave functions. Also, its energy gap has point nodes at the north and south poles of the spherical Fermi surface.

3. Allowed states for Sr_2RuO_4 and spin-orbit coupling as a degeneracy breaking mechanism

We hope that the above example gives insight into decoding the physical properties of a state associated

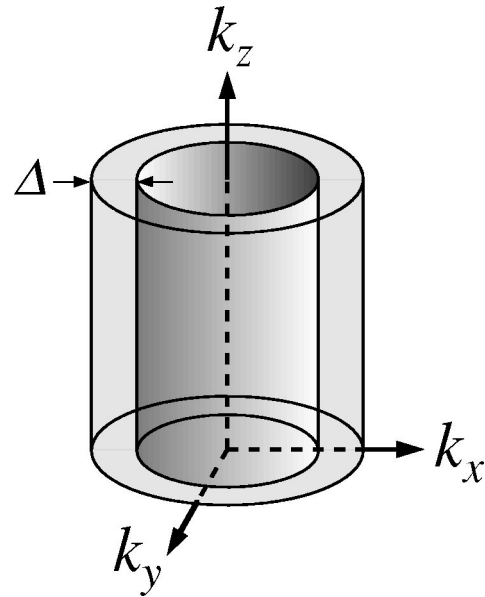


FIG. 21. The energy gap corresponding to the pair state sketched in Fig. 20, which is isotropic on a cylindrical Fermi surface of circular cross section. Image is by K. Deguchi.

with a given \mathbf{d} -vector order parameter. Although we have chosen the order parameter that has been most widely discussed in relation to Sr_2RuO_4 (see Secs. IV.B and IV.C), of course it is not the only triplet state allowed for a tetragonal material. The full list of allowed states is given in Table IV and derived in, for example, Annett (1990), Sigrist and Ueda (1991), Rice and Sigrist (1995), and Machida *et al.* (1996). For the reader interested in more detail, further analysis of three more of these is presented in Appendix D. The states analyzed there, $\Delta_0 \hat{z}k_x$, $\Delta_0(\hat{x}k_x + \hat{y}k_y)$, and $\Delta_0/2(\hat{x} + i\hat{y})(k_x + ik_y)$, have relevance either as two-dimensional analogs of states existing in ^3He or as states that might be adopted in Sr_2RuO_4 in symmetry-breaking fields.

What factors are likely to lead to one of the states in Table IV being favored in Sr_2RuO_4 ? For weak coupling and in the absence of symmetry-breaking fields, it is expected that fully gapped unitary states, if available, will give a larger condensation energy than states with nodes (Rice and Sigrist, 1995). As can be seen from Table IV, many states satisfy this requirement, and all of them are degenerate in a tetragonal crystal field. Splitting the degeneracy further involves the spin part of the wave function. One way that it can occur is through the spin-fluctuation feedback mechanism that was extensively investigated in superfluid ^3He (Leggett, 1975; Vollhardt and Wölfle, 1990). This would be expected to break the degeneracy through a second transition slightly below T_c , and the existing zero-field data give no evidence for this in Sr_2RuO_4 . The other mechanism by which spin-related degeneracy splitting can occur is through spin-orbit coupling, which can lead to a preferential plane for the long-wavelength spin fluctuations that are assumed to be relevant for p -wave pairing. These effects have been investigated by Sigrist *et al.* (1999, 2000) and Ng and Sigrist (2000). It seems likely that in Sr_2RuO_4 , suf-

TABLE IV. Allowed p -wave states on a cylindrical Fermi surface for a tetragonal crystal. References to ^3He are for the analogous three-dimensional states.

Unitary states	Δ/Δ_0	Node	Time-reversal symmetry	^3He
$\hat{\mathbf{x}}k_x + \hat{\mathbf{y}}k_y$	$\sqrt{k_x^2 + k_y^2}$			BW
$\hat{\mathbf{x}}k_y - \hat{\mathbf{y}}k_x$	$\sqrt{k_x^2 + k_y^2}$			
$\hat{\mathbf{x}}k_x - \hat{\mathbf{y}}k_y$	$\sqrt{k_x^2 + k_y^2}$			
$\hat{\mathbf{x}}k_y + \hat{\mathbf{y}}k_x$	$\sqrt{k_x^2 + k_y^2}$			
$\hat{\mathbf{z}}k_x$	$ k_x $	line		
$\hat{\mathbf{z}}(k_x + k_y)$	$ k_x + k_y $	line		
$\hat{\mathbf{z}}(k_x \pm ik_y)$	$\sqrt{k_x^2 + k_y^2}$		broken	ABM
Nonunitary states				
$\hat{\mathbf{x}}k_x + i\hat{\mathbf{y}}k_y$	$ k_x + k_y \uparrow\uparrow$		broken	
	$ k_x - k_y \downarrow\downarrow$			
$\hat{\mathbf{x}}k_y - i\hat{\mathbf{y}}k_x$	$ k_y - k_x \uparrow\uparrow$		broken	
	$ k_x + k_y \downarrow\downarrow$			
$\hat{\mathbf{x}}k_x - i\hat{\mathbf{y}}k_y$	$ k_y - k_x \uparrow\uparrow$		broken	
	$ k_x + k_y \downarrow\downarrow$			
$\hat{\mathbf{x}}k_y + i\hat{\mathbf{y}}k_x$	$ k_x + k_y \uparrow\uparrow$		broken	
	$ k_y - k_x \downarrow\downarrow$			
$(\hat{\mathbf{x}} + i\hat{\mathbf{y}})(k_x + k_y)$	$2(k_x + k_y) \uparrow\uparrow$	line	broken	
	$0 \downarrow\downarrow$			
$(\hat{\mathbf{x}} + i\hat{\mathbf{y}})(k_x + ik_y)$	$2\sqrt{k_x^2 + k_y^2} \uparrow\uparrow$		broken	A1
	$0 \downarrow\downarrow$			

ficient degeneracy splitting will exist to favor one state, but that others are sufficiently close in energy that it may be possible to access them by the application of symmetry-breaking fields.

B. The spin part of the pair wave function of Sr_2RuO_4 from the Knight shift and spin-polarized neutron scattering

We are now in position to discuss the implications of the spin susceptibility measurements of Ishida and co-workers (1998) and Duffy *et al.* (2000) that we introduced in Sec. III.E. If there is sufficient spin-orbit coupling to pin the d vector, then the spin susceptibility for low applied magnetic fields can often identify its direction. If \mathbf{d} has a unique direction in the crystal [as is the case for $\Delta_0 z k_x$, $\Delta_0 z(k_x + k_y)$, or $\Delta_0 z(k_x \pm ik_y)$ from Table IV] then the spin susceptibility is expected to show no change for applied fields perpendicular to \mathbf{d} . This is because the Cooper pairs in the plane of the applied field consist of equal spin pairs and, as discussed in Sec. III.E, these can still form if the Fermi surface is polarized by Zeeman splitting. For applied fields along \mathbf{d} , the opposite is true. The superconducting condensation fixes the spins to lie in the plane perpendicular to the applied magnetic field, and so they cannot polarize along the field direction, and a full Yosida function behavior is expected (Yosida, 1958). If the \mathbf{k} dependence of \mathbf{d} is such that its direction is not uniform for all \mathbf{k} , then the susceptibility will follow a partial Yosida function, falling to one-half of its normal-state value for fields ap-

plied in the ab plane for a two-dimensional state such as $\Delta_0(xk_x + yk_y)$ from Table IV.³⁴

The observation that the Knight shift remains unchanged through T_c for fields applied in the ab plane of Sr_2RuO_4 implies, therefore, that the superconducting state is described by a uniform direction of \mathbf{d} , pointing along the c axis of the crystal. If there were no spin-orbit coupling, the measurements would only imply a uniform direction of \mathbf{d} without specifying that direction in relation to the crystal axes, because the desire of the spins to align along the field direction would rotate \mathbf{d} to lie perpendicular to the applied field. To date, there is no real proof that \mathbf{d} is pinned along c in Sr_2RuO_4 , but it seems likely that there will be sufficient spin-orbit coupling to ensure that this is the case.

The best way to confirm the pinning of \mathbf{d} to c would be to devise an experiment capable of studying the spin susceptibility for fields applied along c . This is not easy by NMR, however. The difficulty is the strong anisotropy of the superconductivity. The need to work at applied magnetic fields a factor of 20 smaller than for $B\parallel ab$ could, in principle, be overcome by the development of even higher sensitivity spectrometers. A more serious problem is the low value of κ for $B\parallel c$. Estim-

³⁴For the three-dimensional equivalent of state listed at the top, the B phase of ^3He , $\mathbf{d} = \Delta_0(\hat{\mathbf{x}}k_x + \hat{\mathbf{y}}k_y + \hat{\mathbf{z}}k_z)$ and the spin susceptibility falls to two-thirds of its normal-state value for any direction of the applied field.

ing the scale of the Meissner effect using Eq. (3.6) shows that it would lead to shifts and broadening of the NMR lines which would be over an order of magnitude *larger* than the scale of K_{spin} . Nevertheless, the shift of the line position may still be detectable with sufficient accuracy, especially because the vortex pinning in high-quality Sr_2RuO_4 is rather weak. We note in passing that the G-L parameters for $B\parallel c$ present no particular barrier to further polarized neutron studies. In contrast to the Knight shift, the neutron measurement obtains information from very short wavelengths, and so is insensitive to the long-wavelength variation of the field profile of the vortex lattice. More work in this area would be desirable.³⁵

C. Time-reversal symmetry breaking probed by muon spin rotation and neutron studies of the flux lattice

As discussed above, some of the possible triplet states for Sr_2RuO_4 break time-reversal symmetry (TRS), since the condensate has an overall magnetic moment because of either the spin or orbital (or both) parts of the pair wave function. At first sight, this might be expected to lead to a large spontaneous magnetic moment appearing at T_c . In fact, TRS-breaking superconductors must still have a Meissner effect, and so compensating screening currents may be set up to ensure that $B=0$ in the bulk of the sample. In addition to this, there is likely to be domain formation, analogous to that seen in ferromagnets. Although these effects mean that no large moment is to be expected, the sample will always contain surfaces and defects at which the Meissner screening of the TRS-breaking moment is not perfect, and a small magnetic signal is expected due to these [see Sigrist and Ueda (1991), and references therein].

1. Muon spin rotation

In light of the discussion above, a search for TRS breaking in superconductors requires a sensitive local probe of the magnetic-field distribution in a solid. In recent years, muon spin relaxation (μSR) has been developed into a technique providing this kind of information (see, for example, Brewer, 1994). In μSR , fully spin-polarized positive muons are incident on a specimen at a sufficiently low flux that they arrive individually on the scale of their decay time ($\sim 2.2 \mu\text{s}$). They come to rest very quickly, and their spins react to the local magnetic environment at the implantation site. When they decay, a positron is emitted in a direction that correlates with the spin direction of the muon at the time of decay. By studying many such positrons, one can deduce the muon polarization function as a function of time after implantation. The form of this function yields considerable information about the local magnetic-field distribution in the solid.

³⁵We are grateful to E.M. Forgan for pointing out the significance of the value of the Ginzburg-Landau κ for various methods of measuring the spin susceptibility.

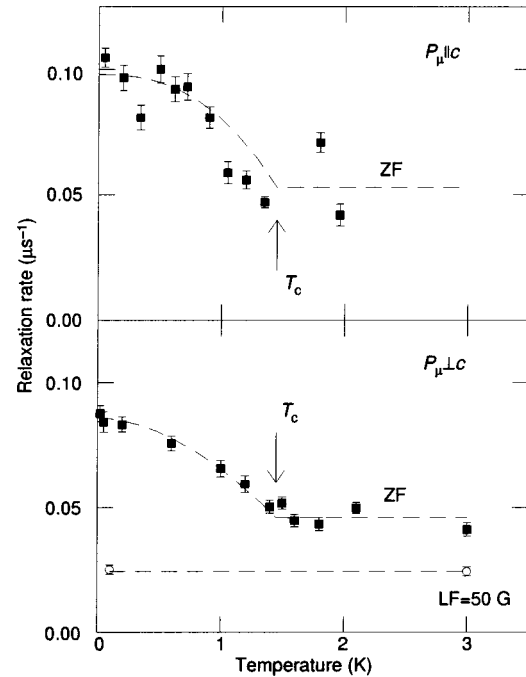


FIG. 22. The muon spin-relaxation rate shows a change on cooling Sr_2RuO_4 through T_c even in zero applied magnetic field, for muons polarized both parallel and perpendicular to the Ru-O planes. The result suggests the development of spontaneous magnetic fields, and gives evidence for a time-reversal symmetry-breaking superconducting state. The open symbols for $P_{\mu}\perp c$ demonstrate the suppression of the extra relaxation in a longitudinal field of 50 G, described in the main text. From Luke *et al.* (1998).

The first study of μSR in Sr_2RuO_4 was reported by Luke and co-workers (1998). In addition to the standard relaxation caused by the dense array of randomly oriented nuclear dipole moments, they observed a spontaneous extra relaxation of the spin-polarization function at the superconducting transition temperature. This extra relaxation is suppressed by the application of a small longitudinal field, indicating that its cause is static on the μs time scale. Furthermore, the fact that it can be best modeled by an exponential indicates that its source is a broad distribution of internal fields from a dilute array of sources. If it had been due to either a dense array of sources or to a unique field at every muon site, a Gaussian relaxation would have been observed. The temperature dependence of the relaxation is shown in Fig. 22. The first experiment was performed on very high quality crystals with $T_c > 1.4$ K. In principle, the extra relaxation could have had some magnetic origin which occurs coincidentally at approximately this temperature. In subsequent work, however, the same group has shown that the spontaneous extra relaxation tracks T_c in poorer samples with T_c as low as 0.7 K (Luke *et al.*, 2000), leaving little doubt that it is an intrinsic feature of the superconductivity.

Luke and co-workers interpreted their results as measurements of the spontaneous fields generated by supercurrents associated with variation of the superconducting order parameter near dilute imperfections in the

material. The locality of the probe makes μSR ideal for their detection, and the fact that the internal fields appear in zero applied field is indicative of broken TRS. Possible sources of these local imperfections are dilute impurities, the muon itself, or the walls of domains in which the TRS-breaking Cooper pair moments are counteroriented. The measured internal field (which is not easy to calculate) is estimated to be 0.5 G, a similar magnitude to that previously observed by the same group in the B phase of UPt_3 (Luke *et al.*, 1993).³⁶

Although, strictly speaking, TRS breaking is not the only possible explanation for the μSR observations, it seems to be the most likely one. As we discuss in Sec. IV.C.3, the existence of TRS breaking has considerable implications for understanding the superconductivity of Sr_2RuO_4 , and the findings of Luke and co-workers are among the most important in the field. It is important, therefore, that they be confirmed by other techniques. One piece of corroborating evidence has come from study and analysis of vortex physics in Sr_2RuO_4 .

2. Magnetic-field distribution of the vortex lattice

Since the work of Abrikosov over 40 years ago, it has been known that if fields higher than the lower critical field are applied to a type-II superconductor, flux penetrates in quantized units surrounded by flowing supercurrents, which are usually referred to as vortices. In the absence of pinning defects, the vortices will arrange in a regular lattice. In Abrikosov's original paper, a square lattice was predicted for an isotropic s -wave superconductor, but it was quickly realized that this was due to a minor numerical error, and that a triangular or hexagonal lattice is the most stable solution. This illustrates an important point about the physics of the vortices; vortex lattice symmetry has no fundamental relationship with the underlying symmetry of the order parameter. Indeed square lattices have been predicted and observed in conventional s -wave superconductors under certain special circumstances (Obst, 1969). Nevertheless, qualitative differences in vortex behavior are expected to exist in superconductors with unconventional order parameters, and several explicit predictions have been made concerning Sr_2RuO_4 . In the spirit of this article, we will concentrate on the aspects of the vortex physics for which experimental investigations have been performed. As we shall see, it turns out that one of these gives supporting evidence for the existence of a TRS-breaking order parameter.

Recent theoretical work has shown that one way in which square rather than hexagonal lattices can occur is through nonlocal effects in London or Ginzburg-Landau

³⁶The observation in UPt_3 was not confirmed in subsequent experiments by another group (Dereotier *et al.*, 1995). In Sr_2RuO_4 , more consistency exists; other groups working at a different muon source have confirmed the result of Luke *et al.* (1998) (Forgan, 2000; Higemoto, 2002).

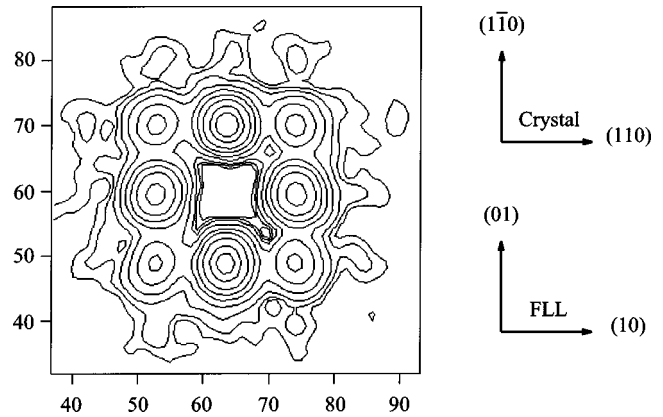


FIG. 23. The diffraction pattern obtained from small-angle neutron scattering from the flux lattice of Sr_2RuO_4 is square for all fields and temperatures at which it can be observed (from Kealey *et al.*, 2000).

treatments, combined with Fermi-surface anisotropy.³⁷ These effects, which apply to standard superconductors with single-component order parameters, lead to the prediction of hexagonal-to-square crossovers and transitions in the H - T phase diagram, and are thought to account satisfactorily for the behavior observed in the borocarbide superconductors (see, for example, Paul *et al.*, 1998). A notable feature of such approaches is the appearance of hexagonal lattices for applied fields near H_{c2} , when the nonlocal effects become less important.

It has recently been realized, however, that there is another scenario in which a square or rectangular solution is more stable. A TRS-breaking state (sometimes also referred to as a “chiral” state) requires the use of a two-component order parameter in Ginzburg-Landau treatments. The consequences of this have been explored in a series of papers by Agterberg and others.³⁸ The first result to emerge is that square or rectangular lattices are expected to be favored over the entire H - T plane in the presence of physically reasonable values of Fermi-surface anisotropy. In a series of measurements that were independent of the above theoretical work, Forgan and collaborators (Riseman *et al.*, 1998; Kealey *et al.*, 2000) observed a square flux lattice by small-angle neutron scattering, as shown in Fig. 23.³⁹ A square lattice was also deduced from studies of muon spin rotation (Aegerter *et al.*, 1998; Luke *et al.*, 2000), but the neutron work established the important fact that *only* square lattices were observed whenever ordered vortices were detected.

³⁷See, for example, de Wilde *et al.* (1997); Kogan *et al.* (1997); Shiraishi and Maki (1999); Wang and Maki (1999).

³⁸For example, see Zhu *et al.* (1997); Agterberg (1998a, 1998b, 2001); Heeb and Agterberg (1999); Kita (1999); Sigrist and Agterberg (1999); Takigawa *et al.* (2002).

³⁹Note the correction of an error in Riseman *et al.* (1998) concerning the orientation of the vortex and crystal lattices [Riseman *et al.*, *Nature* (London) **404**, 629 (2000)]. The correct orientation is shown in Fig. 23.

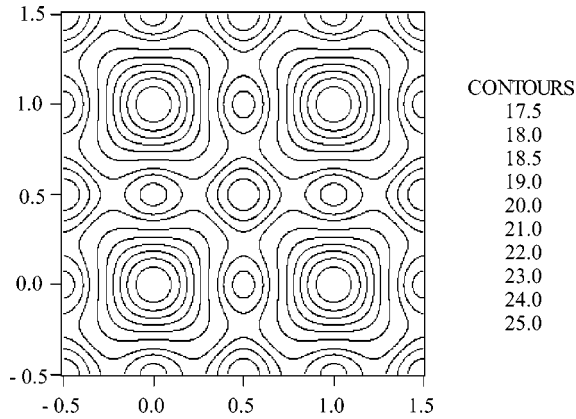


FIG. 24. The magnetic-field distribution in the vortex lattice of Sr₂RuO₄, deduced from Fourier analysis of small-angle neutron-scattering data like those shown in Fig. 23. The existence of field minima between vortices along the (10) direction is predicted by a two-component Ginzburg-Landau treatment. Although a square lattice can be obtained under some assumptions using a single-component Ginzburg-Landau theory, the prediction for its constituent field distribution would be qualitatively different, with saddle points rather than minima in the (10) direction. The contours are magnetic field in mT (from Kealey *et al.*, 2000).

Although the observation of a square lattice gives tentative support for TRS breaking, it could always be argued that similar behavior could be obtained within a treatment based on a single-component order parameter at certain levels of Fermi-surface anisotropy. More persuasive evidence is provided from using the neutron data to deduce the real-space field distribution in the vortex lattice (Kealey *et al.*, 2000). Single- and two-component G-L treatments lead to qualitatively different predictions for the form of this distribution, even when the single-component theory predicts a square lattice. The two-component theory predicts a field minimum rather than a saddle point between the vortices in the (10) direction. As shown in Fig. 24, the experimental data show such a field minimum. They therefore favor the use of the two-component treatment that is a necessary consequence of a TRS-breaking state. In this sense the neutron-scattering studies can be interpreted as providing independent support for the conclusions drawn from the muon spin rotation study of Luke *et al.* (1998, 2000).

3. Implications of TRS breaking at T_c

The evidence that time-reversal symmetry is broken in the superconducting state of Sr₂RuO₄ has important implications. First, it means that of the simplest unitary p -wave states listed in Table IV, only $\mathbf{d}=\hat{\mathbf{z}}(k_x \pm ik_y)$ is consistent with the experimental data provided by NMR, polarized neutron scattering, muon spin rotation, and small-angle neutron scattering.

The second implication of TRS breaking at T_c in a tetragonal material such as Sr₂RuO₄ has a broader significance. On the assumption that the basic pairing

mechanism is in plane, a time-reversal symmetry-breaking d state would have to be an admixture of the form $d_{x^2-y^2} + id_{xy}$ (where these are now d -wave singlet order parameters). In contrast to the p -wave case, the two components of the order parameter have different symmetry-breaking properties, and are not degenerate in a tetragonal crystal field. Thus the time-reversal symmetry-broken state would be entered as a second transition well below T_c . Such a transition has been discussed in the cuprates (for example, see Movshovich, 1998, and references therein).

We regard this as an important point. It means that a nontriplet interpretation for the superconductivity of Sr₂RuO₄ would probably require reversing the conclusions drawn from *four* key independent experiments (Ishida *et al.*, 1998; Luke *et al.*, 1998; Duffy *et al.*, 2000; Kealey *et al.*, 2000).⁴⁰ Instead, the bulk of the currently available evidence points to a triplet order parameter of some kind incorporating TRS breaking as the correct description of the unconventional superconductivity of Sr₂RuO₄.

V. STRUCTURE OF THE SUPERCONDUCTING GAP

We hope that the discussion in Secs. III and IV has successfully conveyed to the reader the main pieces of experimental evidence that point to Sr₂RuO₄ being a triplet superconductor. In this section, we will address the issue of the structure of the superconducting gap, and how it relates to the symmetry constraints imposed by the results discussed previously. Some of the individual experiments that we will discuss are sufficiently complex and difficult to interpret that their conclusions await confirmation; but we believe that a picture of overall consistency is emerging.

A. Evidence for a T -linear quasiparticle density deep in the superconducting state

As shown in Table IV and Sec. IV.A.2, the $\mathbf{d}=\Delta_0\hat{\mathbf{z}}(k_x \pm ik_y)$ state that is strongly suggested by the experiments reviewed in Sec. IV would lead to an energy gap $|\Delta(\mathbf{k})|=(\mathbf{d}\cdot\mathbf{d}^*)=\Delta_0(k_x^2+k_y^2)^{1/2}$. This gives an isotropic energy gap on a two-dimensional Fermi surface in a material with a simple isotropic Fermi surface and pairing interaction. Since Sr₂RuO₄ is a weakly coupled superconductor ($T_c \ll E_F$), the general BCS framework is likely to be applicable, in the sense that a BCS-like gap equation should be obeyed. As shown in Fig. 25, this has the well-known consequence that $\Delta(T)$ is, to a good approximation, fully developed for $T/T_c < 0.4$. The full gapping of the simplest $\mathbf{d}=\Delta_0\hat{\mathbf{z}}(k_x \pm ik_y)$ triplet state

⁴⁰A single d -wave state breaking TRS at T_c can occur in a tetragonal material for interplane Cooper pairing. If such an assumption could be justified, the resultant state would be consistent with the findings of Luke *et al.* (1998) and Kealey *et al.* (2000). It could not, however, be compatible with the conclusions drawn by Ishida *et al.* (1998) or Duffy *et al.* (2000).

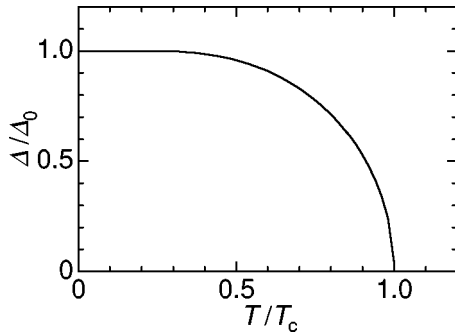


FIG. 25. The temperature dependence of the energy gap predicted by the BCS weak-coupling theory. The essentially full development of this gap below approximately $T_c/4$ means that in the low-temperature limit, the number of thermally excited quasiparticles falls exponentially to zero. In a weak-coupling superconductor with nodes in the gap, qualitatively the same temperature dependence would apply for the gap maximum, but the existence of the gap zeros would lead to more quasiparticle excitation at low temperatures. In this case power-law temperature dependencies would be expected for experiments sensitive to the number of thermally excited quasiparticles.

would then make it thermodynamically indistinguishable from the BCS s -wave state at low temperatures.⁴¹ The main feature of note is that any quantity sensitive to either the number density of thermally excited quasiparticles or the quasiparticle density of states would be expected to become exponentially small for $T \ll T_c$. The BCS predictions for the specific heat, NMR relaxation, ultrasonic attenuation, London penetration depth, and thermal conductivity are discussed in detail in textbooks by Tinkham (1996) and Waldram (1996).

If, on the other hand, the gap in Sr_2RuO_4 contained nodes, the thermodynamics would show quite different behavior. The *average* gap would still have a temperature dependence similar to that of Fig. 25, since the weak-coupling BCS framework would still apply. However, the presence of nodes would allow thermal excitation of quasiparticles down to low temperatures. It is now well established (see, for example, Hardy *et al.*, 1993) that this would be expected to lead to the appearance of power laws rather than exponential behavior for $T \ll T_c$.

Studies of all the properties discussed above have now been performed on Sr_2RuO_4 . It is clear that simple isotropic gapping does not take place, and there seems to be good (although not perfect or complete) evidence for nodes of some kind. It is obviously of crucial importance to establish not just the presence of nodes, but also their position on the Fermi surface, especially since the thermodynamic results have stimulated a large number of ingenious theoretical proposals. Some of the available probes can, in principle, give position-sensitive information, but there are subtleties. In this subsection, let us first review the available experimental data.

⁴¹It would, of course, differ from the BCS s -wave state in many other observables, as discussed in Secs. III and IV.

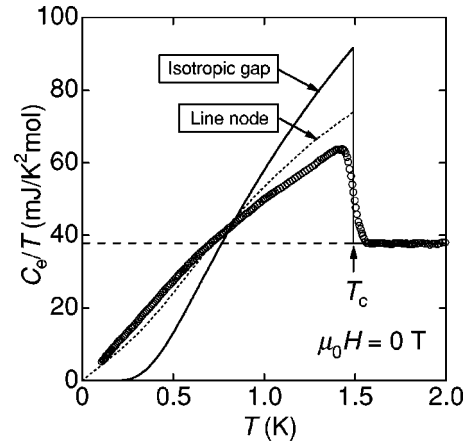


FIG. 26. The electronic specific heat at constant pressure of a very high quality sample of Sr_2RuO_4 with $T_c = 1.48$ K, divided by T . C_e varies linearly with temperature over a large range from 100 mK to above 0.5 K. Also shown are the predictions of weak-coupling theory for a full energy gap (solid line) and a gap with vertical line nodes on a cylindrical Fermi surface (dotted line). Although the latter is a closer match to the data, the fit is far from perfect. Figure after Nishizaki *et al.* (1999).

1. Specific heat

Perhaps the most direct experimental probe of the thermodynamic states in a superconductor is the electronic specific heat at constant pressure (C_e), since it is directly connected with the entropy by the relation:

$$S(T) = \int_0^T \frac{C_e(T') dT'}{T'}. \quad (5.1)$$

The isotropic energy gap $|\Delta(k)| = \Delta_0(k_x^2 + k_y^2)^{1/2}$ will give the same quasiparticle density of states as in an isotropic s -wave superconductor. The magnitude of the specific-heat jump at T_c is $\Delta C_e / \gamma_N T_c = 1.43$ in the weak-coupling limit, where γ_N is the normal-state value of C_e/T , and C_e should decay exponentially to zero at low temperatures.

Early measurements of C_e (Nishizaki *et al.*, 1998) were reviewed in Sec. III, but interpretation of these was complicated by the existence of non-negligible impurity scattering. In fact, the zero-energy density of states deduced from the residual value of C_e/T extrapolated to $T=0$ K was found to decrease systematically with increasing T_c (Nishizaki *et al.*, 1999). Later, Nishizaki and collaborators (Nishizaki *et al.*, 2000) reported the results of a lengthy study of C_e on clean limit crystals with $T_c = 1.48$ K under controlled magnetic fields. Their results in zero applied magnetic field are shown in Fig. 26: C_e/T extrapolates to a value very close to zero and varies linearly with T over a surprisingly wide range of temperatures between 0.1 and 0.5 K, with no sign of an exponential temperature dependence.

At first sight, this power-law behavior of the density of states is strongly suggestive of a gap function with line nodes, but a more careful analysis shows that the data are not fully consistent with this hypothesis either. Since Sr_2RuO_4 is a superconductor with a very low T_c and

long coherence length, it is reasonable to use weak-coupling expressions to model the expected behavior of C_e . The standard formalism for doing so for different nodal structures of the energy gap is given in, for example, Hasselbach *et al.* (1993). Figure 26 shows the fully modeled temperature dependencies for two simple states—an isotropic gap and a gap with vertical line nodes on a single cylindrical Fermi surface. The data are clearly very different from those expected in the case of a single isotropic gap. They more closely resemble the prediction for the gap with line nodes, but the agreement is far from perfect. For example, the normalized jump at T_c is given by $\Delta C_e / \gamma_N T_c$, where γ_N is the normal-state value of C_e / T . Experimentally, this is 0.74 ± 0.02 , compared with predicted values of 1.43 for a full and isotropic gap or 0.95 for vertical line nodes on a simple cylindrical Fermi surface (Maki and Won, 1996; Nishizaki, 1999). A more striking deviation from the simple line node prediction is the very large range of temperature over which an approximately T linear C_e / T is seen. We shall return to this point later.

Single-crystal specific-heat work has also been reported on Sr_2RuO_4 by Langhammer *et al.* (2002). The T_c of their samples was lower than those of the best samples studied by Nishizaki *et al.* (2000), but they stressed various concerns about background subtraction in low-temperature specific-heat studies of Sr_2RuO_4 . Background subtraction was indeed necessary in obtaining the data shown here in Fig. 26, but as we shall discuss below, the basic conclusion of a linear-temperature variation of C_e / T is supported by other experiments.

2. NMR/NQR relaxation rate

Nuclear spin relaxation due to interaction with quasiparticles has played a key role in the history of superconductivity. A peak in the nuclear spin-relaxation rate $1/T_1$ just below T_c was predicted by the BCS theory of s -wave superconductors, and its observation by Hebel and Slichter (1957) was a major step in the verification of the theory (see, for example, the discussion in Tinkham, 1996). As mentioned in Sec. III.A, the observation by Ishida *et al.* (1997) that the Hebel-Slichter peak is absent in Sr_2RuO_4 was one of the first clear pieces of evidence for non- s -wave superconductivity.

The nuclear spin-relaxation rate also gives valuable information about the quasiparticle density well below T_c . For a standard metal, with a temperature-independent quasiparticle density, $1/T_1$ obeys the well-known Korringa law ($1/T_1 \sim T$). If, on the other hand, the quasiparticle density has a linear dependence on temperature, $1/T_1$ is expected to vary as T^3 (see, for example, Kohori *et al.*, 1988). In early samples of Sr_2RuO_4 with strong impurity pair breaking, Korringa-like behavior reappeared below T_c (Ishida *et al.*, 1997). In high quality samples with negligible pair breaking, $1/T$ is completely different, and a good agreement with T^3 is seen all the way down to 100 mK, as shown in Fig. 27 (Ishida *et al.*, 2000). This result is therefore completely consistent with the specific-heat data of Nishizaki

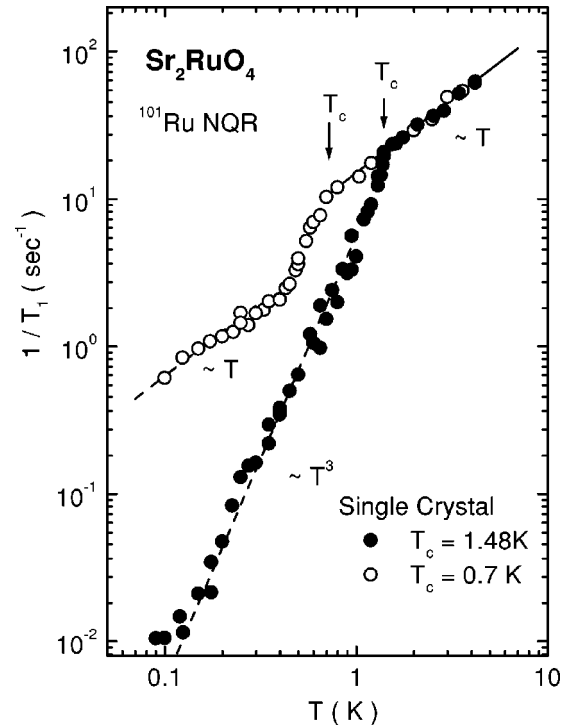


FIG. 27. The nuclear spin-relaxation rate $1/T_1$ in the normal and superconducting states of pure ($T_c = 1.48$ K) and impure ($T_c = 0.7$ K) samples of Sr_2RuO_4 , from Ishida *et al.* (2000). In the impure sample, impurity scattering is the dominant source of quasiparticles at low T , and a linear variation of $1/T_1$ is observed. In the pure sample, thermal excitation dominates, and the cubic variation of $1/T_1$ is fully consistent with the linear variation of C_e / T (see text).

et al. (2000). Similar T^3 variation of $1/T_1$ has also previously been reported in other unconventional superconductors such as UPt_3 (Kohori *et al.*, 1988) and the cuprates.

3. Penetration depth

We continue with discussion of a quantity that yielded profound information about the unconventional superconductivity of the cuprates, the London penetration depth λ_L , which is related to the superfluid density n_s by

$$\frac{1}{\lambda_L^2(T)} = \frac{\mu_0 n_s e^2}{m^*}, \quad (5.2)$$

where m^* is the carrier effective mass. Generalization to a multiband situation is given in Eq. (3.4).

In a standard BCS s -wave state, n_s is essentially fully developed at low temperatures, so $\Delta\lambda_L = \lambda_L(T) - \lambda_L(0)$ is expected to vary exponentially. The observation by Hardy *et al.* (1993) of a linear dependence of $\Delta\lambda_L$ in clean $\text{YBa}_2\text{Cu}_3\text{O}_7$ was, in the eyes of many, the first convincing evidence for nodes in the gap in the cuprates.

In Sr_2RuO_4 , λ_L has been studied by a number of groups. Issues relating to $\lambda_L(0)$ were discussed in Sec. III.C; here we review studies of its temperature depen-

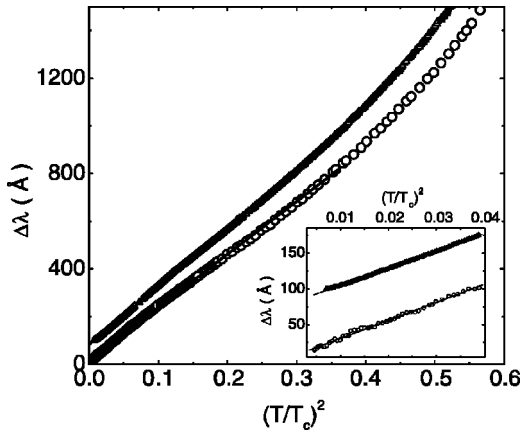


FIG. 28. The T^2 variation of the penetration depth measured at radio frequencies by Bonalde *et al.* (2000). Data are shown from two samples, with $T_c = 1.44$ and 1.39 K, respectively, and the traces have been shifted for clarity. The inset shows the low-temperature region below 0.2 K.

dence. The most complete report so far has come from Bonalde *et al.* (2000), who worked at radio frequencies. Their data for $\lambda_L^2(0)/\lambda_L^2(T)$ are shown in Fig. 28, along with various theoretical fits as described in the caption. Their key experimental observation is that of a T^2 dependence of $\Delta\lambda_L$ at low T in samples with T_c of 1.39 and 1.44 K. This basic conclusion was also reached by Hein *et al.* (2001a), who reported a microwave study.

The simplest expectation for $\Delta\lambda_L$ if a superconductor has line nodes and a two-dimensional Fermi surface is a linear- T dependence (for example, see Hardy *et al.*, 1993). In the cuprates, T^2 is sometimes observed in disordered samples. Both Bonalde *et al.* and Hein *et al.* point out that their data seem to be incompatible with theories of line nodes plus disorder. On the contrary, it is likely that extreme clean limit and nonlocal effects are important, something which is also discussed in some detail by Hein *et al.* (2001b).

A further issue has been raised by Morinari and Sigrist (2000), who have pointed out that for chiral superconductors, a T^2 dependence would be observed for a surface measurement of λ_L even for a superconductor whose energy gap contains no nodes. A bulk measurement on the same sample could then give a different result, i.e., exponential behavior. As discussed in Sec. IV, there is good evidence for a chiral state in Sr_2RuO_4 , and Luke *et al.* (2000) have reported something looking more exponential for $\lambda_L(T)$ on the basis of a muon spin rotation study. The data are of lower resolution than those of Fig. 28, but they were obtained from the bulk (via the vortex lattice) rather than the surface. Higher-resolution bulk $\lambda_L(T)$ data are clearly desirable to clarify the situation.

The work so far has shown that the London penetration depth in Sr_2RuO_4 contains some rich physics. However, it seems fair to comment that due to some special features of the superconducting state, a number of complications of interpretation exist in Sr_2RuO_4 that did not

exist in the cuprates. Consequently, the information obtained to date about nodal structure is somewhat less definitive.

4. Thermal conductivity in zero applied magnetic field

Thermal conductivity is experimentally defined as the ratio of the temperature gradient to the heat current passing through the sample: $\kappa = (P/A)/|\nabla T|$, where P/A is the heat current per unit area. Formal expressions are derived for κ due to electrons and phonons in Ziman's classic text (1960), but as he points out, a simple, useful, and physically transparent formula results from treating the problem with kinetic theory. In this approximation

$$\kappa = (1/3)Cv\ell, \quad (5.3)$$

where C is the specific heat of the particles carrying heat, v is their velocity, and ℓ is their mean free path. This formula gives the essential contributions to thermal conductivity regardless of the relevant particles. For thermal conduction by electronic quasiparticles, the specific heat is C_e and the velocity is the Fermi velocity v_F ; the phononic contribution would be estimated by using C_{ph} and the average phonon velocity.

In real materials, the presence of multiple bands and anisotropy complicates the interpretation of thermal conductivity, but there are limiting situations in which important information can be extracted. If the thermal conduction is dominated by quasiparticles, and we are at sufficiently low temperature that the scattering of quasiparticles is dominated by impurities, rather than by other quasiparticles or phonons, ℓ is independent of temperature. In this limit, κ varies according to the temperature dependence of the quasiparticle specific heat. Thus, κ provides important alternative information on the superconducting gap structure. In the first instance, we consider the information that it can give on the temperature dependence of the specific heat with no applied field. We will then discuss two experiments that have profited from the tensor nature of κ to combine thermal-conductivity measurements with applied magnetic fields to obtain direction-sensitive information.

As mentioned in Sec. III, the first measurements of κ in Sr_2RuO_4 were reported by Suderow *et al.* (1998). They established that the thermal conductivity in the superconducting state was dominated by a quasiparticle contribution, but obtained data only from samples with strong impurity pair breaking. Work on high quality samples with negligible impurity pair breaking was reported later by Izawa *et al.* (2001); Tanatar, Nagai, *et al.* (2001); and Tanatar, Suzuki, *et al.* (2001). The results agree closely, and are summarized in Fig. 29. As seen in the figure, κ/T has a linear- T variation, extrapolating close to zero. Again, this is in qualitative agreement with the results of direct measurements of C_e/T discussed above. Above T_c , κ/T is temperature independent, and its value is accurately predicted using the Wiedemann-Franz law and resistivity measurements on the same

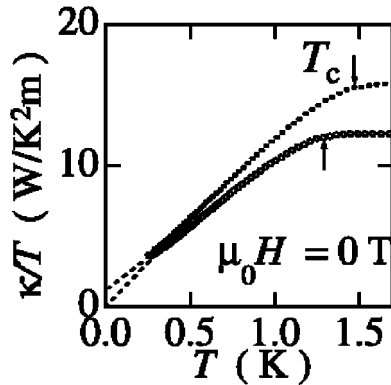


FIG. 29. The in-plane thermal conductivity κ divided by T shows a linear temperature dependence. Since κ is dominated by the same quasiparticles as C_e/T , this result, like that for nuclear relaxation shown in Fig. 27, adds to the consistent picture that has emerged for the temperature dependence of thermally excited quasiparticles in Sr₂RuO₄. The thermal-conductivity result was obtained independently by Izawa *et al.* (2001) and Tanatar, Nagai, *et al.* (2001); the data shown are from the latter paper, for two samples with slightly different values of T_c .

sample. This is good evidence that over the whole temperature range of Fig. 29, the thermal conductivity is dominated by the quasiparticle contribution.

B. The issue of gap nodes and their position

When the thermal conductivity and electronic specific-heat measurements are coupled with the NQR results, a consistent overall experimental picture emerges. The quasiparticle density of states in Sr₂RuO₄ varies linearly in temperature from $T \approx T_c/2$ to at least as low as 100 mK. This dependence is very different from that expected for a fully and isotropically gapped Fermi surface, and the observation raises at least two important questions. Does the gap function of Sr₂RuO₄ contain nodes, and if so, what kind are they? Most of the papers referenced above assumed that the existence of nodes was already settled. With such strong evidence for a simple power-law dependence of the quasiparticle density, it is certainly tempting to postulate nodes of some kind. However, some caution is still appropriate. As seen in Fig. 26, simple vertical line nodes on a cylindrical Fermi surface are consistent with the appearance of a T -linear quasiparticle density at very low reduced temperatures. The observations on Sr₂RuO₄ discussed so far show it occurring at remarkably high temperatures, and do not extend to the very low-temperature region where the prediction is most robust.⁴²

Another feature of the experiments reviewed above is that they were primarily sensitive to the existence of

quasiparticles in the superconducting state, rather than to the regions of \mathbf{k} space in which they are being excited. If there are nodes, it is crucially important to identify their type and position. With this in mind, we now review several thermal-conductivity and ultrasound experiments that should have sensitivity to the position of vertical line nodes on a cylindrical Fermi surface. The ultrasound work had the additional advantage of going to lower temperatures than have so far been reached using the other techniques.

1. In-plane quasiparticle thermal conductivity in applied magnetic fields

The “standard” way in which thermal conductivity has been used as a directional probe of nodal structure in superconductors has involved varying a combination of directions of heat current and magnetic field, and probing the quasiparticle heat current. This approach has yielded information about heavy-fermion superconductors such as UPt₃,⁴³ and, notably, line nodes in the d -wave state of the cuprates (e.g., see Aubin *et al.*, 1997).

In Sr₂RuO₄, the in-plane thermal conductivity κ_{ab} is dominated by quasiparticles below 2 K, as seen in Fig. 29, and it has been adopted as a directional probe by Izawa *et al.* (2001); Tanatar, Nagai, *et al.* (2001); and Tanatar, Suzuki, *et al.* (2001). In the experiment by Izawa *et al.*, the in-plane thermal conductivities with the heat current along the [110] and [100] directions were measured with the magnetic field rotating within the layer. The largest anisotropy observed was twofold, but by repeating for both directions of heat current, they could show that this was dominated by differences due to the quasiparticles moving parallel or perpendicular to the vortices. Superimposed on this twofold anisotropy, a small fourfold anisotropy of less than 0.3% was extracted, as shown in Fig. 30. For several reasons, the authors argued that there is little reason to associate this fourfold term with nodes either. Empirically, it is much smaller as a fraction of the total quasiparticle conductivity than the effect seen in YBa₂Cu₃O₇. It is also approximately a factor of 20 weaker than the predictions of some recent calculations for the expected effect of vertical nodes by Dahm *et al.* (2002). Finally, and perhaps most persuasively, a fourfold anisotropy of this magnitude can be estimated taking into account the much larger anisotropy of H_{c2} (which was first measured by Mao *et al.*, 2000). The observed fourfold anisotropy seems to be mainly due to the tetragonal band structure rather than to line nodes.

The studies by Tanatar and co-workers (2001) gave results for the in-plane anisotropy of the quasiparticle thermal conductivity that are in agreement with those of

⁴²The rf study of Bonalde *et al.* (2000) shows that the surface penetration depth varies as T^2 down to 50 mK, but, as discussed in Sec. V.A.3 above, special care needs to be taken when interpreting penetration depth measurements on Sr₂RuO₄.

⁴³See, e.g., Suderow, Aubin, *et al.* (1997); Suderow, Brison, *et al.* (1997); Suderow *et al.* (1998).

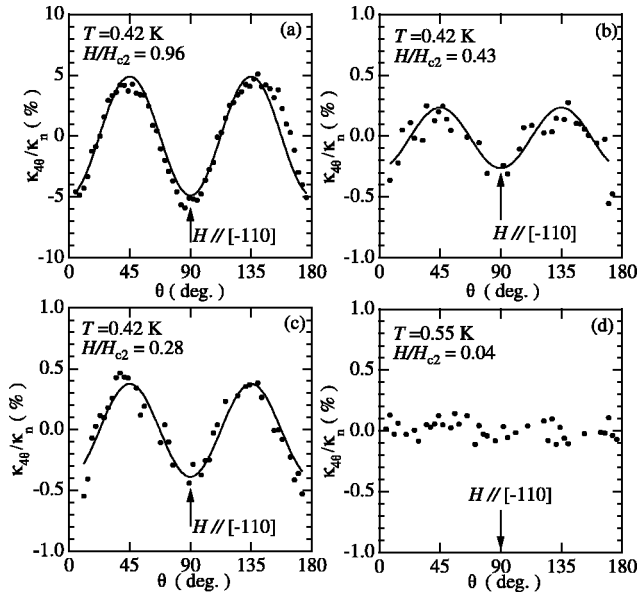


FIG. 30. In addition to the twofold term discussed in the text, a small fourfold term can be extracted from the in-plane thermal conductivity. The data shown are from the $T_c = 1.45$ K sample used by Izawa *et al.* (2001), with the heat current along $[110]$. The interpretation of such data is discussed in the text.

Izawa *et al.*, but the extent to which these experiments have ruled out the presence of line nodes is open to question. The physical processes involved in understanding heat transport due to nodal quasiparticles in applied magnetic fields are far from trivial. Several effects related to the interactions between quasiparticles and vortices and have to be taken into account. These include Doppler shifting of the quasiparticle energy spectrum in a circulating supercurrent, and related changes to the characteristic scattering times associated with impurities and Andreev scattering from vortices.⁴⁴ All of these effects are expected to show a fairly strong anisotropy as the field is cycled between nodal and antinodal directions, but they partially cancel, and there has to be a concern about the quantitative accuracy of predictions for the anisotropy. In fact, calculations in slightly different limits by Dahm *et al.* (2002) and Tewordt and Fay (2001) reach rather different conclusions. The latter argue that p states with horizontal and vertical nodes would give very similar results. This conclusion is partly based on the assumption that the p states would give only twofold anisotropy on the Fermi surface, which would be hard to distinguish from anisotropies due to quasiparticle motion parallel and perpendicular to the vortices. Tewordt and Fay further point out that the fairly strong fourfold anisotropy attributed by Aubin

⁴⁴For discussion and additional references, the reader is referred to the papers by Izawa *et al.* (2001); Tanatar, Nagai, *et al.* (2001); Tanatar, Suzuki, *et al.* (2001); and Tewordt and Fay (2001).

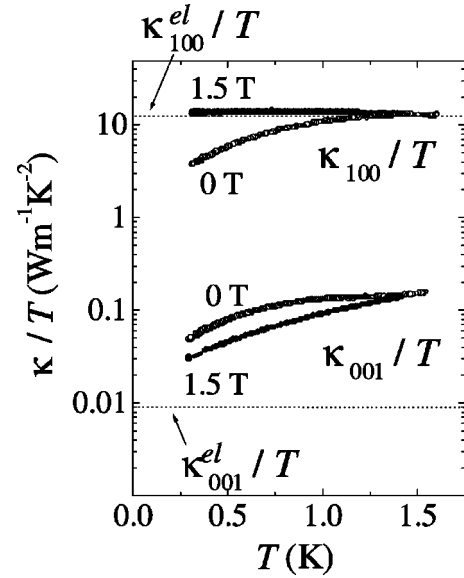


FIG. 31. Although the in-plane thermal conductivity is dominated by quasiparticles, the major contribution to the much smaller out-of-plane thermal conductivity comes from phonons (Tanatar, Suzuki, *et al.*, 2001). Furthermore, when the sample is driven normal in an applied field of 1.5 T, the thermal conductivity in the two directions shows the opposite change of sign. The fact that the out-of-plane conductivity is *higher* in the superconducting state where there are fewer quasiparticles suggests that phonon-quasiparticle scattering is the dominant process. This opened the way to a novel experiment searching for vertical line nodes, as described in the text.

et al. (1997) to line nodes in $\text{YBa}_2\text{Cu}_3\text{O}_7$ (footnote 45) is only consistent with their calculation due to the rather square Fermi surface in this material. In Sr_2RuO_4 , the γ sheet is much more circular (Fig. 11), so even a fourfold term may not show up so strongly.

2. Out-of-plane phonon thermal conductivity combined with in-plane magnetic fields

Given the uncertainties mentioned above, it is useful that Tanatar *et al.* also adopted a novel complementary approach. They measured the out-of-plane thermal conductivity κ_c , to which the quasiparticle contribution might be expected to be far smaller in such an anisotropic material. This is indeed the case, as shown in Fig. 31. Not only is κ_c an order-of-magnitude larger than the predicted quasiparticle value when $T \approx T_c$, but it *falls* when the quasiparticle density is increased by driving the sample normal in an applied magnetic field. In this low-temperature metallic state, κ_c has a T^2 dependence, which Tanatar *et al.* argue to be consistent with a thermal conductivity dominated by phonons whose main

⁴⁵Although the anisotropy was only 0.4% of the *total* κ , the measurement was performed at the fairly high temperature of 6.8 K where phonons still dominate the thermal conductivity. In terms of the quasiparticle contribution, the signal was approximately 4%.

scattering mechanism is from quasiparticles rather than from sample boundaries.⁴⁶ They estimate that the dominance of the phonon contribution persists deep into the superconducting state, still accounting for nearly 90% of κ_c at 0.3 K.

These properties of the interlayer thermal conductivity opened the way to an alternative method for probing the existence of nodal quasiparticles. Since the number of phonons is determined purely by the temperature and is constant in H , the variation of κ_c with respect to the direction and magnitude of H simply reflects the variation of the quasiparticles generated by magnetic fields. In the experiment, κ_c was measured while the magnetic field was applied parallel to the layers with an accuracy of better than $\Delta\theta=0.1^\circ$, and rotated within the plane in steps of $\Delta\phi=10^\circ$. Although the upper critical field H_{c2} shows anisotropy amounting to about 4%, maximum in the [110] direction, the anisotropy of κ_c at 0.3 K was less than the experimental precision of 2% between 0.3 and 1.2 T. No evidence was seen for the large (~30%) variation in quasiparticle density predicted by Vekhter *et al.* (1999) as the field was rotated from a nodal to an antinodal direction.

This technique is new, and although it has the advantage of avoiding some of the complex magnetic-field-related effects on quasiparticle scattering described above, it is not above criticism. It is a fairly indirect probe, and its interpretation awaits a full theoretical treatment. Nevertheless, the failure to find any measurable anisotropy is striking, and the experiment provides no support for the existence of vertical nodes.

In summary, then, two classes of directional thermal-conductivity studies have failed to find any convincing evidence for the existence of vertical nodes on the Fermi surface of Sr₂RuO₄. That is not, however, the same as saying that they conclusively rule them out.⁴⁷ More theoretical and experimental work will be needed before this technique can yield a completely definitive result one way or the other.

3. Ultrasound attenuation

Another technique that has been used to study the nodal structure in Sr₂RuO₄ is ultrasonic attenuation. Attenuation of longitudinal ultrasound waves played a significant role in the study of the quasiparticle spectrum in

⁴⁶This is supported by the observation that the measured κ_c is at least a factor of 8 smaller than that expected for a phonon term with dominant boundary scattering.

⁴⁷In fact, there is a further complication of interpretation. As shown in Fig. 32, specific-heat measurements under field suggest that except at very low temperature and low field, substantial numbers of quasiparticles are excited. If the orbital-dependent effects first suggested by Agterberg *et al.* (1997) and discussed in Sec. VI are important, these quasiparticles may originate from one or two Fermi-surface sheets on which the induced gap magnitude is small. If so, this would be a source of isotropic quasiparticles that may mask the anisotropy introduced by the nodal quasiparticles.

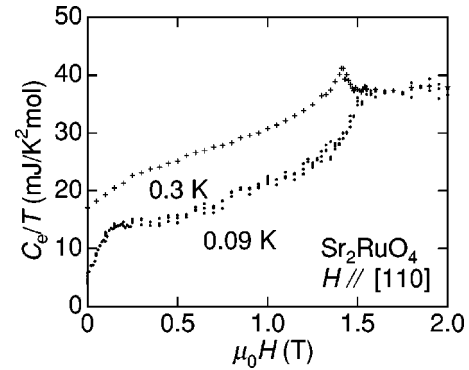


FIG. 32. The specific heat under magnetic fields applied parallel to the ab planes of Sr₂RuO₄ (Nishizaki *et al.*, 2000). It should be noted that quasiparticle excitation under magnetic fields is strongly nonlinear, most probably reflecting the orbital dependence of the superconductivity (see the discussion in Sec. VI). A substantial number of quasiparticles exists unless temperature is below 0.3 K and field is below 0.2 T.

conventional superconductors. Like the nuclear relaxation rate, the behavior of the ultrasonic attenuation below T_c provided essential verification of one of the coherence factors of BCS theory, as explained in, for example, Waldram (1996) and Tinkham (1996). Attenuation using a variety of polarizations has since been used to obtain information on the superconducting state of unconventional superconductors such as UPt₃ (for example, see Shivaram *et al.*, 1986; Ellman *et al.*, 1996).

Before going on to describe the work on Sr₂RuO₄ in detail, we should outline the technique and its terminology. Sound waves are attenuated in metals because of electron-phonon coupling—more precisely, coupling between the phonon strain field and a stress tensor that describes the flow of electron momentum. The stress tensor should take into account the electronic structure of any real material. The results of ultrasound studies are expressed either as the attenuation α or the viscosity η . In the “hydrodynamic” limit (when the wavelength of the sound is much longer than the electron mean free path), the two are related by

$$\alpha = \frac{(2\pi\nu)^2}{\rho c_s^3} \eta_{\text{mode}}, \quad (5.4)$$

where ρ is the mass density and ν and c_s are the frequency and sound velocity, respectively, for the relevant mode. The full specification of the mode requires definition of its polarization and propagation directions. For in-plane propagation in a layered tetragonal material such as Sr₂RuO₄, the modes of relevance are longitudinal and transverse in-plane polarized, traveling in the (100) and (110) directions. These are conventionally labeled L100, T100, L110, and T110, respectively.⁴⁸

⁴⁸In terms of the normal modes for the tetragonal lattice, these modes correspond to the elastic constants C_{11} , C_{66} , $(C_{11}+C_{12}+2C_{66})/2$, and $(C_{11}-C_{12})/2$, respectively. See, for example, Okuda *et al.* (2002).

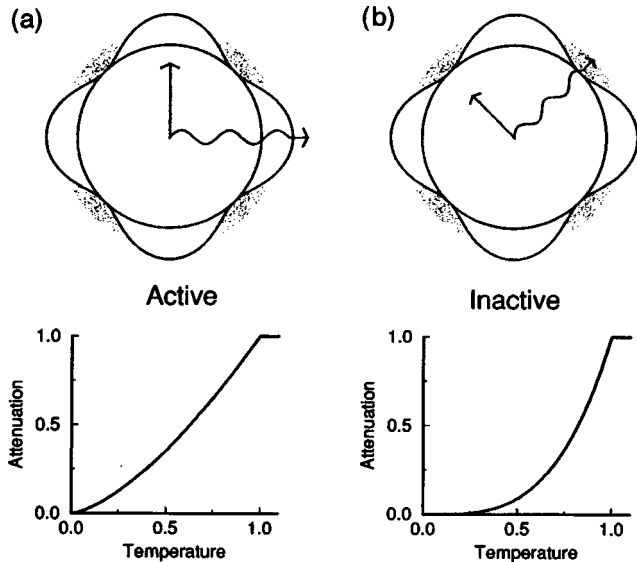


FIG. 33. The idea of “active” and “inactive” nodes as probed by ultrasound attenuation, from Moreno and Coleman (1996). Active nodes lead to approximately a $T^{1.5}$ power-law dependence of the attenuation, while for inactive nodes, this is suppressed by a factor of T^2 to $T^{3.5}$. The powers of 1.5 and 3.5 are dependent on the use of an approximate form for the electron stress tensor, but the T^2 suppression factor is not (see text).

In the superconducting state, the attenuation occurs because of coupling between the phonons and the Bogoliubov quasiparticles. If the state is fully gapped, this means that the attenuation drops exponentially towards zero at low temperatures. The situation with the presence of gap nodes has been discussed in, for example, a very clear paper by Moreno and Coleman (1996). At sufficiently low temperatures, the quasiparticles exist only near the nodes. If there is a nonzero matrix element between these nodal quasiparticles and the injected phonon, the node is “active.” If, however, the matrix element is zero for a quasiparticle right at the node, the sea of nodal quasiparticles is much less efficient at absorbing the phonons, since the absorption grows from zero for quasiparticles away from the nodes. For these “inactive” nodes, the attenuation drops off much faster, as the power law for active nodes multiplied by T^2 . If the assumption of an isotropic electronic stress tensor is used, conditions for (in)activity exist and are shown in Fig. 33. The consequences of each case are also shown. In this approximation, active and inactive nodes lead to $T^{1.5}$ and $T^{3.5}$ attenuation, respectively.

In Sr_2RuO_4 , studies of ultrasonic attenuation have been reported by Matsui *et al.* (2000, 2001) from 0.17 K to T_c and by Lupien *et al.* (2001) from 40 mK to T_c . The Lupien results are summarized in Fig. 34. They were obtained from high quality single crystals with $T_c = 1.37$ K (defined from the maximum of the dissipative component of the ac susceptibility χ''), and studies of the frequency dependence were used to establish that the experiments were performed in the hydrodynamic limit. Their first key finding was the persistence of power laws in the attenuation of all relevant sound polariza-

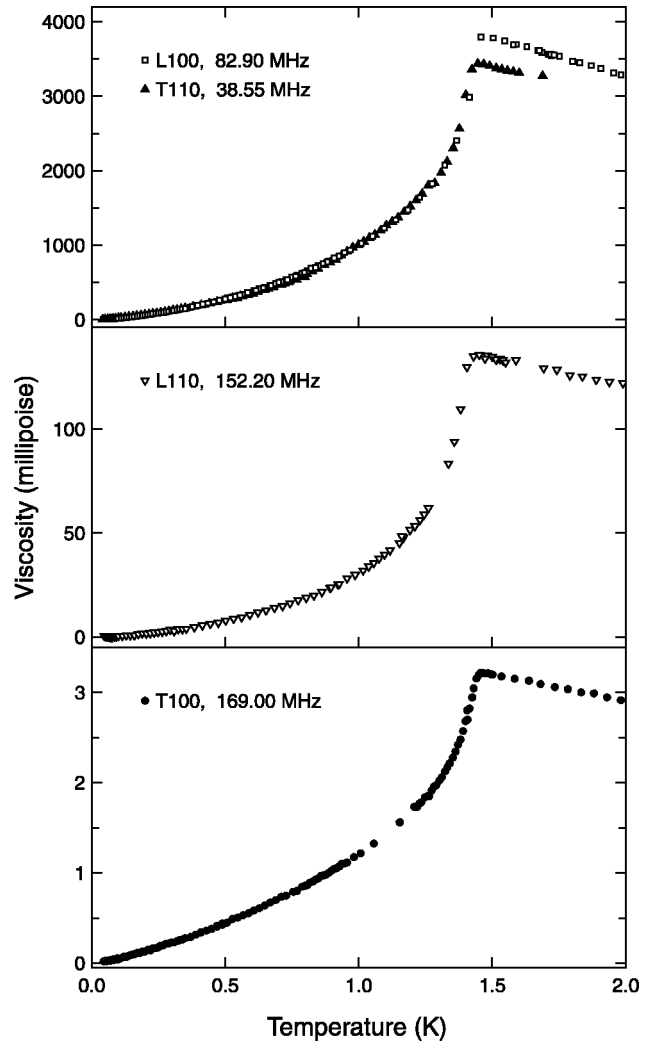


FIG. 34. The ultrasonic attenuation of the four modes relevant to searches for vertical line nodes in Sr_2RuO_4 (Lupien *et al.*, 2001), expressed in terms of the viscosity (see text).

tions to the lowest temperatures studied. This appears to answer one of the questions left slightly open by the studies reported so far. It seems hard to imagine this behavior occurring unless there are indeed nodes or zeros of some kind in the superconducting gap.

The second striking and at first unexpected feature of the data shown in Fig. 34 is the enormous normal-state anisotropy. The L110 mode is attenuated by a factor of 30 less than L100, and for the transverse modes, the effect is higher still. T100 has a full factor of 1000 lower attenuation than T110. An effect of this size was unprecedented.

A theory of this unusual normal-state behavior is clearly a necessary precursor to interpretation of the superconducting state data. Walker *et al.* (2001) have made progress in that direction, by abandoning the usual course of working with the electron stress tensor appropriate to an isotropic electron fluid. In particular, they showed that the square planar configuration of the ruthenium ion lattice, combined with the tight-binding nature of the $4d$ electrons, can lead to very large changes from the predictions of the isotropic fluid assumption. In

a tightly bound square lattice, a transverse sound wave traveling along the $[100]$ direction does not stretch the nearest-neighbor Ru-Ru bond. Since the conduction electrons have strong Ru character, this wave does not couple to them (at least at the order of nearest-neighbor coupling), and so it is not attenuated. Walker *et al.* argued that the extremely low T100 attenuation observed by Lupien *et al.* (2001) is evidence that nearest-neighbor interactions are dominant in determining the ultrasonic attenuation in Sr_2RuO_4 . Using this assumption, and performing numerical calculations based on a tight-binding approximation to the Fermi surface of Sr_2RuO_4 from Mazin and Singh (1997), they are able to account for many of the basic features of the normal-state ultrasound attenuation.⁴⁹

Walker *et al.* then used the same electron stress tensor to analyze the behavior expected in the superconducting state in the presence of various nodal structures. Their results are as follows. For vertical line nodes anywhere along the $[110]$ direction, the T100, L100, and L110 modes would be active, and T110 inactive. For vertical nodes along the $[100]$ direction, L100, L110, and T110 are predicted to be active, and T100 inactive. The credibility of conclusions such as these depends on the same model at least partially explaining the normal-state behavior. If this were not the case, there would always be suspicion about interpretation in the superconducting state. Indeed, Walker *et al.* gave an explicit example of a different prediction of nodal activity that arises from the application of the isotropic electron stress tensor to Sr_2RuO_4 .⁵⁰

Where, then, does the discussion of this section leave us regarding the nodal structure of Sr_2RuO_4 ? The ultrasound data show power-law behavior down to less than $T_c/30$, so the existence of nodes or gap zeros of some kind is very likely indeed. However, the same data do not give clear evidence of inactivity of any of the ultra-

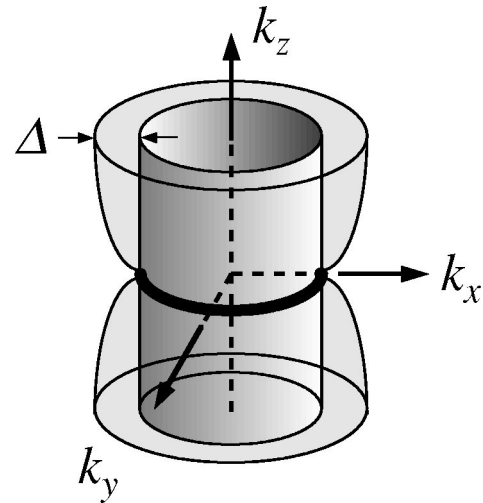


FIG. 35. A horizontal line node in a superconducting energy gap on a cylindrical Fermi surface.

sound modes relevant to this tetragonal material. The observed powers are $T^{1.8}$ for L100, T110, and L110, and $T^{1.4}$ for T100. While there is a small difference of 0.4 in the powers, it is much less than the difference of 2 expected if there were inactivity in some modes due to the presence of vertical line nodes. The ultrasonic attenuation results do not, therefore, appear to support the existence of vertical line nodes at any position along either the $[100]$ or $[110]$ directions of the Brillouin zone of Sr_2RuO_4 .

C. Summary

Although the detailed interpretation of each of the measurements described in this section has some associated complications, none of the observations contradict the following basic conclusion. The energy gap of Sr_2RuO_4 contains nodes, and no conclusive evidence has emerged to show that they are vertical line nodes, in spite of several studies designed to investigate this point. This conclusion applies not only to models that propose actual vertical line nodes, but also to those that propose very small gap minima. We note again that the angular-dependent measurements performed so far have all been concerned with investigating the quasiparticle density, and are not sensitive to phase. This means that they would also have detected gap zeros or deep gap minima. If a gap minimum is small enough for power laws to persist down to $T_c/30$, then angular probes on a similar temperature scale would see thermally excited quasiparticles that would be essentially indistinguishable from those produced by “proper” vertical line nodes.

A natural way to account for this combination of evidence is to postulate the existence of horizontal line nodes, zeros, or deep gap minima going around the Fermi surface, as sketched in Fig. 35. The existence of this type of node in a material with such a strongly two-dimensional electronic structure is surprising. Efforts to justify it theoretically and prove or disprove its existence

⁴⁹There are, however, several reasons for caution. As acknowledged by Walker *et al.*, it is somewhat surprising that the electron-phonon interaction should be so dominated by the nearest-neighbor term, while higher-order terms are significant in determining the Fermi-surface shape. Also, some of the numerical success of the calculation depends on details of the tight-binding parametrization of the Fermi surface by Mazin and Singh. The parametrization derived from the experimentally determined Fermi surface (for example, see Bergemann *et al.*, 2000, 2002) is different from that of Mazin and Singh (1997). Bergemann (private communication) points out that using these “real” parameters in conjunction with the model of Walker *et al.* degrades that model’s prediction of the normal-state attenuation.

⁵⁰The use of the isotropic electron stress tensor gives, for example, the prediction that the L100 mode is inactive for vertical line nodes appearing anywhere along the $[110]$ direction in the Brillouin zone (see, for example, Graf and Balatsky, 2000 and Wu and Joynt, 2001). Recently, Tewordt and Fay (2002) made predictions about ultrasonic attenuation in applied magnetic fields, but as they stated in their paper, they also worked with an isotropic electron stress tensor.

experimentally will be important aspects of future investigation into the superconductivity of Sr_2RuO_4 .

VI. TOWARDS A THEORY

As stated in Sec. I, this review is primarily concerned with aspects of the experimental work that have been carried out so far on Sr_2RuO_4 . Our main goal has been to establish what we regard to be an important checklist of facts with which any eventual theory for the superconductivity of Sr_2RuO_4 will have to be compatible. It is not our intention to make any attempt at a comprehensive review of the large amount of theoretical work that has been published. Constraints of length, author time, and expertise all argue against such an approach. However, we feel that the article would be incomplete without some comments on theoretical issues. These we will give qualitatively and from an experimentalist's perspective. In the first (and probably most important) subsection, we compile a summary of the facts that place constraints on the symmetries of the superconducting state. These constraints will need to be matched by any successful theory. If they are all true, they are sufficiently tight to rule out the majority of the theoretical approaches suggested so far. We will not, however, have the temerity to dissect these treatments in detail; we prefer to let their authors decide for themselves. We then give an outline of the lines of reasoning that appear to succeed in incorporating the main experimental facts. In doing so, we do not endorse them as the only such approaches that are possible. Our neglect to reference and discuss other theoretical work in this section does not indicate any lack of respect, and we hope that the relevant authors forgive our omission. In the third subsection we make a few remarks on a slightly separate issue, that of the mechanism of the superconductivity. A correct theory for this is likely to be a longer-term quest, especially since there are still some fairly major gaps in relevant experimental knowledge.

A. Summary of the main experimental constraints on the symmetry of the Sr_2RuO_4 order parameter

We believe that arguably the most important experimental facts that place real constraints on the superconducting order parameter of Sr_2RuO_4 are as follows:

- (i) The Cooper pairs are in a spin-triplet state, with a d vector that is aligned perpendicular to the Ru-O planes. The main papers supporting this are Ishida *et al.* (1998); Duffy *et al.* (2000); Ishida *et al.* (2001a), and the situation was reviewed in detail in Secs. III.E and IV.B.
- (ii) The superconducting state is time-reversal symmetry breaking. The main piece of evidence comes from Luke *et al.* (1998), supported by Kealey *et al.* (2000), as reviewed in Sec. IV.C.
- (iii) All quasiparticles are paired at $T=0$ (Secs. V.A and V.B).
- (iv) The superconducting energy gap contains nodes, zeros, or very deep gap minima. The form of

these nodes is still uncertain, but little evidence has emerged to suggest that they are vertical line nodes (Sec. V.B).

These are by no means the only important experiments performed on Sr_2RuO_4 (indeed their presumed success depended on many other pieces of work as discussed in other sections of this review), but they play a special role. The following objective statement can be made concerning facts (i)–(iii): As long as none of the experiments or their basic interpretation is subsequently proved to be false, the order parameter of the superconducting state of Sr_2RuO_4 is already quite tightly defined. On the reasonable assumption that a unitary state exists in a paramagnetic material such as Sr_2RuO_4 , they strongly suggest that the basic symmetries of the superconducting state are described by $\mathbf{d} = \Delta_0 \hat{\mathbf{z}}(k_x \pm ik_y)$. If this is indeed the case, the challenge is how to reconcile this symmetry with the evidence that has accumulated in favor of line nodes. The key issue is that for the unitary p states listed in Table IV, the existence of vertical line nodes implies symmetries that are incompatible with facts (i), (ii), or both. One way around this difficulty is to postulate an f -wave instability (for example, see Graf and Balatsky, 2000; Hasegawa *et al.*, 2000; Dahm *et al.*, 2002). However, theoretical objections have been raised regarding the stability of nodes in such a state (Zhitomirsky and Rice, 2001), and we will concentrate here on theoretical work within a basic p -wave scenario.

B. Promising theoretical scenarios

1. Horizontal line nodes and orbital-dependent superconductivity

The possible existence of horizontal line nodes in Sr_2RuO_4 is, at first sight, surprising. Given the extreme two dimensionality of the material (see, e.g., Bergemann *et al.*, 2000), it seems reasonable to work in the two-dimensional approximation used to construct Table IV. By definition, any line node listed there is vertical. Indeed, interlayer processes of some kind are needed to produce horizontal nodes. An important question is whether it is necessary to invoke a *purely* interlayer pairing mechanism (a hypothesis adopted by, for example, Hasegawa *et al.*, 2000). In light of the extremely two-dimensional motion of the quasiparticles, it surely seems to be most likely that the primary pairing mechanism is in plane. A key question is whether horizontal line nodes are compatible with such pairing, and with the other experimental symmetry constraints discussed above. This issue has been addressed recently by Zhitomirsky and Rice (2001). They considered whether details of the real electronic structure of Sr_2RuO_4 could lead to a state with “accidental” horizontal line nodes, due to interlayer processes taking place within the basic scenario of an in-plane pairing attraction. The existence of such nodes would not imply any change to the fundamental symmetries implied by $\mathbf{d} = \Delta_0 \hat{\mathbf{z}}(k_x \pm ik_y)$.

In their paper, Zhitomirsky and Rice followed a line of reasoning that began soon after the discovery of the

superconductivity and elucidation of the basic electronic structure of Sr₂RuO₄. The key underlying point was first raised by Agterberg *et al.* (1997). They noted that although Sr₂RuO₄ has three Fermi-surface sheets, the strong orbital character (with the γ sheet based on Ru d_{xy} orbitals and α and β based on hybridized Ru d_{xz} and d_{yz} orbitals) implies that it might best be regarded as consisting of two almost decoupled electronic subsystems. Normally, interband Cooper pair scattering in a multiband superconductor leads to approximately the same superconducting gap opening simultaneously on all sheets of the Fermi surface. If the electronic subsystems are sufficiently decoupled, however, this might not be the case. Dominant gapping on one Fermi-surface sheet might then induce only a smaller gap on the other two (or vice versa), leading to an enhanced quasiparticle density of states at intermediate temperature before all the gaps fully open as $T \rightarrow 0$. Qualitative support for this picture is provided from several sources. A first example is the Ru-orbital dependence of the susceptibility, which is suggestive of a dominant pairing interaction in one subsystem (for example, see Imai *et al.*, 1998; Sidis *et al.*, 1999). Second, aspects of the dependence of the specific heat on magnetic field seem to be consistent with a two-gap structure (Nishizaki *et al.*, 1999 and see Fig. 32).

Agterberg *et al.* (1997) coined the term “orbital-dependent superconductivity” (ODS) for this idea of different dominant and induced energy gaps on different Fermi-surface sheets. It may not be an ideal name, because it risks confusion with, for example, the orbital moment of $L=1$ Cooper pairs, but it is now in widespread use. The concept of ODS has received a slightly unfortunate treatment in the experimental literature, with a number of groups constructing fits based on the slightly restrictive original assumptions of Agterberg *et al.* (1997). The failure of fits of this kind to match new data is a reflection on one particular form of ODS-based assumptions rather than on the concept itself, which certainly has more appeal.

Zhitomirsky and Rice (2001) generalized and extended ODS to consider interplane processes. They pointed out that the detailed Fermi-surface data of Bergemann *et al.* (2000) were consistent with an out-of-plane quasiparticle hopping with major differences between the (α, β) and γ sheets. For the former, the layer-to-layer hopping is direct, but for the latter, first-order processes are banned, and the hopping occurs via a second-order γ -(α, β)- γ process. They set up a model for interlayer, interband scattering of triplet Cooper pairs incorporating this kind of process, in what they refer to as the “spirit of tight binding.” Using this model, they derived the following results. First, the direct in-plane scattering of Cooper pairs induces the same form (but different magnitude) of nodeless gap,

$$\mathbf{d}_1(\mathbf{k}) \propto \hat{\mathbf{z}}(\sin k_x a + i \sin k_y a), \quad (6.1)$$

on all the Fermi-surface sheets. Second, including the interlayer processes leads to a second gap of the form

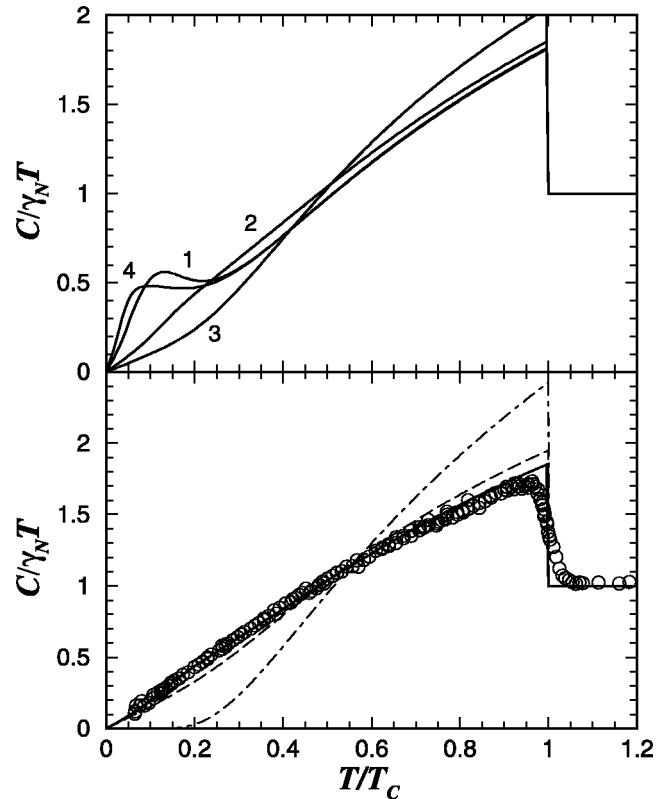


FIG. 36. The predictions of the most recent orbital-dependent superconductivity model of Zhitomirsky and Rice for C_e/T in Sr₂RuO₄. The upper panel shows calculations for various combinations of the three-variable coupling parameters in the theory (two related to in-plane interband coupling and one to interlayer interband coupling; see text). The lower panel shows the best fit that can be obtained to the data of Nishizaki *et al.* (1999) (solid line) and a repeat of the predictions for full isotropic gapping or vertical line nodes on a cylindrical Fermi surface (see Fig. 26).

$$\mathbf{d}_2(\mathbf{k}) \propto \hat{\mathbf{z}} \left(\sin \frac{k_x a}{2} \cos \frac{k_y a}{2} + i \sin \frac{k_y a}{2} \cos \frac{k_x a}{2} \right) \cos \frac{k_z c}{2}, \quad (6.2)$$

which has a horizontal line node.

This model has the appealing feature that it satisfies all the experimental constraints described in Sec. VI.A above, since the node is an “accident of induction,” and does not require any fundamental change to the symmetries that seem to be required of the order parameter. By using the experimentally measured values for the sheet-by-sheet quasiparticle effective mass, Zhitomirsky and Rice could perform a three-parameter fit to the specific-heat data of Nishizaki *et al.* (1999), with the results shown in Fig. 36. Obtaining a good match is never as impressive with three free parameters as with none, but the success of this calculation is nevertheless encouraging.

Two aspects of the ultrasonic attenuation studies (Sec. V.B.3) that we have not so far discussed in detail may also lend some support to the “refined ODS” picture of Zhitomirsky and Rice. First, Lupien *et al.* (2001) noted that $\alpha(T)$ just below T_c decays much faster than the

expectation for the “active” case, despite the reasonable agreement at temperatures much below T_c . In fact, a two-component model with the sum of the power law and a BCS temperature dependence provides a good description of $\alpha(T)$ all the way up to T_c . This is qualitatively consistent with the temperature-dependent two-component gap of Zhitomirsky and Rice; it would be interesting to see if an explicit calculation using parameters consistent with those used to fit the specific heat gave good quantitative agreement with the ultrasound data. A second point was raised by Walker *et al.* (2001), who noted that interlayer coupling might be responsible for the observation that the T100-mode attenuation is stronger than the others at low temperatures.⁵¹

We do not aim to propose the Zhitomirsky-Rice model as being the only route to understanding the symmetries and gap structure of Sr_2RuO_4 , or as being correct in all its details. In fact, it has recently been realized that, contrary to the statement made in their paper, the horizontal line node in \mathbf{d}_2 is only marginally stable. In the presence of the admixtures of \mathbf{d}_1 that are implicit in Fig. 36, point nodes would form (Bergemann, 2002).

Although several features of the model remain controversial, it is attractive because the basic assumptions on which it is based seem plausible, and because the nodal structure that it suggests is consistent with all the main experimental facts as they are currently known. We believe that it is also important to distinguish between Zhitomirsky and Rice’s specific calculation and the more general physics of orbital-dependent superconductivity. The latter seems certain to play an important role in the development of a successful theory for Sr_2RuO_4 superconductivity, even if the former does not prove to be the final answer.

2. Symmetry-conserving gap minima as an alternative to vertical line nodes

As stressed in Sec. VI.A above, p states containing vertical line nodes are not consistent with the symmetry constraints that are apparently imposed by experiment. Several authors, however, have investigated the possibility of highly anisotropic gaps that preserve the basic symmetries of $\mathbf{d} = \Delta_0 \hat{\mathbf{z}}(k_x \pm ik_y)$ but have such deep gap minima that they could lead to a quasiparticle density similar to that given by vertical line nodes. Even if the gap in such pictures actually had a zero, this would be different from a gap node because it would not be accompanied by a phase reversal. Examples of this kind of calculation can be found in papers by Miyake and Narikiyo (1999) and Nomura and Yamada (2000). In both cases, orbital dependence is taken into account since gaps of different magnitudes are predicted for the (α, β) and γ Fermi-surface sheets. The gap minima on

the β sheet resulting from the calculation of Nomura and Yamada are extremely deep, approximating to zeros. Combining these with the weaker features calculated for α and γ gives a fairly good fit to the specific-heat data shown in Fig. 26.

The attractive feature of these calculations is that the stability of the nodalike gap minima does not seem to be in question. However, we note again that these vertical features would be expected to be revealed by the angle-dependent probes discussed in Sec. V.B. No convincing evidence for them has yet emerged, although each of the experiments performed so far has its drawbacks. It seems likely that further experimental work will be required for one class of theory to be strongly favored over the other.

C. Remarks on the mechanism

An understanding of the basic symmetries and nodal structure of the order parameter of Sr_2RuO_4 is obviously an important step on the way to a complete theory, but it is only a step. For example, even if the model described above turns out to be correct, it will be only the starting point for a theory of the basic pairing mechanism. The widely held assumption is that the mechanism will involve spin-fluctuation-mediated pairing of some kind, but there certainly is not universal agreement over the best way to construct a theory.⁵² As reviewed in Sec. II.D, by far the most striking feature so far seen in the dynamical susceptibility is the incommensurate peak at around $(0.6\pi, 0.6\pi)$. In the absence of orbital-dependent effects, it would be natural either to concentrate on this or make some estimate or calculation of the dynamical susceptibility summed over all the bands. However, there is good evidence that orbital dependence plays a major role, leaving extra issues open: Is the behavior of γ or (α, β) dominant in producing the superconductivity? Are the incommensurate fluctuations a help or a hindrance to pairing in the triplet channel? The fit shown in Fig. 36 is based on a dominant gap opening on the γ sheet of the Fermi surface. This seems reasonable, since it has the largest electron masses and the largest mass enhancement, but it is a model-dependent observation.

At the moment, the experimental knowledge of the dynamical susceptibility is incomplete. It is certainly important that it be improved, but further insight into orbital dependence may be required before even the improved data can be used to best effect. A full understanding of the mechanism of the superconductivity is one of the major outstanding issues concerning Sr_2RuO_4 .

⁵¹In fact, the point made by Walker *et al.* is not specific to the Zhitomirsky-Rice model. It is concerned with any instance in which horizontal line nodes occur because of interlayer processes.

⁵²Examples of published theoretical work in this area include Mazin and Singh (1997, 1999); Miyake and Narikiyo (1999); Monthoux and Lonzarich (1999); Kuwabara and Ogata (2000); Nomura and Yamada (2000); Sato and Kohmoto (2000); Kuroki *et al.* (2001).

VII. MULTIPLE SUPERCONDUCTING PHASES

In this section, we turn our attention to attempts to study multiphase behavior in the superconductivity of Sr₂RuO₄. The work so far has generated more questions than answers, and is ongoing. At first, we considered omitting this section since many of the results presented are more preliminary than in other parts of the article. However, we prefer to include it, partly because it is appropriate to discuss multiple phases in the general context of triplet pairing, and partly because the surprising results that are emerging are likely to have a bearing on future work designed to understand the superconducting state of Sr₂RuO₄ in more depth.

A. The existence of a second phase in a symmetry-breaking magnetic field

At several points in this article, we have emphasized the fact that the complexity and internal degrees of freedom inherent in triplet order parameters lead to degeneracy. In the absence of explicit degeneracy-breaking mechanisms, order parameters with different symmetries and nodal structures have the same T_c . In real materials, the degeneracy is split to favor only one symmetry at T_c ; in Sr₂RuO₄ spin-orbit coupling has been invoked as a way to understand the alignment of the d vector along the c axis that is suggested by experiment (see Sec. IV.A). A qualitative feature of triplet pairing is that even if one state is favored at T_c , there are so many near degeneracies that complicated phase diagrams can result. This is well known to be the case in superfluid ³He, where the A and B phases exist in zero applied magnetic field and the A1 phase is stabilized in applied fields (see, for example, the discussion in Sec. IV and the phase diagrams shown in Vollhardt and Wölfle, 1990). The complicated phase diagrams observed in UPt₃ are also often taken to be evidence in favor of triplet pairing.

In Sr₂RuO₄, the basic $\mathbf{d} = \Delta_0 \hat{\mathbf{z}}(k_x \pm ik_y)$ state that seems to be favored by experiment is itself twofold degenerate, and Agterberg (1998a) pointed out that this degeneracy would be expected to lift in magnetic fields near H_{c2} applied in the ab plane. In essence, the applied field would stabilize a state with a vertical line node corresponding to $\Delta_0 \hat{\mathbf{z}}k_x$, where the x direction is along the field (see Appendix D.3). The nodes would thus rotate with an in-plane field, and one of the signals of this state was predicted to be an in-plane anisotropy of the upper critical field. Mao *et al.* (2000) were the first to report a search for such a state, using ac susceptibility measurements and a special two-axis rotator that allowed precise in-plane field alignment. They observed an in-plane anisotropy of the upper critical field, and initially associated it with Agterberg's prediction. However, its magnitude was not what was expected, and was temperature

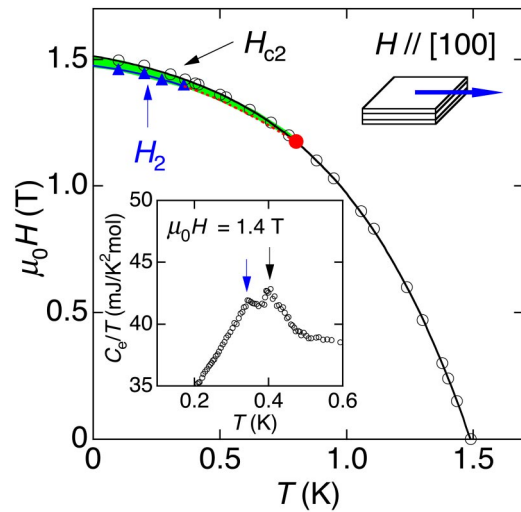


FIG. 37. The empirically deduced superconducting phase diagram for Sr₂RuO₄ for magnetic fields applied precisely in the ab plane. Below 0.8 K, thermodynamic measurements provide evidence of a split superconducting transition, as evidenced by the C_e/T data shown in the inset. The data suggest the existence of a bicritical point at approximately (0.8 K, 1.2 T). See Deguchi *et al.* (2002) (Color in online edition).

dependent, to the extent that it even changed sign near T_c .⁵³

The study by Mao *et al.* uncovered preliminary evidence for multiple phase behavior *not* predicted by Agterberg. It appeared that there may be a second phase at high fields and low temperatures, with a bicritical point somewhere near 0.8 K. Since then, high-resolution specific-heat and thermal-conductivity measurements (reviewed in Yaguchi *et al.*, 2002) have uncovered considerable evidence that such a second phase does indeed exist. To observe it, the field has to be aligned to the ab plane with considerable accuracy. For in-plane thermal conductivity κ , the field dependence up to T_c has the same characteristic shape for any angle between the field and the planes of greater than 3°. As the field is moved closer to the plane, there is an abrupt onset of a sharp jump in κ/T just below H_{c2} , seemingly indicative of a rapid entropy release (Tanatar, Nagai, *et al.*, 2001). The most direct thermodynamic evidence comes from the specific heat. If the field is aligned in the planes to within 0.5°, the single peak seen at all other angles splits into two, as shown in the inset to Fig. 37.

The thermal-conductivity and specific-heat data can be combined to construct the phase diagram for Sr₂RuO₄ that is shown in Fig. 37. The feature in the specific heat provides evidence that a change of phase is taking place, but little is known so far about the nature of the phase transition or the symmetry of the state between H_2 and H_{c2} . The data suggest the presence of a bicritical point at approximately (0.8 K, 1.2 T) that was not part of the original prediction of Agterberg. This does not mean that the prediction was incorrect. It is a

⁵³This issue was subsequently discussed by Sigrist (2000) in terms of spin-orbit coupling.

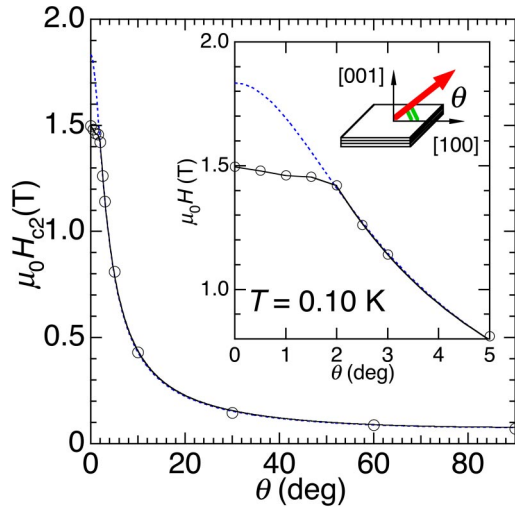


FIG. 38. Evidence that the second phase shown in Fig. 37 is accompanied by a limiting of H_{c2} . As the field is rotated into the plane (conditions under which the second phase is observed), the upper critical field changes sharply from obeying the predictions of Ginzburg-Landau anisotropic effective-mass theory to falling below its predictions. From Deguchi *et al.* (2002) (Color in online edition).

robust property of a twofold-degenerate state to exhibit a split transition under a symmetry-breaking field. On the assumption that the main superconducting phase of Sr_2RuO_4 does involve time-reversal symmetry breaking as discussed in Sec. IV.C, the fact the transition to $\Delta_0 \hat{z} k_x$ has not been observed in the higher-temperature region near T_c seems to indicate that the relevant region of phase space is quite narrow. The split transition that *has* been observed at low temperatures is therefore probably due to some separate mechanism.

B. Unusual upper critical-field limiting

A striking feature of the split transition that is not immediately apparent from Fig. 37 is the fact that it seems to be accompanied by a value of H_{c2} that is lower than that expected for an extrapolation of the main superconducting phase. This can be seen in several ways. First, $H_{c2} \parallel ab$ falls to below the low-temperature value in comparison to that of $H_{c2} \parallel c$ if the gradients near T_c are normalized. A graphic way to demonstrate this is to plot H_{c2} measured at 100 mK as a function of the angle between the field and the ab plane (Fig. 38). It appears to follow the prediction of a Ginzburg-Landau anisotropic effective-mass theory very well until the field comes to within approximately 2° of the ab plane, at which point it deviates strongly and sharply from the predicted angular dependence (see inset to Fig. 38). This is very surprising, because a phase change would usually be made to increase the condensation energy and therefore the critical-field scale.

A well-known mechanism for limiting upper critical fields in superconductors is the Pauli limit, which occurs when the Pauli-susceptibility-based energy gain for splitting a singlet pair exceeds the superconducting conden-

sation energy, leading to a first-order phase transition. For weak-coupling isotropic superconductors, the transition is expected at $\mu_0 H/T_c \approx 1.8$ T/K, the value often referred to as the Clogston-Chandrasekhar limit (see, for example, Clogston, 1962 or WalDRAM, 1996). In triplet superconductors, a form of spin limiting would be expected for some combinations of applied field and d vector, but for other combinations it should be completely absent. In Sr_2RuO_4 , the order parameter favored by the experiments reviewed in Secs. III–V should result in no spin limiting for applied fields in the plane. One view that could be taken is, therefore, that the upper critical field limiting provides evidence against the whole triplet pairing interpretation in Sr_2RuO_4 . The much-quoted value of 1.8 T/K is not exact, and may be lowered in some circumstances. Here, the observation occurs at approximately 1 T/K.

While we cannot rule out such an interpretation, several comments should be made. The first is that, to our knowledge, no Pauli limiting feature as abrupt as that shown in Fig. 38 has been observed in other layered superconductors. In fact, a more standard puzzle is why the assumed singlet superconductivity survives to *higher* than the Clogston-Chandrasekhar limit. The second point is that the data on Sr_2RuO_4 do not support the idea of a single limiting transition. On the contrary, as the precision of the measurements has improved, increasingly convincing evidence has emerged for a double transition, defining a second superconducting phase as shown in Fig. 37. The third point is the extreme sensitivity of the H_{c2} limiting to accurate field alignment. For a spin-limiting mechanism, the precise alignment of the field relative to the crystal axes is not expected to be crucial. Rather, the limiting should depend primarily on the field value. In Sr_2RuO_4 , the limiting for the [100] and [110] field directions occurs at a similar $\Delta\theta$, even though the field values are different due to the in-plane anisotropy of H_{c2} . A fourth comment concerns the relationship of critical fields to the normal-state dispersion. For $\theta > 2^\circ$, the fit shown in Fig. 38 gives a convincing match to the Ginzburg-Landau anisotropic effective-mass expression for the angular dependence of the critical fields. However, the value of the effective-mass anisotropy that is extracted is far below that which would be estimated from the Fermi-surface warping, which is well known (see Secs. II and III.C). In other words, the puzzle of the critical field in Sr_2RuO_4 goes well beyond the limiting to 1.5 T for fields exactly aligned in the plane. We are intrigued by a possible link to orbital-dependent superconductivity. Could the field disrupt some of the interband, interlayer coupling discussed by Zhitomirsky and Rice (2001) and others?

C. Summary

The experiments described in this section have uncovered evidence for a nontrivial superconducting phase diagram for Sr_2RuO_4 in applied magnetic fields. The features that have been seen are intriguing, but far from understood. In that sense, this section is much more pre-

liminary than others in this review, but further phase diagram investigation seems destined to be one of the major areas of experimental activity on Sr_2RuO_4 for the near future.

VIII. CONCLUSIONS AND FUTURE WORK

A. Main conclusions and their strength

At the end of a review such as this, the central question of importance to the reader (and reviewers) must concern the conclusions and the strength with which they can be drawn. In the case of Sr_2RuO_4 , the main issues are whether the superconductivity is unconventional and if so, whether it involves spin-singlet or -triplet pairing. It is particularly important that we take a purely objective view on the latter point. The original proposal of triplet superconductivity (Rice and Sigrist, 1995; Baskaran, 1996) was beautiful, intriguing, and influential. As a consequence, the vast majority of the experimental literature has been centered on a triplet interpretation and the extent to which it fits the data. A feature of science is that one tends to find what one looks for. Unless an experiment has both an absolutely unambiguous interpretation and the capability to discriminate between the received wisdom and other possibilities, there is the danger of building that received wisdom on shaky foundations.

With the above considerations in mind, we will now attempt a critical summary of the key discriminatory experiments on Sr_2RuO_4 as discussed during this review. They are as follows:

- (i) The superconductivity is unconventional, in the sense that it does not involve standard s -wave singlet pairing. The evidence for this seems to be so overwhelming that we can state it as a conclusion with high confidence.
- (ii) The spin susceptibility as measured by the NMR Knight shift (Ishida *et al.*, 1998, 2001a) and magnetic neutron scattering (Duffy *et al.*, 2000) does not change as Sr_2RuO_4 enters the superconducting state (Sec. III.E). Some analysis is required to extract the spin susceptibility from the raw experimental data in each case, but the following objective statement can be made. If the spin susceptibility is deduced correctly in the above experiments, spin-triplet pairing is the only conclusion that can be drawn.
- (iii) Muon spin rotation experiments (Luke *et al.*, 1998, 2000) have provided evidence that time-reversal symmetry (TRS) is broken at T_c in Sr_2RuO_4 . Supporting evidence for TRS breaking can be found from small-angle neutron-scattering studies of the vortex lattice by Kealey *et al.* (2000). The latter experiment is not, however, sensitive to whether the symmetry is broken at T_c or not, so the important observation of TRS breaking is, for the moment, reliant principally on the muon spin rotation results.

- (iv) Studies of the energy gap (Sec. V) show that it contains either line nodes, lines of zeros, or very deep gap minima. A key question is whether these are vertical or horizontal. Experiments that should be sensitive to vertical nodes or gap minima have failed to find convincing evidence for their existence. A process of elimination then favors horizontal line nodes, but this conclusion can be drawn with much less certainty than (i)–(iii). In (ii) or (iii), the published work (or at least its interpretation by the authors concerned) would have to be simply incorrect for the basic conclusion to be overturned. In the case of the energy-gap studies, we reach our “conclusion” based on the overall evidence from a series of experiments, each of which is subject to uncertainty of interpretation.

Given the current state of knowledge, we think that a *definitive* statement that Sr_2RuO_4 is a triplet superconductor is premature. However, it certainly seems to be favored by the experimental evidence. The best way to express this may well be to ask the inverse question. What would be the cost of a *nontriplet* interpretation of the superconductivity in Sr_2RuO_4 ? The following assessment can be made. A basic triplet scenario would survive if (iii) and (iv) were overturned but (ii) proved to be robust. A simple singlet picture would also have problems if (ii) were judged to be inconclusive but (iii) were fully confirmed (see the argument of Sec. IV.C.3). In fact, it seems likely that both (ii) and (iii) would need to be reversed or substantially altered for a credible nontriplet interpretation of the superconductivity of Sr_2RuO_4 . It seems to us that that such a series of developments is unlikely, but in some ways it is best left to the reader to make his/her own judgement.

If we adopt the view that (ii) and (iii) are both correct, the constraints on the order parameter are strong. Of the simple unitary p -wave states, one of the form $\mathbf{d} = \Delta_0 \hat{\mathbf{z}}(k_x \pm ik_y)$ [or more generally, $\mathbf{d} = \Delta_0 \hat{\mathbf{z}}(f_x \pm if_y)$, where f is an odd function] is required. If the energy gap contained vertical line nodes on all Fermi-surface sheets, no unitary p -wave state is compatible, and a nonunitary p - or f -wave state would be necessary. Each of these would in turn present difficulties of interpretation. If the real electronic structure is taken into account through the orbital-dependent superconductivity discussed in Sec. VI, a wider range of gap structures is still consistent with the experiments to date. For example, horizontal line nodes, as mildly favored by the existing evidence [Sec. V and (iv) above], might be compatible with (ii) and (iii).

B. Outstanding issues and desirable future work

It is important that we discuss some of the outstanding issues surrounding the unconventional superconductivity of Sr_2RuO_4 . In doing so, we give special emphasis to anything that appears to challenge the interpretation of a TRS-breaking triplet state, to summarize some key ar-

eas of research for the future. If all of the experiments we list could be done satisfactorily, the issue of the order-parameter symmetry of Sr_2RuO_4 would be settled one way or the other.

- (i) The single biggest void in the experimental understanding of Sr_2RuO_4 (and all other postulated triplet superconductors) is work that confirms or denies the existence of odd parity (the symmetry of the orbital part of the pair wave function). Ideas exist on how this might be accomplished based on the experience gained with the cuprates of phase-sensitive investigations of the order parameter. Some of these involve tunneling, and in a triplet superconductor, this raises the additional issue of the strength of coupling expected between singlet and triplet condensates (see Sec. III.D). Indeed, some concerns have already been expressed regarding the magnitude of the Josephson coupling that can be observed between Sr_2RuO_4 and *s*-wave superconductors (see footnote 27).
- (ii) Substantial extra weight would be lent to the interpretation of the spin susceptibility studies in relation to $\mathbf{d}=\hat{\mathbf{z}}(k_x\pm k_y)$ if a successful measurement could be made of the spin susceptibility with an applied field along the *c* axis of Sr_2RuO_4 . The prediction is that (assuming sufficiently strong pinning of the *d* vector to the crystal axes) the spin susceptibility should follow the basic Yosida function for this orientation. The experiment would not be easy (see Sec. IV.B), but it is highly desirable.
- (iii) If, as suggested by muon spin rotation, time-reversal symmetry is broken in the superconducting state of Sr_2RuO_4 , this should have observable consequences on other properties. Such consequences appear to have been observed in the field distribution of the vortex lattice (see Sec. IV.C.2), but no degeneracy splitting under symmetry-breaking fields has been resolved (see Sec. VII). In fact, the “chirality” of the superconducting state should have a much wider range of consequences. Many of these have been discussed extensively in theoretical literature, which we have not been able to review here.⁵⁴ Our decision not to review that literature was based on the lack of supporting experimental evidence to date. Examples exist, such as the intriguing flux creep experiments by Mota and collaborators (1999, 2000) that were interpreted in terms of chiral vortices by Sigrist and Agterberg (1999). However, for complete confidence that the order parameter is really based on the fundamental symmetries of \mathbf{d}

$=\Delta_0\hat{\mathbf{z}}(k_x\pm k_y)$, it is desirable that some other consequences of chirality be observed. The same considerations apply to another topic for which theory but essentially no experiment currently exists, that of collective modes.

- (iv) It is clearly important that the multiphase behavior outlined in Sec. VII be understood. This applies particularly to the issue of critical-field limiting. This could either prove to be a route to deep understanding of the triplet state in Sr_2RuO_4 , or a first step to revising or unraveling the triplet interpretation.
- (v) Further clarification of the nodal structure of the energy gap is necessary. The experiments that currently seem to contradict the presence of vertical lines of nodes or zeros should be performed at lower temperatures and/or lower magnetic fields to see if their results still hold. Further experiments should be performed to confirm or deny the presence of horizontal nodes or zeros by direct observation rather than indirect inference.
- (vi) Parallel with attempts to finalize our knowledge of superconducting condensate symmetry, it is important that there is a continuation of experiments likely to yield information pertinent to a proper theory of the superconductivity mechanism. Detailed study of the dynamical susceptibility is likely to be a crucial part of this process. It seems clear that it will also be very important to be able to decouple such information into its orbital, or Fermi-surface sheet specific, components.

C. Sr_2RuO_4 in a broader context

In this article, we have striven to remain focused on the unconventional superconductivity of Sr_2RuO_4 and the experimental constraints on its order parameter. As discussed, evidence has accumulated in favor of a particular triplet order parameter. That classification cannot yet be made with certainty, but a growing number of results would need to be proven false for any nontriplet interpretation to be acceptable.

Whatever the final answer concerning the superconducting symmetry, we believe that Sr_2RuO_4 will have a lasting significance. It has provided a beautiful example of the kind of work possible when one encounters a form of novel quantum order in a material with a relatively simple electronic structure that can be grown to very high purity. Experimental investigations on Sr_2RuO_4 have been possible with a level of precision that can be achieved only very rarely. The fact that such detailed knowledge is becoming available gives hope that a genuinely detailed understanding of the underlying physics can be achieved. There is a growing realization that this will require a “real-life” approach in which the actual electronic structure is taken carefully into account. If that proves to be a formidable task in Sr_2RuO_4 (which might indeed be the case), it is sobering to think that it would be next to impossible for the fascinating

⁵⁴Some examples are the Hall effect in the absence of any external field (Goryo, 2000) unusual flux-flow conductivity (Kato, 2000), and chiral optical absorption (e.g., Matsumoto and Sigrist, 1999).

materials in which an equivalent level of experimental knowledge is never likely to be achieved.

Another way in which we believe that Sr_2RuO_4 will prove to be influential is in altering preconceptions that have existed concerning transition-metal oxides. Until recently, these were presumed by physicists to be complex and defect ridden. In some cases, this is undoubtedly true, but in others, it is not. In recent years, evidence has emerged that has shown that several ordered cuprates such as $\text{YBa}_2\text{Cu}_3\text{O}_7$ exist in extremely pure form, but this was based on experiments performed deep in the superconducting state. Sr_2RuO_4 has yielded an explicit demonstration of the levels of purity that can be achieved, and of an intriguing ground state that can be observed *only* in the high-purity limit. The discoveries reviewed in this article have led to the investigation of a series of related ruthenates (and other transition-metal oxides), resulting in the discovery of fascinating magnetic and metallic ground states. To date, none of these has been grown with sufficient purity to yield mean free paths as long as those achieved for Sr_2RuO_4 , leaving open the intriguing possibility of the discovery of more examples of unconventional superconductivity. In fact, such a discovery in a complementary material may ultimately prove to be one of the most important routes to understanding the mechanism of the pair binding in Sr_2RuO_4 itself. We hope that in writing this article, we have conveyed some of our enthusiasm for the search.

ACKNOWLEDGMENTS

In the course of our work on Sr_2RuO_4 , we have enjoyed collaborations and discussions with a large number of people. We will not give a long list here, since those concerned feature prominently in the text and/or list of references. In connection with preparing this article, we gratefully acknowledge help given by C. Bergemann, K. Deguchi, T. Katsufuji, and T. Nomura. We would particularly like to thank M.R. Walker and C. Bergemann for their detailed comments on the first draft of the manuscript. The amendments that we were able to make in response to those comments have, in our view, substantially improved the article. This work was carried out with support from the Royal Society, Leverhulme Trust, and EPSRC in the United Kingdom; the CREST program of the Japan Science and Technology Corporation; the “Novel Quantum Phenomena in Transition-Metal Oxides” program of the Japanese Ministry of Education, Culture, Sports, Science, and Technology; and the Japanese Society for the Promotion of Science.

APPENDIX A: ADDITIONAL DETAILS OF THE NORMAL-STATE PHYSICS OF Sr_2RuO_4

1. Hall effect and magnetoresistance

The temperature dependence of the Hall effect in Sr_2RuO_4 is relatively complicated, as shown in Fig. 39, the general features of which have been observed by two

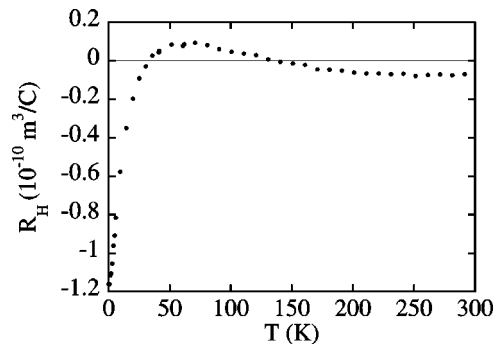


FIG. 39. The temperature dependence of the weak-field Hall coefficient of Sr_2RuO_4 (in the configuration $j \parallel ab$, $H \parallel c$), from Mackenzie, Hussey, *et al.* (1996).

groups (Shirakawa *et al.*, 1995; Mackenzie, Hussey, *et al.*, 1996). It is small and negative at high temperatures, crosses over to become positive between 130 and 30 K, and becomes negative again below 30 K. Between 30 and 1 K, it varies rapidly with temperature, but below 1 K it becomes almost temperature independent. The Hall effect at finite temperature is notoriously sensitive to details of the temperature dependence of the scattering rate, the local curvature of the Fermi surface, and the local Fermi velocity (see, e.g., Ong, 1991). In a multi-band material such as Sr_2RuO_4 with electrons and holes, strong temperature dependencies are no surprise.⁵⁵ At sufficiently low temperature, however, the mean free path becomes approximately independent of quasiparticle velocity, because the scattering is dominated by elastic scattering from a static distribution of impurities and defects. In this limit, R_H in a quasi-two-dimensional material is temperature independent, with a value that is simply related to the Fermi-surface topography, as discussed in a beautiful paper by Ong (1991). It seems very likely that the crossover to a temperature independent R_H below 1 K indicates entry to this regime. Indeed, it will be shown in Appendix A.3 that a successful calculation of the low-temperature value of $-1.1 \text{ m}^3/\text{C}$ can be made on the basis of the Fermi-surface topography measured using quantum oscillations. Again, this suggests that the main features of the Hall effect can be understood using Fermi-liquid-based transport theory within the relaxation-time approximation. While we believe that caution should be exercised before attaching physical significance to any temperature dependence of R_H in Sr_2RuO_4 (see the discussion in Mackenzie, Hussey, *et al.*, 1996), a correlation between $R_H(T)$ and $[\rho(T)]^2$ has been stressed by Miyazawa *et al.* (1999), and calculations of the temperature dependence of R_H have been reported by Mazin *et al.* (2000) and Noce and Cuoco (1999b).

The magnetoresistance of single-crystal Sr_2RuO_4 has been studied by Hussey *et al.* (1998) for field and current

⁵⁵Multiple bands also complicate the interpretation of the thermoelectric power, which was studied in Sr_2RuO_4 by Yoshino *et al.* (1996).

combinations parallel and perpendicular to the RuO_2 planes. At low temperatures, where there is coherent transport perpendicular to the planes, the transverse magnetoresistance for both field orientations can be understood within conventional Boltzmann transport theory. The long low-temperature mean free path of these very pure single crystals results in pronounced deviations from quadratic field dependencies at high fields, for which the weak-field limit is exceeded (Hussey *et al.*, 1998; Schofield and Cooper, 2000). The magnetoresistance has also been studied to lower fields by Jin *et al.* (1998) and Jin, Liu, and Lichtenberg (1999). Aspects of their data and particularly their interpretation differ from those discussed by Hussey *et al.* and Schofield and Cooper. Very high-field magnetoresistance (up to 33 T) was reported by Ohmichi *et al.* (2000, 2001b), who were able to perform the measurements thanks to the development of a novel sample rotator based on piezoresistive drives (Ohmichi *et al.*, 2001a). Magnetotransport in Sr_2RuO_4 has been analyzed in a quantum critical scenario by Noce and Cuoco (2000) and Noce *et al.* (2000).

2. Calculation of bulk properties using quantum oscillation parameters

The data reviewed in Sec. II yield very strong evidence that the normal state of Sr_2RuO_4 is a Fermi liquid. A useful check on this important conclusion is whether the “microscopic” data of Table II can be used to calculate the bulk properties summarized in Sec. II.A. The relative simplicity of the Fermi surface of Sr_2RuO_4 implies that estimates of some properties can be made within a simple two-dimensional approximation, in which we treat the Fermi surface as three cylinders with the average k_F values given in Table II. In Secs. A.2 to A.5 we give some specific examples of this.

3. Luttinger volume

Luttinger’s theorem states that in a correlated electron metal, the Fermi volume should be unchanged by the interactions. An important check on whether Sr_2RuO_4 can be completely described within a Fermi-liquid picture is that the observed Fermi surface should account for the existence of exactly four electrons per formula unit in the three bands that are observed to cross E_F . If fewer than four were seen to participate in the Fermi liquid, it would not be possible to completely exclude the existence of some second normal-state fluid, however unlikely this might seem.

The measured k_F values and the hole, electron, and electron character of α , β , and γ give a total of 4.05. The error of approximately 1% is entirely consistent with the experimental precision and the two-dimensional approximation used, so we can conclude that Luttinger’s theorem is satisfied. The quantum oscillation measurements do not establish the hole or electron character of an individual pocket directly, so in performing this calculation, we have used information from the band-structure calculations. Given the good agreement between experiment and theory on the areas of each sheet,

this seems reasonable. Further experimental justification comes from an analysis of the Hall effect (see below).

4. Electronic specific heat

The electronic specific heat γ_{el} is another quantity that should be calculable to within experimental precision and the small uncertainty of our two-dimensional approximation. Considering the definition of the cyclotron mass,

$$m^* = \frac{\hbar^2}{2\pi} \frac{\partial A_e}{\partial k}, \quad (\text{A1})$$

that of the density of states per unit volume from a single Fermi-surface sheet,

$$g(\varepsilon_F) = \int \frac{dS_F}{4\pi^3} \frac{1}{|\nabla\varepsilon|} \quad (\text{A2})$$

(a surface integral where S_F is the Fermi surface), and that of γ_{el} ,

$$\gamma_{\text{el}} = \frac{\pi^2}{3} k_B^2 g(\varepsilon_F), \quad (\text{A3})$$

the electronic specific heat in J/mol K^2 can be expressed in terms of the cyclotron masses measured with $B \parallel c$ as

$$\gamma_{\text{el}} = \frac{\pi N_A k_B^2 a^2}{\hbar^2} \sum_i m_i^*, \quad (\text{A4})$$

where N_A is Avogadro’s number, a is the in-plane lattice constant of 3.87 Å, and i is the band index.⁵⁶ Although Eq. (A4) has been derived here using oversimplified one-electron language, it is exact for a Fermi liquid (for example, see Leggett, 1975). Using the values of m^* from Table II gives $\gamma_{\text{el}} = 38.6 \text{ mJ/mol K}^2$, in complete agreement, within experimental error, with those obtained from bulk measurements on the same crystals (see Sec. II.A).

5. In-plane transport

In a two-dimensional multiband material, the low-temperature conductivity $\sigma_{xx} = 1/\rho$ is given by

$$\sigma_{xx} = \frac{e^2 \ell}{\hbar d} \sum_i k_F^i, \quad (\text{A5})$$

where ℓ is the mean free path and d is the interlayer spacing. For this expression to be exact, the Fermi surface must be a cylinder with a circular cross section (a condition that did not apply in the analysis of Luttinger’s theorem or the specific heat), and the mean free path must be \mathbf{k} independent. This “isotropic- ℓ ” limit is a fairly good approximation if the temperature is low enough that elastic impurity and defect scattering is dominant over inelastic (temperature-dependent) scattering. Since ρ is a sample-dependent quantity, it cannot

⁵⁶We emphasize that the precise functional form of Eq. (A4) holds only for two dimensions.

be calculated in any absolute sense. However, measured values of the residual resistivity of samples used for quantum oscillations correspond to mean free paths of 1400–3000 Å, in line with the estimates obtained from Dingle analyses (see below).

Within the approximations of two dimensions, circular Fermi-surface cross sections, and isotropic ℓ , an expression can be derived for the absolute value of the Hall coefficient, making use of Ong's treatment of the Hall conductivity in two dimensions (Ong, 1991). As discussed by Mackenzie, Hussey, *et al.* (1996),

$$R_H = \frac{\sigma_{xy}}{\sigma_{xx}^2} = \frac{2\pi d \sum_i (-1)^{n_i}}{e \left(\sum_i k_F^i \right)^2}, \quad (\text{A6})$$

where $n_i=1$ if the Fermi-surface sheet i has electron character and 2 if it has hole character. As expected, the Hall coefficient depends only on the geometry of the Fermi surface and not on the mean free path. Note that Eq. (A6) is valid only in the weak-field limit at low temperatures. The k_F values from Table II then give a calculated Hall coefficient of $-0.9 \times 10^{-10} \text{ m}^3/\text{C}$. Given the approximations used in deriving Eq. (A6), the existence of electrons and holes, and the strong temperature dependence between 1 and 30 K, this is a fairly successful estimate of the measured value of $-1.15 \text{ m}^3/\text{C}$ (Fig. 39). If there were not two Fermi-surface sheets with electron character and one with hole character, the calculated value would be in serious disagreement with experiment.

6. Resistive anisotropy

The general expression for the components of the conductivity tensor was given by, for example, Ziman (1972):

$$\sigma_{ij} = \frac{1}{4\pi^3} \frac{e^2}{\hbar} \int \frac{v_i \cdot v_j}{|\nu|} \tau dS_F, \quad (\text{A7})$$

where v_i is the component of the velocity in direction i , and $\tau = \ell/|\nu|$ is the relaxation time and the integral is over the Fermi surface. In a material with one Fermi-surface sheet and any nearly two-dimensional dispersion (the only criterion is that $\nu_{\perp} \ll |\nu|$), Eq. (A7) can be used to derive the conductivity ratio

$$\frac{\sigma_{\perp}}{\sigma_{xx}} = 2 \frac{\langle \nu_{\perp}^2 \rangle}{\nu_F^2}, \quad (\text{A8})$$

where $\langle \rangle$ denotes an average through the Brillouin zone. [We note that in the notation usually associated with Eq. (A7), $\sigma_{\perp} = \sigma_{zz}$ and $|\nu_F| = |\nu|$.] Taking the values for $\langle \nu_{\perp}^2 \rangle$ from Table II, and generalizing to the multi-band situation in the isotropic- ℓ approximation,

$$\frac{\sigma_{\perp}}{\sigma_{xx}} = 2 \frac{\sum_i k_F^i \langle \nu_{\perp}^2 \rangle_i}{\sum_i k_F^i} \quad (\text{A9})$$

gives a value of 3800 for the resistive anisotropy. There is considerable variation in the quoted experimental values, but the latest data yield a value of 4000 (Ohmichi *et al.*, 2000).

7. Other quantum oscillation work on Sr₂RuO₄

The information in Table II is sufficient to underpin the discussion of the superconductivity in Secs. III–VI, but we also note that Sr₂RuO₄ is being used to develop new areas of research in the field of quantum oscillations themselves. Bergemann and co-workers (Bergemann *et al.*, 1999; Julian *et al.*, 1999) have reported the use of piezoresistive microlevers to measure the dHvA effect in the magnetic torque of Sr₂RuO₄. Observing oscillations from the γ surface in a 1- μg sample demonstrated that the technique is capable of excellent sensitivity even when the excitation current in the lever is low enough to allow the sample to be cooled to less than 200 mK. A variant of quantum oscillations, the acoustic dHvA effect, has been investigated by Matsui and co-workers (1998, 2000). In a recent study of low-temperature c -axis resistivity, Ohmichi, Maeno, *et al.* (1999) have presented evidence for the observation of chemical-potential oscillations, whose existence had been discussed theoretically by several authors (e.g., Shoenberg, 1984; Alexandrov and Bratkovsky, 1996; Nakano, 1997, 2000) and observed and discussed in an organic metal (Harrison *et al.*, 1996). Finally, cyclotron-type resonances have been observed by two groups, although different interpretations have been given for the results obtained (Hill *et al.*, 2000; Ardavan *et al.*, 2001).

8. High-temperature and high-pressure normal-state transport

The majority of work discussed in this article concerns the normal-state properties of Sr₂RuO₄ at low temperatures and ambient pressure. This does not mean that other regimes are without interest. In particular, Sr₂RuO₄ is an ideal material in which to study a phenomenon that is now acknowledged to be a feature of many correlated electron materials, namely, a surprising fragility of the Fermi-liquid metallic state. The power-law transport behavior associated with the Fermi liquid is lost at a much lower-temperature scale (tens of kelvin) than would be simply understood in terms of the observed mass renormalization. This issue was addressed by Tyler *et al.* (1998), who studied in-plane and out-of-plane resistivity to temperatures in excess of 1300 K. In this paper, they also discussed the apparent violation of the Mott-Ioffe-Regel limit seen in high-temperature transport. High-temperature transport has also been studied by Berger *et al.* (1998). Their experimental results differ from those of Tyler *et al.* (1998), and in fact bear a strong similarity to data later obtained by Ikeda *et al.* (2000) for the bilayer ruthenate Sr₃Ru₂O₇.

High-pressure work on Sr₂RuO₄ was first reported by Shirakawa *et al.* (1997), who observed a decrease of the superconducting transition temperature in applied pressures of up to 12 kbar. They also studied low-

temperature normal-state transport, but did not clearly resolve any changes over this range of pressure. Much higher pressures of approximately 100 kbar were employed by Yoshida, Nakamura, *et al.* (1998) to study normal-state behavior above 4 K. There is a clear motivation to perform more high-pressure work on Sr_2RuO_4 in an effort to obtain insight into the spin fluctuations that many believe to be responsible for the superconductivity.

APPENDIX B: ISSUES CONCERNING ANGLE-RESOLVED PHOTOEMISSION SPECTROSCOPY IN Sr_2RuO_4

Angle-resolved photoemission spectroscopy (ARPES) has seen a huge growth in investment and interest over the past two decades. The technique of photoemission spectroscopy is based on measuring the momentum and energy of electrons ejected from a sample in response to radiation by photons, usually in the ultraviolet. In principle, it yields important information about the electronic band structure and Fermi surface, and (through line-shape analysis) is sensitive to many-body effects. Angular resolution allows this to be combined with Fermi-surface mapping. Although this mapping can be performed on materials with three-dimensional electronic structure, the technique is most suited to quasi-two-dimensional materials. In principle, ARPES is suitable for addressing crucial questions about correlated electron physics in the cuprates. This has motivated research leading to impressive advances in parallel data acquisition and, notably, resolution.

The suitability of ARPES for cuprates study is based on more than just two dimensionality. In those materials, it has proved to be impossible to perform any accurate quasiparticle spectroscopy with the bulk techniques such as quantum oscillations that have played such a key role in the physics of Sr_2RuO_4 . Experimental difficulties such as huge superconducting critical fields have so far proved to be insurmountable.⁵⁷ ARPES can be performed above and below the superconducting transition temperature, and has been used to address many of the key issues in cuprate physics. Although ARPES has these advantages, the most important problem is that it is fundamentally a probe of surface physics. The information that it yields comes from at best the top few atomic layers, which are commonly assumed to be representative of the bulk. Its surface sensitivity is well appreciated by ARPES researchers, and in the cuprates, many controversies have arisen due to different interpretations of the existing experimental data. There is an

inherent instability about placing great emphasis on the results of a developing technique when it is being used to study materials such as cuprates, which apparently show entirely new physics. It was interesting to see how ARPES functioned when studying a material for which it was possible to obtain detailed complementary information about electronic structure and correlations. This might be assumed to be a common situation, but it is not. For various reasons, quasi-two-dimensional systems for which there is detailed information from quantum oscillations have not been widely studied by ARPES. Sr_2RuO_4 , with its close structural similarity to the cuprates, provides a special opportunity in this regard.

Angle-integrated photoemission work on Sr_2RuO_4 has been used to study correlation effects,⁵⁸ but the angle-resolved studies have generated the most interest. The first studies were performed by Lu *et al.* (1996) and Yokoya *et al.* (1996a, 1996b) before the results of the dHvA work discussed in Sec. II were widely known. Both groups concentrated on the apparent observation of an “extended Van Hove singularity” just below the Fermi level over a fairly wide region of the Brillouin zone near the M point.⁵⁹ They emphasized the similarity between this feature and one that had been widely observed in the cuprates. It was immediately clear, however, that these results could not be representative of the bulk in Sr_2RuO_4 . They predicted a significantly different Fermi-surface topography from that predicted by electronic structure calculations and observed in the dHvA studies (Mackenzie *et al.*, 1997). Various suggestions for resolving the discrepancy were made by Yokoya *et al.* (1997), but subsequently shown to be inadequate (Mackenzie, Ikeda, *et al.*, 1998).

The significant discrepancy between ARPES and dHvA on one of the first occasions in which a detailed comparison had been possible was a serious concern, and a substantial body of work has gone into its investigation. Several theoretical scenarios based on modifications to the electronic structure near surfaces and/or photoemission cross sections have been proposed,⁶⁰ and detailed experimental investigations performed. The first direct experimental evidence for a surface effect of some kind playing an important role in the photoemission was reported by Puchkov *et al.* (1998). They observed a strong dependence of the spectra near the M point on fairly small changes in the incident photon energy. Then Matzdorf *et al.* (2000) discovered a surface atomic reconstruction in a scanning-tunneling microscopy study of the surface of Sr_2RuO_4 . Band reflection due to surface reconstruction was discussed in relation

⁵⁷Because of the superconductivity, it is not possible to work on a well-understood metallic state at laboratory-accessible dc magnetic fields. Even if it were, there is good evidence that the metallic state of most cuprates is not a Fermi liquid, and it is not clear what the quantum oscillatory signal from such a state would be. In some cuprates, the superconducting critical temperatures and fields can be depressed by doping, but in these cases, the resultant materials are often disordered.

⁵⁸For example, see Inoue *et al.* (1996, 1998). There has also been a study of x-ray fluorescence emission, by Kurmaev *et al.* (1998).

⁵⁹This scenario was also discussed in Schmidt *et al.* (1996) and Okuda *et al.* (1999).

⁶⁰For example, see Seibel and Winter (1998); Liebsch and Lichtenstein (2000).

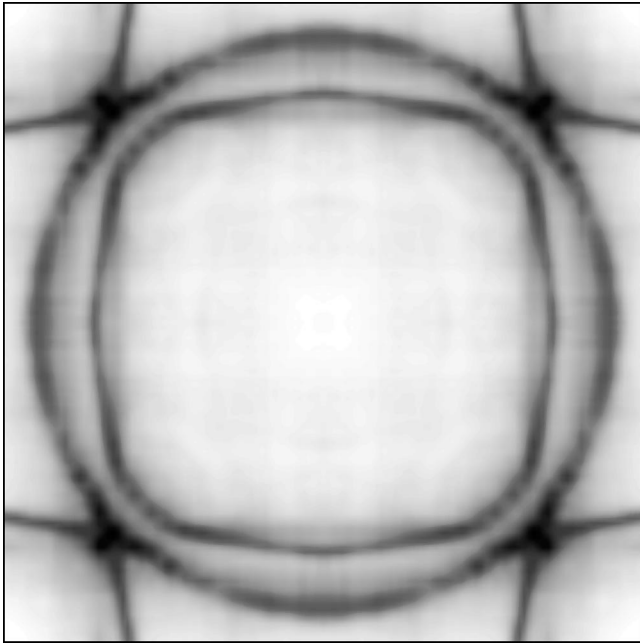


FIG. 40. The Fermi surface of Sr_2RuO_4 reported by Damascelli *et al.* (2000) after the use of a special sample preparation technique to remove a purely surface-related feature near the M point of the Brillouin zone.

to a new generation of ARPES measurements (for example, see Damascelli *et al.*, 2000; Ding *et al.*, 2001).

The precise relationship of the surface reconstruction of Matzdorf *et al.* (2000) to the photoemission spectra would be relatively difficult to calculate. Its existence strongly suggests that the observed signals are a mixture from surface layers with inhomogeneous properties, and the situation is further complicated by calculations suggesting that the top layer might even be ferromagnetic.

Much of the need to model the behavior near the M point was overcome by the empirical discovery of Damascelli *et al.* (2000) in which they showed that they could deliberately degrade the surface layer and apparently remove its contribution to the ARPES spectra. This was achieved by reversing the usual “good practice” of low-temperature cleaving, and instead cleaving at 180 K. This might have been expected both to remove the signal from the surface (or top layer) and at the same time broaden or degrade the assumed “bulk” contribution (i.e., that from lower layers). Instead, it removed the former and actually sharpened the latter, resulting in the ARPES-derived Fermi surface shown in Fig. 40. This Fermi surface agrees well with that predicted by electronic structure calculations. The areas of the α and β sheets differ slightly from those predicted by, for example, Oguchi (1995), but this feature is also seen in dHvA. The ARPES work also gives angular information that cannot be obtained from dHvA in isolation (for a discussion, see Bergemann *et al.*, 2000).

That Fermi-surface data of the quality shown in Fig. 40 can be obtained from a multiband material such as Sr_2RuO_4 is a testament to the advances that have been made with ARPES. It does not, however, mean the end

to all uncertainty or controversy regarding the detail of how to interpret ARPES data. For example, the interpretation of Damascelli *et al.* (2000) and Puchkov *et al.* (1998) that the surface-related features should be understood in terms of a surface state has since undergone some revision (Damascelli *et al.*, 2001; Liebsch, 2001; Shen *et al.*, 2001). A question of more fundamental importance is whether the story that has unfolded regarding Sr_2RuO_4 (and other outstanding controversies regarding ARPES) will lead to the development of robust experimental methods for separating signals genuinely representative of the bulk from those due purely to surface effects. It will be vital to develop this capability for the community to have confidence in ARPES results on materials for which there is no independent experimental check on bulk electronic structure from probes such as dHvA. If it can be done, then Sr_2RuO_4 will have made an important long-term contribution to the development of a very important technique. Another area in which we believe that Sr_2RuO_4 should prove useful is in line-shape analysis. As ARPES resolution improves still further, it will be interesting to compare line shapes from Sr_2RuO_4 , where there is so much independent data about electron correlations, with those obtained from other materials in which ARPES is the often the primary source of such information.

APPENDIX C: THE “3-K” PHASE OF Sr_2RuO_4 -Ru

As the program of crystal growth of Sr_2RuO_4 proceeded in the years immediately following the discovery of superconductivity, it was observed that the ac susceptibility of some growth batches occasionally appeared to show weak diamagnetism up to temperatures as high as 3 K (Maeno *et al.*, 1996). It was soon clear that this was fully double the intrinsic T_c of 1.5 K expected of pure Sr_2RuO_4 (Mackenzie, Haselwimmer, *et al.*, 1998a, 1998b), raising questions about its origin. It was then noticed that the anomalous diamagnetic signals occurred in samples in which x-ray diffraction revealed the presence of small concentrations of Ru metal. Polishing crystals from these batches showed small platelets of Ru embedded in the Sr_2RuO_4 . The platelets had approximate thickness of 1 μm and length and width of 1–30 μm . The interplatelet separation was of order 10 μm , and the region of Ru inclusion was usually at the central portion of a cross section through the grown crystal rod. The density of inclusions is very similar wherever they occur, and they have no unique preferred orientation relative to the crystal axes of the Sr_2RuO_4 . Spatially resolved electron-probe analysis showed no sign of any concentration gradient of Ru or Sr_2RuO_4 on the approach to an interface, nor of any resolvable oxidation of the Ru metal.

As discussed by Maeno *et al.* (1998), all of the above observations are consistent with eutectic solidification in

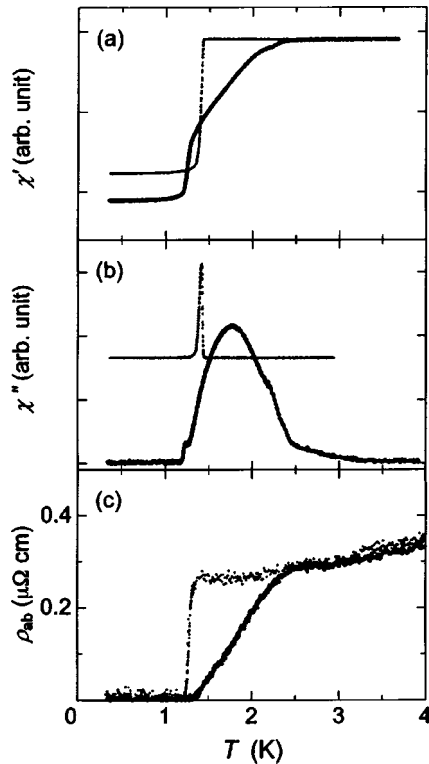


FIG. 41. (a) In-phase and (b) out-of-phase components of the ac susceptibility, and (c) in-plane resistivity, for typical crystals of Sr_2RuO_4 with and without Ru platelets (large and small symbols, respectively). Crystals without the platelets show sharp transitions at 1.4–1.5 K, while those containing platelets show the broad transitions displayed by the 3-K superconductivity. From Maeno *et al.* (1998).

a Ru-rich melt.⁶¹ The important consequence of this is that in the two-phase region, the volume fraction of Ru is dependent on the composition of the eutectic point, and not on details of the growth conditions. This removes some of the uncertainty in comparing different “3-K phase” samples. Typical susceptibility and resistivity data from single- and two-phase crystals are shown in Fig. 41. Everything points to the existence of some spatially inhomogeneous second superconducting phase. Of most interest from the point of view of ruthenate superconductivity is why the two-phase sample should have such an enhanced T_c . As shown by Maeno and co-workers, it is not purely an effect of the ruthenium, for several reasons. First, the T_c of pure Ru metal is only 0.5 K. Second, the large diamagnetic shielding suggests that it is predominantly a surface effect. Third, the anisotropy of the superconducting critical fields is related to that of the crystal lattice of Sr_2RuO_4 , although there is no unique orientation of the Ru platelets relative to this

⁶¹The principles are described, for example, in P. Gordon, *Principles of Phase Diagrams in Materials Systems* (McGraw-Hill, New York, 1968), Chap. 6.

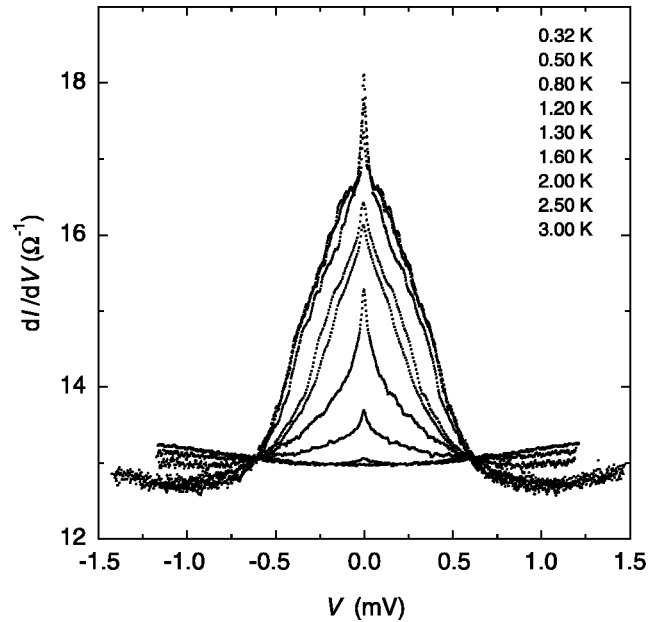


FIG. 42. Tunneling spectra for c -axis break junctions containing Ru platelets. The large peak in the conductance at zero bias is evidence for the existence of Andreev bound states, which are evidence in favor of unconventional superconductivity. The sharp central peak survives all the way to the T_c of the 3-K phase. From Mao, Nelson, *et al.* (2001).

lattice. Taken together, these observations strongly suggest a picture of surface superconductivity at the Ru- Sr_2RuO_4 interface, residing dominantly in Sr_2RuO_4 (Maeno *et al.*, 1998).

The properties of the 3-K phase were investigated in detail by Ando *et al.* (1999). They showed that although the critical-field anisotropy relates to the anisotropic electronic structure of Sr_2RuO_4 , its value is approximately 3, compared to 20 for pure Sr_2RuO_4 . This suggests a hybrid state existing, by proximity, in both the strongly anisotropic Sr_2RuO_4 and the much more isotropic Ru. Important evidence that the 3-K phase superconducting state is unconventional came from Mao, Nelson, *et al.* (2001). In their experiment, tunneling c -axis break junctions were made from two-phase crystals. Zero-bias conduction peaks are seen, as shown in Fig. 42. The fact that the sharp central feature persists to well above the T_c of pure Sr_2RuO_4 suggests that it is intrinsic to the 3-K phase. This interpretation is supported by the fact that the broad outer features can be suppressed at low temperatures by working in a magnetic field that exceeds the critical field of bulk Sr_2RuO_4 but not that of the 3-K phase. The conclusion drawn by Mao *et al.* is that there is a strong tendency to form surface Andreev bound states in the interface region of Ru- Sr_2RuO_4 . Since these states indicate an order parameter with a direction-dependent phase (see Sec. III.D), these results are good evidence in favor of unconventional superconductivity in the 3-K phase of Sr_2RuO_4 -Ru.

Sigrist and Monien (2001) have constructed a phenomenological theory for the 3-K phase, based on a gen-

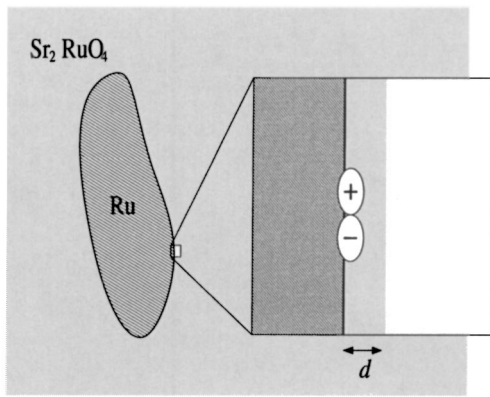


FIG. 43. Interface order parameter proposed by Sigrist and Monien (2001) for the 3-K phase. A p -wave state nucleates at the interface, with amplitude in both Sr_2RuO_4 and Ru. Its wave function has lobes parallel and nodes perpendicular to the interface.

eralized Ginzburg-Landau formalism. Their assumption is that there exists a superconducting surface state with a higher T_c than that of the bulk. Their key findings are that the lowered symmetry of the interface promotes a superconducting state with a different symmetry to that in the bulk. More precisely, they argue that the k_x, k_y degeneracy of the basic $\Delta_0 \hat{z}(k_x \pm ik_y)$ state postulated for the bulk is lifted, and that the component of this state oriented as shown in Fig. 43 is the lowest-energy solution. They argue that the phase structure is particularly favorable for the formation of Andreev bound states, and that their solution is therefore consistent with the findings of Mao, Nelson, *et al.* (2001). A prediction of their theory is that near T_c , H_{c2} should not have the standard $(1 - T/T_c)$ dependence, but instead should vary as $(1 - T/T_c)^{0.5}$. This arises because although only the component shown in Fig. 43 exists in zero applied field, the application of the field allows the other component to stabilize as well. A second consequence of this would be an enhancement of the critical field at low temperatures, an effect that is predicted to be strongest for fields along the crystallographic c axis.

Recently, the critical fields of 3-K phase material were studied to higher precision by Wada and co-workers (2002). Their results are shown in Fig. 44. Near T_c , H_{c2} has a temperature dependence closer to the Sigrist-Monien prediction than to that for a standard superconductor, and upward curvature is seen for $H \parallel c$. Another feature of the data (first reported by Ando *et al.*, 1999) is the existence of hysteresis for $H \parallel ab$ at high fields and low temperatures.

It will be interesting to examine the properties of the 3-K phase in more detail, to further check the theory of Sigrist and Monien. As they point out, measurements isolating one interface would be particularly desirable. The problem with bulk measurements is that they involve averaging over the inhomogeneity that is inevita-

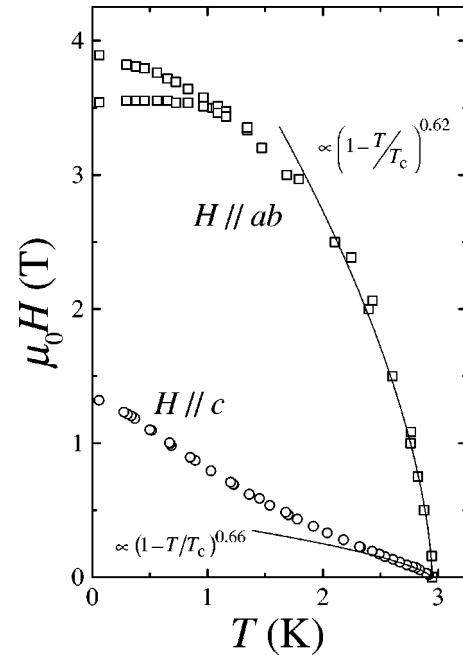


FIG. 44. Upper critical-field data obtained for the 3-K phase by Wada *et al.* (2002). Several features are in qualitative agreement with the predictions of Sigrist and Monien (2001), namely, (a) the unusual temperature dependence near T_c for both field orientations and (b) the enhancement and upward curvature seen for $H \parallel c$. The split data for $H \parallel ab$ at low temperatures represent the fact that the transition becomes hysteretic in that region.

bly present in a two-phase eutectic solidification.⁶² Confirmation of the basic picture proposed by the theory would be powerful evidence in favor of the triplet order parameter for bulk Sr_2RuO_4 that Sigrist and Monien used as an input parameter in their calculation. It might also be possible to address the fascinating issue of the superconducting mechanism in Sr_2RuO_4 . Understanding the reason for T_c enhancement at an interface is an obvious way to gain insight into the determining factors in the bulk.⁶³ The 3-K phase of Sr_2RuO_4 is a striking example of the role of phase rules in materials science, but it has turned out to be of broader interest than that alone.

APPENDIX D: FURTHER EXAMPLES OF VECTOR ORDER PARAMETERS

Earlier in the article, we presented an analysis of the vector order parameter that has been most discussed in relation to Sr_2RuO_4 , namely, $\mathbf{d} = \Delta_0 \hat{z}(k_x \pm ik_y)$. We be-

⁶²Examples of interesting work that is subject to this difficulty include Jin *et al.* (2000) and Hildebrand *et al.* (2001).

⁶³It is possible, however, that T_c is raised mainly because of a change to the density of states due to interface stress. Sigrist and Monien argue that the behavior of the Σ_3 phonon mode observed by Braden *et al.* (1998) makes this a plausible scenario.

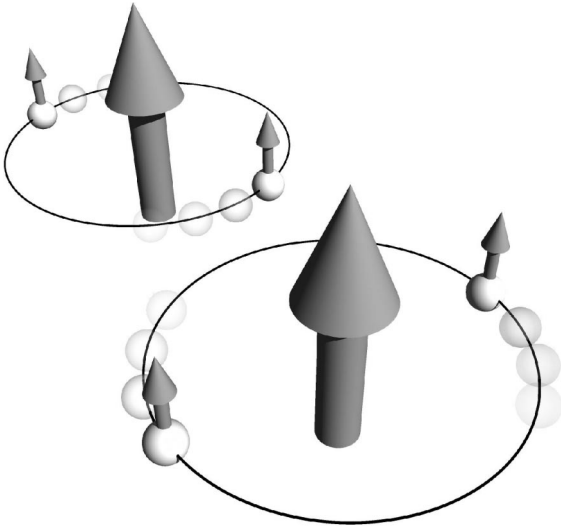


FIG. 45. Cooper pair \mathbf{S} and \mathbf{L} vectors for $\mathbf{d} = \Delta_0/2(\hat{\mathbf{x}} + i\hat{\mathbf{y}})(k_x + ik_y)$. The large arrows denote \mathbf{L} and the small arrows the spins of the electrons in a pair. Both \mathbf{S} and \mathbf{L} are aligned out of plane. Only one spin direction is paired, so it is a nonunitary state in which TRS is broken by both spin and orbital parts. This is the two-dimensional analog of the A1 phase of ³He. Image by K. Deguchi.

lieve that some readers would find it useful to see additional worked examples. Our goal is not a detailed theoretical analysis, but an attempt to enable someone new to the field to deduce the basic symmetries, spin directions, and nodal structures associated with a given d vector. In our opinion, this kind of “practical working guide” to decoding vector order parameters is absent from most of the literature. We have chosen three extra order parameters for analysis. Two of them are two-dimensional analogs of the A1 and B phases that exist in ³He, chosen to emphasize the possible links between the physics of that superfluidity (on which much of the source literature on d vectors concentrates) and the superconductivity of Sr₂RuO₄. The third example concerns a state with vertical line nodes that Sr₂RuO₄ would be expected to adopt in symmetry-breaking fields if its order parameter in the absence of such fields is indeed closely related to $\mathbf{d} = \Delta_0\hat{\mathbf{z}}(k_x \pm ik_y)$.⁶⁴

1. An example of the nonunitary state—the two-dimensional analog of the A1 phase of superfluid ³He

This triplet state has the order parameter

⁶⁴In keeping with the discussion of Sec. IV and Table IV, we adopt a two-dimensional convention, which neglects the interlayer processes that may be important in Sr₂RuO₄. This would still be a useful approximation if the interlayer processes are “additional” to the underlying in-plane ones, i.e., they do not lead to any fundamental changes in symmetry.

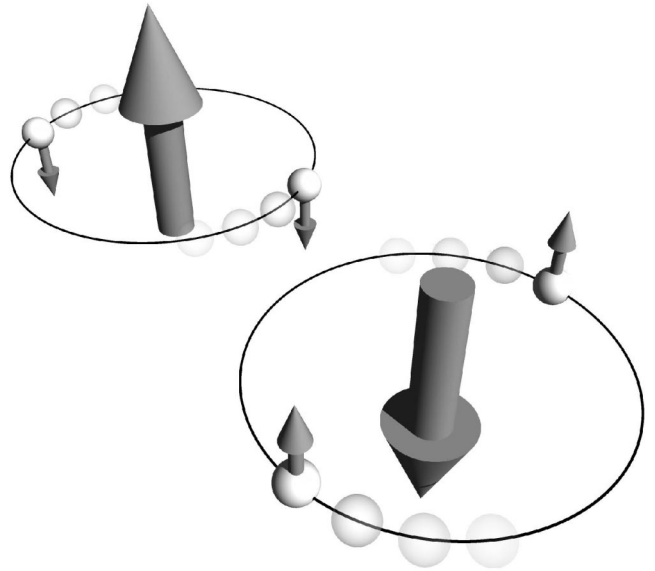


FIG. 46. Cooper pair \mathbf{S} and \mathbf{L} vectors for $\mathbf{d} = \Delta_0(\hat{\mathbf{x}}k_x + \hat{\mathbf{y}}k_y)$. The large arrows denote \mathbf{L} and the small arrows the spins of the electrons in a pair. The state consists of an equal superposition of pairs with \mathbf{S} antiparallel to \mathbf{L} , with no favored direction. It therefore respects TRS. This is the two-dimensional analog of the BW, or A phase of ³He. Image by K. Deguchi.

$$\begin{aligned} \mathbf{d} &= \Delta_0/2(\hat{\mathbf{x}} + i\hat{\mathbf{y}})(k_x + ik_y) \\ &= \Delta_0/2 \left\{ \begin{bmatrix} k_x + ik_y \\ 0 \\ 0 \end{bmatrix} + i \begin{bmatrix} 0 \\ k_x + ik_y \\ 0 \end{bmatrix} \right\}. \end{aligned} \quad (\text{D1})$$

In ³He this phase emerges in a very narrow temperature region just below T_c in an applied magnetic field, until it changes to the A phase at lower temperatures. As depicted in Fig. 45, the $S=1$ spin pairs, as well as the orbital angular momentum, are pointing in the c direction (assuming that the z direction for spin corresponds to the c direction of the crystal). Time-reversal symmetry is thus broken in both orbital and spin space. The state is nonunitary because

$$\mathbf{d} \times \mathbf{d}^* = -i\Delta_0\hat{\mathbf{z}}(k_x^2 + k_y^2) \quad (\text{D2})$$

remains nonzero. There are therefore two energy gaps,

$$|\Delta(\mathbf{k}) \pm| = (k_x^2 + k_y^2)^{1/2}(1 \pm 1) = 2(k_x^2 + k_y^2)^{1/2} \text{ or } 0. \quad (\text{D3})$$

Thus the spin-up species has an isotropic gap, whereas the spin-down species has a zero gap and they remain as quasiparticles. As a consequence, half of the Fermi surface remains ungapped.

2. The two-dimensional analog of the B phase of superfluid ³He

A two-dimensional Balian-Werthamer state is described by

$$\mathbf{d} = \Delta_0(\hat{\mathbf{x}}k_x + \hat{\mathbf{y}}k_y) = \Delta_0 \begin{bmatrix} k_x \\ k_y \\ 0 \end{bmatrix}. \quad (\text{D4})$$

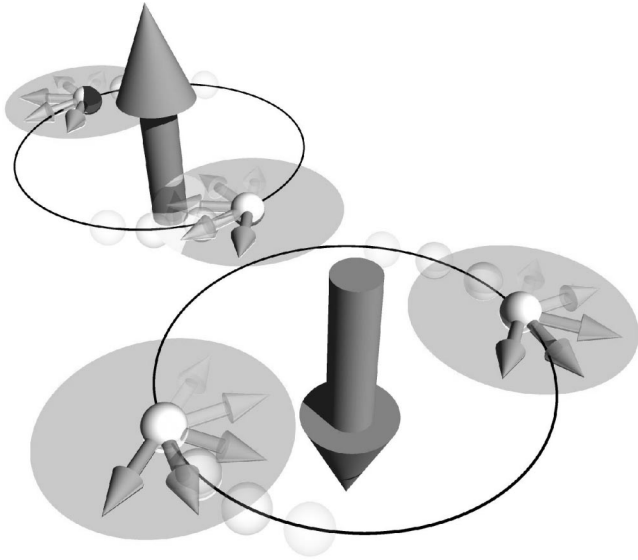


FIG. 47. Cooper pair \mathbf{S} and \mathbf{L} vectors for $\mathbf{d} = \Delta_0 \hat{z} k_x$. The large arrows denote \mathbf{L} and the small arrows the spins of the electrons in a pair. There is equal spin pairing for any quantization axis in the plane, similar to Fig. 20. Here, though, there is no favored direction of \mathbf{L} , so TRS is respected. Image by K. Deguchi.

Since this order parameter can also be expressed as

$$\mathbf{d} = \Delta_0/2\{(\hat{x} + i\hat{y})(k_x - ik_y) + (\hat{x} - i\hat{y})(k_x + ik_y)\}, \quad (\text{D5})$$

it can be thought of as the superposition of the two states with parallel and antiparallel combinations of spin and orbital wave functions, with quenched overall orbital angular momentum, as depicted in Fig. 46. In this state the spin, as well as the orbital momentum, is quantized along the c direction, but time-reversal symmetry remains unbroken since there is no net value for either

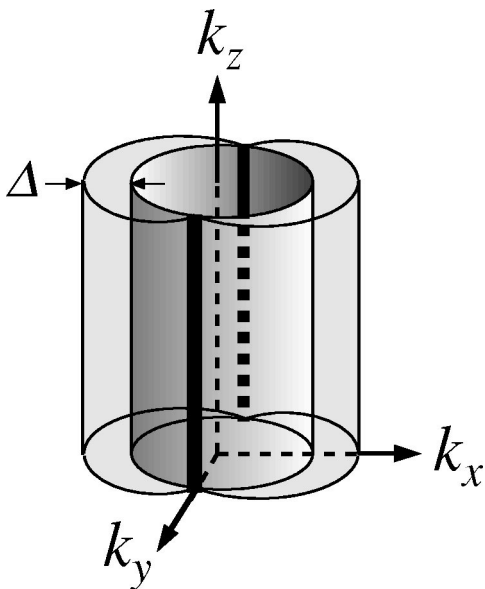


FIG. 48. Energy gap corresponding to $\mathbf{d} = \Delta_0 \hat{z} k_x$, which has vertical line nodes on a cylindrical Fermi surface. Image by K. Deguchi.

quantity. The cross product $\mathbf{d} \times \mathbf{d}^* = 0$, so the state is unitary. The energy gap $|\Delta(\mathbf{k})| = (k_x^2 + k_y^2)^{1/2}$ is nodeless, as sketched in Fig. 21.

3. A final example, of possible relevance to Sr₂RuO₄ in symmetry-breaking fields

In the presence of certain symmetry-breaking fields, the degeneracy of the two components of an order parameter such as $\mathbf{d} = \Delta_0 \hat{z}(k_x \pm ik_y)$ can be broken (see the discussion in Sec. VII), providing the state

$$\mathbf{d} = \Delta_0 \hat{z} k_x = \Delta_0 \begin{bmatrix} 0 \\ 0 \\ k_x \end{bmatrix}. \quad (\text{D6})$$

The spins have the same properties as those for $\mathbf{d} = \Delta_0 \hat{z}(k_x \pm ik_y)$ (see the analysis in Sec. IV.A.2). Since $\mathbf{d} = \Delta_0 \hat{z} k_x$ can be written as $\mathbf{d} = \Delta_0/2\hat{z}\{(k_x + ik_y) + (k_x - ik_y)\}$, it can be seen to consist of a superposition of $L_z = +1$ and -1 states, as depicted in Fig. 47. Again, there is no overall spin or orbital angular momentum, so time-reversal symmetry is respected. The state is also unitary.

In contrast to $\mathbf{d} = \Delta_0 \hat{z}(k_x \pm ik_y)$, the energy gap of $\mathbf{d} = \Delta_0 \hat{z} k_x$ has nodes

$$|\Delta(\mathbf{k})| = |k_x|. \quad (\text{D7})$$

These would be vertical line nodes on a cylindrical Fermi surface, as sketched in Fig. 48.

REFERENCES

- Abrikosov, A. A., and L. P. Gor'kov, 1960a, Zh. Eksp. Teor. Fiz. **39**, 1781 [Sov. Phys. JETP **12**, 1243].
 Abrikosov, A. A., and L. P. Gor'kov, 1960b, Zh. Eksp. Teor. Fiz. **42**, 1088 [Sov. Phys. JETP **15**, 752].
 Aegerter, C. M., S. H. Lloyd, C. Ager, S. L. Lee, S. Romer, H. Keller, and E. M. Forgan, 1998, J. Phys.: Condens. Matter **10**, 7445.
 Agterberg, D. F., 1998a, Phys. Rev. Lett. **80**, 5184.
 Agterberg, D. F., 1998b, Phys. Rev. B **58**, 14 484.
 Agterberg, D. F., 1999, Phys. Rev. B **60**, R749.
 Agterberg, D. F., 2001, Phys. Rev. B **64**, 052502.
 Agterberg, D. F., T. M. Rice, and M. Sigrist, 1997, Phys. Rev. Lett. **78**, 3374.
 Akima, T., S. Nishizaki, and Y. Maeno, 1999, J. Phys. Soc. Jpn. **68**, 694.
 Alexandrov, A. S., and A. M. Bratkovsky, 1996, Phys. Rev. Lett. **76**, 1308.
 Anderson, P. W., 1959, Phys. Rev. Lett. **3**, 325.
 Ando, T., T. Akima, Y. Mori, and Y. Maeno, 1999, J. Phys. Soc. Jpn. **68**, 1651.
 Androes, G. M., and W. D. Knight, 1961, Phys. Rev. **121**, 779.
 Annett, J. F., 1990, Adv. Phys. **39**, 83.
 Annett, J. F., 1995, Contemp. Phys. **36**, 423.
 Aoki, D., A. Huxley, E. Ressouche, D. Braithwaite, J. Flouquet, J. P. Brison, E. Lhotel, and C. Paulsen, 2001, Nature (London) **413**, 613.
 Ardavan, A., R. S. Edwards, E. Rzepniewski, J. Singleton, and S. J. Blundell, 2001, Physica B **294**, 379.

- Aubin, H., K. Behnia, M. Ribault, R. Gagnon, and L. Taillefer, 1997, *Phys. Rev. Lett.* **78**, 2624.
- Balian, R., and N. R. Werthamer, 1963, *Phys. Rev.* **131**, 1553.
- Barrett, S. E., D. J. Durand, C. H. Pennington, C. P. Slichter, T. A. Friedmann, J. P. Rice, and D. M. Ginsberg, 1990, *Phys. Rev. B* **41**, 6283.
- Baskaran, G., 1996, *Physica B* **224**, 490.
- Bednorz, J. G., and K. A. Müller, 1986, *Z. Phys. B: Condens. Matter* **64**, 189.
- Bergemann, C., 2002, private communication.
- Bergemann, C., J. S. Brooks, L. Balicas, A. P. Mackenzie, S. R. Julian, Z. Q. Mao, and Y. Maeno, 2001, *Physica B* **294**, 371.
- Bergemann, C., S. R. Julian, A. P. Mackenzie, S. Nishizaki, and Y. Maeno, 2000, *Phys. Rev. Lett.* **84**, 2662.
- Bergemann, C., S. R. Julian, A. P. Mackenzie, A. W. Tyler, D. E. Farrell, Y. Maeno, and S. Nishizaki, 1999, *Physica C* **318**, 444.
- Bergemann, C., A. P. Mackenzie, S. R. Julian, D. Forsythe, and E. Ohmichi, 2002, *Adv. Phys.* (in press).
- Berger, H., L. Forro, and D. Pavuna, 1998, *Europhys. Lett.* **41**, 531.
- Bonalde, I., B. D. Yanoff, D. J. Van Harlingen, M. B. Salamon, and Y. Maeno, 2000, *Phys. Rev. Lett.* **85**, 4775.
- Braden, M., O. Friedt, Y. Sidis, P. Bourges, M. Minakata, and Y. Maeno, 2002, *Phys. Rev. Lett.* **88**, 197002.
- Braden, M., A. H. Moudden, S. Nishizaki, Y. Maeno, and T. Fujita, 1997, *Physica C* **273**, 248.
- Braden, M., W. Reichardt, S. Nishizaki, Y. Mori, and Y. Maeno, 1998, *Phys. Rev. B* **57**, 1236.
- Brewer, J. H., 1994, in *Encyclopedia of Applied Physics*, edited by G. L. Trigg (VCH, New York), Vol. 11, p. 23.
- Brison, J. P., L. Glemot, H. Suderow, A. Huxley, S. Kambe, and J. Flouquet, 2000, *Physica B* **280**, 165.
- Callaghan, A., C. W. Moeller, and R. Ward, 1966, *Inorg. Chem.* **5**, 1572.
- Carter, S. A., B. Batlogg, R. J. Cava, J. J. Krajewski, W. F. Peck, Jr., and L. W. Rupp Jr., 1995, *Phys. Rev. B* **51**, 17 184.
- Cava, R. J., B. Batlogg, K. Kiyono, H. Takagi, J. J. Krajewski, W. F. Peck, L. W. Rupp, and C. H. Chen, 1994, *Phys. Rev. B* **49**, 11 890.
- Chashechkina, E. I., I. J. Lee, S. E. Brown, D. S. Chow, W. G. Clark, M. J. Naughton, and P. M. Chaikin, 2001, *Synth. Met.* **119**, 13.
- Chmaissem, O., J. D. Jorgensen, H. Shaked, S. Ikeda, and Y. Maeno, 1998, *Phys. Rev. B* **57**, 5067.
- Choi, M. Y., P. M. Chaikin, and R. L. Greene, 1984, *Phys. Rev. B* **34**, 7727.
- Clarke, D. G., and S. P. Strong, 1997, *Adv. Phys.* **46**, 545.
- Clogston, A. M., 1962, *Phys. Rev. Lett.* **9**, 266.
- Clogston, A. M., A. C. Gossard, V. Jaccarino, and Y. Yafet, 1964, *Rev. Mod. Phys.* **36**, 170.
- Dahm, T., H. Won, and K. Maki, 2002, cond-mat/0006301.
- Dalichaouch, Y., M. C. de Andrade, D. A. Gajewski, R. Chau, P. Visani, and M. B. Maple, 1995, *Phys. Rev. Lett.* **75**, 3938.
- Damascelli, A., D. H. Lu, K. M. Shen, N. P. Armitage, R. Ronning, D. L. Feng, C. Kim, Z. X. Shen, T. Kimura, Y. Tokura, Z. Q. Mao, and Y. Maeno, 2000, *Phys. Rev. Lett.* **85**, 5194.
- Damascelli, A., K. M. Shen, D. H. Lu, and Z. X. Shen, 2001, *Phys. Rev. Lett.* **87**, 239702.
- de Boer, P. K., and R. A. de Groot, 1999, *Phys. Rev. B* **59**, 9894.
- Deguchi, K., M. Tanatar, Z. Mao, T. Ishiguro, and Y. Maeno, 2002, *J. Phys. Soc. Jpn.* **71**, 2839.
- Dereotier, P. D., A. Huxley, A. Yaouanc, J. Flouquet, P. Bonville, P. Imbert, P. Pari, P. C. M. Gubbens, and A. M. Mulders, 1995, *Phys. Lett. A* **205**, 239.
- de Wilde, Y., M. Iavarone, U. Welp, V. Metlushko, A. E. Koshelev, I. Aranson, G. W. Crabtree, P. L. Gammel, D. J. Bishop, and P. C. Canfield, 1997, *Physica C* **282-287**, 355.
- Ding, H., S. C. Wang, H. B. Yang, T. Takahashi, J. C. Campuzano, and Y. Maeno, 2001, *Physica C* **364**, 594.
- Duffy, J. A., S. M. Hayden, Y. Maeno, Z. Mao, J. Kulda, and G. J. McIntyre, 2000, *Phys. Rev. Lett.* **85**, 5412.
- Ellman, B., L. Taillefer, and M. Poirer, 1996, *Phys. Rev. B* **54**, 9043.
- Forgan, E. M., 2000, private communication.
- Forgan, E. M., A. P. Mackenzie, and Y. Maeno, 1999, *J. Low Temp. Phys.* **117**, 1567.
- Fukuzumi, Y., K. Mizuhashi, K. Takanaka, and S. Uchida, 1996, *Phys. Rev. Lett.* **76**, 684.
- Gardner, J. S., G. Balakrishnan, and D. McK. Paul, 1995, *Physica C* **252**, 303.
- Gardner, J. S., G. Balakrishnan, D. McK. Paul, and C. Haworth, 1996, *Physica C* **265**, 251.
- Geibel, C., C. Schank, F. Jähring, B. Buschinger, A. Grauel, T. Lühmann, P. Gegenwart, R. Helfrich, P. H. P. Reinders, and F. Steglich, 1994, *Physica B* **199&200**, 128.
- Goryo, J., 2000, *Phys. Rev. B* **61**, 4222.
- Graf, M. J., and A. V. Balatsky, 2000, *Phys. Rev. B* **62**, 9697.
- Hardy, W. N., D. A. Bonn, D. C. Morgan, R. X. Liang, and K. Zhang, 1993, *Phys. Rev. Lett.* **70**, 3999.
- Harrison, N., R. Bogaerts, P. H. P. Reinders, J. Singleton, S. J. Blundell, and F. Herlach, 1996, *Phys. Rev. B* **54**, 9977.
- Hase, I., and Y. Nishihara, 1996, *J. Phys. Soc. Jpn.* **65**, 3957.
- Hasegawa, Y., K. Machida, and M. Ozaki, 2000, *J. Phys. Soc. Jpn.* **69**, 336.
- Hasselbach, K., J. R. Kirtley, and J. Flouquet, 1993, *Phys. Rev. B* **47**, 509.
- Hebel, L. C., and C. P. Slichter, 1957, *Phys. Rev.* **107**, 901.
- Heeb, R., and D. F. Agterberg, 1999, *Phys. Rev. B* **59**, 7076.
- Hein, M. A., R. J. Ormeno, and C. E. Gough, 2001a, *J. Phys.: Condens. Matter* **13**, L65.
- Hein, M. A., R. J. Ormeno, and C. E. Gough, 2001b, *Phys. Rev. B* **64**, 024529.
- Higemoto, W., 2002, private communication.
- Hildebrand, M. G., M. Reedyk, T. Katsufuji, and Y. Tokura, 2001, *Phys. Rev. Lett.* **87**, 227002.
- Hill, S., J. S. Brooks, Z. Q. Mao, and Y. Maeno, 2000, *Phys. Rev. Lett.* **84**, 3374.
- Hirai, T., Y. Tanuma, Y. Tanaka, J. Inoue, and S. Kashiwaya, 2001, *Physica C* **357**, 1580.
- Hirai, T., N. Yoshida, Y. Tanaka, J. Inoue, and S. Kashiwaya, 2001, *J. Phys. Soc. Jpn.* **70**, 1885.
- Honerkamp, C., and M. Sigrist, 1998a, *Prog. Theor. Phys.* **100**, 53.
- Honerkamp, C., and M. Sigrist, 1998b, *J. Low Temp. Phys.* **111**, 895.
- Huang, Q., J. L. Soubeyroux, O. Chmaissem, I. Natali Sora, A. Santoro, R. J. Cava, J. J. Krajewski, and W. F. Peck, Jr., 1994, *J. Solid State Chem.* **112**, 355.
- Hussey, N. E., A. P. Mackenzie, J. R. Cooper, S. Nishizaki, Y. Maeno, and T. Fujita, 1998, *Phys. Rev. B* **57**, 5505.
- Ikeda, S., Y. Maeno, S. Nakatsuji, M. Kosaka, and Y. Uwatoko, 2000, *Phys. Rev. B* **62**, R6089.
- Imai, T., A. W. Hunt, K. R. Thurber, and F. C. Chou, 1998, *Phys. Rev. Lett.* **81**, 3006.

- Inoue, I. H., A. Kimura, A. Harasawa, A. Kakizaki, Y. Aiura, S. Ikeda, and Y. Maeno, 1998, *J. Phys. Chem. Solids* **59**, 2205.
- Inoue, I. H., H. Makino, Y. Aiura, I. Hase, Y. Maeno, Y. Haruyama, S. Nishizaki, T. Fujita, and Y. Nishihara, 1996, *Czech. J. Phys.* **46**, Suppl. S5, 2699.
- Ishida, K., Y. Kitaoka, K. Asayama, S. Ikeda, S. Nishizaki, Y. Maeno, K. Yoshida, and T. Fujita, 1997, *Phys. Rev. B* **56**, R505.
- Ishida, K., H. Mukuda, Y. Kitaoka, K. Asayama, Z. Q. Mao, Y. Mori, and Y. Maeno, 1998, *Nature (London)* **396**, 658.
- Ishida, K., H. Mukuda, Y. Kitaoka, Z. Q. Mao, H. Fukazawa, and Y. Maeno, 2001a, *Phys. Rev. B* **63**, 060507(R).
- Ishida, K., H. Mukuda, Y. Kitaoka, Z. Q. Mao, Y. Mori, and Y. Maeno, 2000, *Phys. Rev. Lett.* **84**, 5387.
- Ishida, K., H. Mukuda, Y. Minami, Y. Kitaoka, Z. Q. Mao, H. Fukazawa, and Y. Maeno, 2001b, *Phys. Rev. B* **64**, 100501.
- Izawa, K., H. Takahashi, H. Yamaguchi, Y. Matsuda, M. Suzuki, T. Sasaki, T. Fukase, Y. Yoshida, R. Settai, and Y. Onuki, 2001, *Phys. Rev. Lett.* **86**, 2653.
- Jin, R., Y. Liu, and F. Lichtenberg, 1999, *Phys. Rev. B* **60**, 10 418.
- Jin, R., Y. Liu, Z. Q. Mao, and Y. Maeno, 2000, *Europhys. Lett.* **51**, 341.
- Jin, R., Yu. Zadorozhny, D. G. Schlom, Y. Liu, F. Lichtenberg, and J. G. Bednorz, 1998, *J. Phys. Chem. Solids* **59**, 2215.
- Jin, R., Yu. Zadorozhny, D. G. Schlom, Y. Mori, Y. Maeno, and Y. Liu, 1999, *Phys. Rev. B* **59**, 4433.
- Julian, S. R., A. P. Mackenzie, G. G. Lonzarich, C. Bergemann, R. K. W. Haselwimmer, Y. Maeno, S. Nishizaki, A. W. Tyler, S. Ikeda, and T. Fujita, 1999, *Physica B* **259-261**, 928.
- Kato, Y., 2000, *J. Phys. Soc. Jpn.* **69**, 3378.
- Katsufuji, T., M. Kasai, and Y. Tokura, 1996, *Phys. Rev. Lett.* **76**, 126.
- Kealey, P. G., T. M. Riseman, E. M. Forgan, A. P. Mackenzie, L. M. Galvin, S. L. Lee, D. McK. Paul, R. Cubitt, D. F. Agterberg, R. Heeb, Z. Q. Mao, and Y. Maeno, 2000, *Phys. Rev. Lett.* **84**, 6094.
- Kita, T., 1999, *Phys. Rev. Lett.* **83**, 1846.
- Kogan, V. G., M. Bullock, B. Harmon, P. Miranovic, L. Dobrosavljevic-Grujic, P. L. Hammel, and D. J. Bishop, 1997, *Phys. Rev. B* **55**, 8693.
- Kohori, Y., T. Kohara, H. Shibai, Y. Oda, Y. Kitaoka, and K. Asayama, 1988, *J. Phys. Soc. Jpn.* **57**, 395.
- Kurmaev, E. Z., S. Stadler, D. L. Ederer, Y. Harada, S. Shin, M. M. Grush, T. A. Callcott, R. C. C. Perera, D. A. Zatsopin, N. Ovechkina, M. Kasai, Y. Tokura, T. Takahashi, K. Chandrasekaran, R. Vijayaraghavan, and U. V. Varadaraju, 1998, *Phys. Rev. B* **57**, 1558.
- Kuroki, K., M. Ogata, R. Arita, and H. Aoki, 2001, *Phys. Rev. B* **63**, 060506.
- Kuwabara, T., and M. Ogata, 2000, *Phys. Rev. Lett.* **85**, 4586.
- Langhammer, C., F. Steglich, M. Lang, and T. Sasaki, 2002, *Eur. Phys. J. B* **26**, 413.
- Larkin, A. I., 1965, *Zh. Eksp. Teor. Fiz., Pis'ma Red.* **2**, 205 [*JETP Lett.* **2**, 130 (1965)].
- Laube, F., G. Goll, H. v. Löhneysen, M. Fogelstrom, and F. Lichtenberg, 2000, *Phys. Rev. Lett.* **84**, 1595.
- Lee, I. J., S. E. Brown, W. G. Clark, M. J. Strouse, M. J. Naughton, W. Kang, and P. M. Chaikin, 2002, *Phys. Rev. Lett.* **88**, 017004.
- Leggett, A. J., 1975, *Rev. Mod. Phys.* **47**, 331.
- Lichtenberg, F., A. Catana, J. Mannhart, and D. G. Schlom, 1992, *Appl. Phys. Lett.* **60**, 1138.
- Liebsch, A., 2001, *Phys. Rev. Lett.* **87**, 239701.
- Liebsch, A., and A. Lichtenstein, 2000, *Phys. Rev. Lett.* **84**, 1591.
- Lu, D. H., M. Schmidt, T. R. Cummins, S. Schuppler, F. Lichtenberg, and J. G. Bednorz, 1996, *Phys. Rev. Lett.* **76**, 4845.
- Luke, G. M., Y. Fudamoto, K. M. Kojima, M. I. Larkin, J. Merrin, B. Nachumi, Y. J. Uemura, Y. Maeno, Z. Q. Mao, Y. Mori, H. Nakamura, and M. Sigrist, 1998, *Nature (London)* **394**, 558.
- Luke, G. M., Y. Fudamoto, K. M. Kojima, M. I. Larkin, B. Nachumi, Y. J. Uemura, J. E. Sonier, Y. Maeno, Z. Q. Mao, Y. Mori, and D. Agterberg, 2000, *Physica B* **289**, 373.
- Luke, G. M., A. Keren, L. P. Le, W. D. Wu, Y. J. Uemura, D. A. Bonn, L. Taillefer, and J. D. Garrett, 1993, *Phys. Rev. Lett.* **71**, 1466.
- Lupien, C., W. A. MacFarlane, C. Proust, L. Taillefer, Z. Q. Mao, and Y. Maeno, 2001, *Phys. Rev. Lett.* **86**, 5986.
- Machida, K., M. Ozaki, and T. Ohmi, 1996, *J. Phys. Soc. Jpn.* **65**, 3720.
- Mackenzie, A. P., 1999, *J. Supercond.* **12**, 543.
- Mackenzie, A. P., R. K. W. Haselwimmer, A. W. Tyler, G. G. Lonzarich, Y. Mori, S. Nishizaki, and Y. Maeno, 1998a, *Phys. Rev. Lett.* **80**, 161.
- Mackenzie, A. P., R. K. W. Haselwimmer, A. W. Tyler, G. G. Lonzarich, Y. Mori, S. Nishizaki, and Y. Maeno, 1998b, *Phys. Rev. Lett.* **80**, 3890.
- Mackenzie, A. P., N. E. Hussey, A. J. Diver, S. R. Julian, Y. Maeno, S. Nishizaki, and T. Fujita, 1996, *Phys. Rev. B* **54**, 7425.
- Mackenzie, A. P., S. Ikeda, Y. Maeno, T. Fujita, S. R. Julian, and G. G. Lonzarich, 1998, *J. Phys. Soc. Jpn.* **67**, 385.
- Mackenzie, A. P., S. R. Julian, A. J. Diver, G. G. Lonzarich, N. E. Hussey, Y. Maeno, S. Nishizaki, and T. Fujita, 1996c, *Physica C* **263**, 510.
- Mackenzie, A. P., S. R. Julian, A. J. Diver, G. J. McMullan, G. G. Lonzarich, Y. Maeno, S. Nishizaki, and T. Fujita, 1996a, in *Proceedings of the 2nd Conference on Physical Phenomena at High Magnetic Fields*, edited by Z. Fisk, L. Gor'kov, D. Meltzer, and R. Schrieffer (World Scientific, Singapore), p. 537.
- Mackenzie, A. P., S. R. Julian, A. J. Diver, G. J. McMullan, M. P. Ray, G. G. Lonzarich, Y. Maeno, S. Nishizaki, and T. Fujita, 1996b, *Phys. Rev. Lett.* **76**, 3786.
- Mackenzie, A. P., S. R. Julian, G. G. Lonzarich, Y. Maeno, and T. Fujita, 1997, *Phys. Rev. Lett.* **78**, 2271.
- Mackenzie, A. P., and Y. Maeno, 2000, *Physica B* **280**, 148.
- Mackenzie, A. P., Y. Maeno, and S. R. Julian, 2002, *Phys. World* **15** (4), 33.
- MacLaughlin, D. E., 1976, *Solid State Phys.* **31**, 1.
- Maeno, Y., 1997, *Physica C* **282**, 206.
- Maeno, Y., 2000, *Physica B* **281&282**, 865.
- Maeno, Y., T. Ando, Y. Mori, E. Ohmichi, S. Ikeda, S. Nishizaki, and S. Nakatsuji, 1998, *Phys. Rev. Lett.* **81**, 3765.
- Maeno, Y., H. Hashimoto, K. Yoshida, S. Nishizaki, T. Fujita, J. G. Bednorz, and F. Lichtenberg, 1994, *Nature (London)* **372**, 532.
- Maeno, Y., S. Nakatsuji, and S. Ikeda, 1999, *Mater. Sci. Eng., B* **63**, 70.
- Maeno, Y., S. Nishizaki, and Z. Q. Mao, 1999, *J. Supercond.* **12**, 535.
- Maeno, Y., S. Nishizaki, K. Yoshida, S. Ikeda, and T. Fujita, 1996, *J. Low Temp. Phys.* **105**, 1577.
- Maeno, Y., T. M. Rice, and M. Sigrist, 2001, *Phys. Today* **54**, 42.

- Maeno, Y., K. Yoshida, H. Hashimoto, S. Nishizaki, S. Ikeda, M. Nohara, T. Fujita, A. P. Mackenzie, N. E. Hussey, J. G. Bednorz, and F. Lichtenberg, 1997, *J. Phys. Soc. Jpn.* **66**, 1405.
- Maki, K., and E. Puchkaryov, 1999, *Europhys. Lett.* **45**, 263.
- Maki, K., and E. Puchkaryov, 2000, *Europhys. Lett.* **50**, 533.
- Maki, K., E. Puchkaryov, G. F. Wang, and H. Won, 2000, *Chin. J. Phys. (Taipei)* **38**, 386.
- Maki, K., and H. Won, 1996, *Ann. Phys. (Leipzig)* **5**, 320.
- Mao, Z. Q., Y. Maeno, and H. Fukazawa, 2000, *Mater. Res. Bull.* **35**, 1813.
- Mao, Z. Q., Y. Maeno, Y. Mori, S. Sakita, S. Nimori, and M. Udagawa, 2001, *Phys. Rev. B* **63**, 144514.
- Mao, Z. Q., Y. Maeno, S. Nishizaki, T. Akima, and T. Ishiguro, 2000, *Phys. Rev. Lett.* **84**, 991.
- Mao, Z. Q., Y. Mori, and Y. Maeno, 1999, *Phys. Rev. B* **60**, 610.
- Mao, Z. Q., K. D. Nelson, R. Jin, Y. Liu, and Y. Maeno, 2001, *Phys. Rev. Lett.* **87**, 037003.
- Martinez, J. L., C. Prieto, J. Rodriguez-Carvajal, A. Deandres, M. Valletregi, and J. M. Gonzalez-Calbet, 1995, *J. Magn. Magn. Mater.* **140**, 179.
- Matsui, H., M. Yamaguchi, Y. Yoshida, A. Mukai, R. Settai, Y. Onuki, H. Takei, and N. Toyota, 1998, *J. Phys. Soc. Jpn.* **67**, 3687.
- Matsui, H., Y. Yoshida, A. Mukai, R. Settai, Y. Onuki, H. Takei, N. Kimura, H. Aoki, and N. Toyota, 2000, *J. Phys. Soc. Jpn.* **69**, 3769.
- Matsui, H., Y. Yoshida, A. Mukai, R. Settai, Y. Onuki, H. Takei, N. Kimura, H. Aoki, and N. Toyota, 2001, *Phys. Rev. B* **63**, 060505(R).
- Matsumoto, M., and M. Sigrist, 1999, *J. Phys. Soc. Jpn.* **68**, 724.
- Matzdorf, R., Z. Fang, Ismail, J. D. Zhang, T. Kimura, Y. Tokura, K. Terakura, and E. W. Plummer, 2000, *Science* **289**, 746.
- Mazin, I. I., D. A. Papaconstantopoulos, and D. J. Singh, 2000, *Phys. Rev. B* **61**, 5223.
- Mazin, I. I., and D. J. Singh, 1997, *Phys. Rev. Lett.* **79**, 733.
- Mazin, I. I., and D. J. Singh, 1999, *Phys. Rev. Lett.* **82**, 4324.
- McMullan, G. J., M. P. Ray, and R. J. Needs, 1996, *Physica B* **224**, 529.
- Millis, A. J., S. Sachdev, and C. M. Varma, 1988, *Phys. Rev. B* **37**, 4975.
- Minakata, M., and Y. Maeno, 2001, *Phys. Rev. B* **63**, 180504(R).
- Mineev, V. P., and K. V. Samokhin, 1999, *Introduction to Unconventional Superconductivity* (Gordon and Breach, Amsterdam).
- Mishonov, T., and E. Penev, 2000, *J. Phys.: Condens. Matter* **12**, 143.
- Miyake, K., and O. Narikiyo, 1999, *Phys. Rev. Lett.* **83**, 1423.
- Miyazawa, M., H. Kontani, and E. Yamada, 1999, *J. Phys. Soc. Jpn.* **68**, 1625.
- Monthoux, P., and G. G. Lonzarich, 1999, *Phys. Rev. B* **59**, 14 598.
- Moreno, J., and P. Coleman, 1996, *Phys. Rev. B* **53**, R2995.
- Morinari, T., and M. Sigrist, 2000, *J. Phys. Soc. Jpn.* **69**, 2411.
- Mota, A. C., E. Dumont, A. Amann, and Y. Maeno, 1999, *Physica B* **261**, 934.
- Mota, A. C., E. Dumont, J. L. Smith, and Y. Maeno, 2000, *Physica C* **332**, 272.
- Movshovic, R., M. A. Hubbard, M. B. Salamon, A. V. Balatsky, R. Yoshizaki, J. L. Sarrao, and M. Jaime, 1998, *Phys. Rev. Lett.* **80**, 1968.
- Mukuda, H., K. Ishida, Y. Kitaoka, K. Asayama, R. Kanno, and M. Takano, 1999a, *Phys. Rev. B* **60**, 12 279.
- Mukuda, H., K. Ishida, Y. Kitaoka, K. Asayama, Z. Q. Mao, Y. Mori, and Y. Maeno, 1998, *J. Phys. Soc. Jpn.* **67**, 3945.
- Mukuda, H., K. Ishida, Y. Kitaoka, K. Asayama, Z. Q. Mao, Y. Mori, and Y. Maeno, 1999b, *Physica B* **259-261**, 944.
- Nakano, M., 1997, *J. Phys. Soc. Jpn.* **66**, 19.
- Nakano, M., 2000, *Phys. Rev. B* **62**, 45.
- Neumeier, J. J., M. F. Hundley, M. G. Smith, J. D. Thompson, C. Allgeier, H. Xie, W. Yelon, and J. S. Kim, 1994, *Phys. Rev. B* **50**, 17 910.
- Ng, K. K., and M. Sigrist, 2000, *Europhys. Lett.* **49**, 473.
- Nishizaki, S., 1999, Ph.D. thesis (Kyoto University).
- Nishizaki, S., Y. Maeno, S. Farner, S. Ikeda, and T. Fujita, 1998, *J. Phys. Soc. Jpn.* **67**, 560.
- Nishizaki, S., Y. Maeno, and T. Fujita, 1996, *J. Phys. Soc. Jpn.* **65**, 1876.
- Nishizaki, S., Y. Maeno, and Z. Q. Mao, 1999, *J. Low Temp. Phys.* **117**, 1581.
- Nishizaki, S., Y. Maeno, and Z. Q. Mao, 2000, *J. Phys. Soc. Jpn.* **69**, 572.
- Noce, C., G. Buseillo, and M. Cuoco, 2000, *Europhys. Lett.* **51**, 195.
- Noce, C., and M. Cuoco, 1999a, *Int. J. Mod. Phys. B* **13**, 1157.
- Noce, C., and M. Cuoco, 1999b, *Phys. Rev. B* **59**, 2659.
- Noce, C., and M. Cuoco, 2000, *Phys. Rev. B* **62**, 9884.
- Nomura, T., and K. Yamada, 2000, *J. Phys. Soc. Jpn.* **69**, 3678.
- Obst, B., 1969, *Phys. Lett.* **28A**, 662.
- Oguchi, T., 1995, *Phys. Rev. B* **51**, 1385.
- Ohmichi, E., H. Adachi, Y. Mori, Y. Maeno, T. Ishiguro, and T. Oguchi, 1999, *Phys. Rev. B* **59**, 7263.
- Ohmichi, E., Y. Maeno, and T. Ishiguro, 1999, *J. Phys. Soc. Jpn.* **68**, 24.
- Ohmichi, E., Y. Maeno, S. Nagai, Z. Q. Mao, M. A. Tanatar, and T. Ishiguro, 2000, *Phys. Rev. B* **61**, 7101.
- Ohmichi, E., S. Nagai, Y. Maeno, T. Ishiguro, H. Mizuno, and T. Nagamura, 2001a, *Rev. Sci. Instrum.* **72**, 1914.
- Ohmichi, E., S. Nagai, Y. Maeno, Z. Q. Mao, and T. Ishiguro, 2001b, *Physica B* **294**, 375.
- Okuda, T., M. Kotsugi, K. Nakatsuji, M. Fujikawa, S. Suga, Y. Tezuka, S. Shin, M. Kasai, Y. Tokura, and H. Daimon, 1999, *J. Phys. Soc. Jpn.* **68**, 1398.
- Okuda, T., T. Suzuki, Z. Q. Mao, Y. Maeno, and T. Fujita, 2002, *J. Phys. Soc. Jpn.* **71**, 1134.
- Ong, N. P., 1991, *Phys. Rev. B* **43**, 193.
- Paul, D. McK., C. V. Tomy, C. M. Aegerter, R. Cubitt, S. H. Lloyd, E. M. Forgan, S. L. Lee, and M. Yethiraj, 1998, *Phys. Rev. Lett.* **80**, 1517.
- Perez-Navarro, A., J. Costa-Quintana, and F. Lopez-Aguilar, 2000, *Phys. Rev. B* **61**, 10 125.
- Pfleiderer, C., M. Uhlarz, S. M. Hayden, R. Vollmer, H. von Lohneysen, N. R. Bernhoeft, and G. G. Lonzarich, 2001, *Nature (London)* **412**, 58.
- Puchkov, A. V., Z. X. Shen, T. Kimura, and Y. Tokura, 1998, *Phys. Rev. B* **58**, R13 322.
- Radtke, R., K. Levin, H.-B. Schüttler, and M. R. Norman, 1993, *Phys. Rev. B* **48**, 653.
- Randall, J. J., and R. Ward, 1959, *J. Am. Chem. Soc.* **81**, 2629.
- Rice, T. M., and M. Sigrist, 1995, *J. Phys.: Condens. Matter* **7**, L643.
- Rickayzen, G., 1969, in *Superconductivity*, edited by R. D. Parks (Dekker, New York), p. 91.

- Riseman, T. M., P. G. Kealey, E. M. Forgan, A. P. Mackenzie, L. M. Galvin, A. W. Tyler, S. L. Lee, C. Ager, D. McK. Paul, C. M. Aegerter, R. Cubitt, Z. Q. Mao, T. Akima, and Y. Maeno, 1998, *Nature (London)* **396**, 242 [note correction: *Nature (London)* **404**, 629 (2000)].
- Sakita, S., S. Nimori, Z. Q. Mao, Y. Maeno, N. Ogita, and M. Udagawa, 2001, *Phys. Rev. B* **63**, 134520.
- Sato, M., and K. Kohmoto, 2000, *J. Phys. Soc. Jpn.* **69**, 3505.
- Saxena, S. S., P. Agarwal, K. Ahilan, F. M. Grosche, R. K. W. Haselwimmer, M. J. Steiner, E. Pugh, I. R. Walker, S. R. Julian, P. Monthoux, G. G. Lonzarich, A. Huxley, I. Sheikin, D. Braithwaite, and J. Flouquet, 2000, *Nature (London)* **406**, 587.
- Schmidt, M., T. R. Cummins, M. Burk, D. H. Lu, N. Nucker, S. Schuppler, and F. Lichtenberg, 1996, *Phys. Rev. B* **53**, 14 761.
- Schofield, A. J., 1995, *Phys. Rev. B* **51**, 11 733.
- Schofield, A. J., 1999, *Contemp. Phys.* **40**, 95.
- Schofield, A. J., and J. R. Cooper, 2000, *Phys. Rev. B* **62**, 10 779.
- Seibel, E., and H. Winter, 1998, *J. Phys.: Condens. Matter* **10**, 5197.
- Servant, F., S. Raymond, B. Fak, J. P. Brison, P. Lejay, and J. Flouquet, 2002, *Phys. Rev. B* **65**, 184511.
- Servant, F., S. Raymond, B. Fak, P. Lejay, and J. Flouquet, 2000, *Solid State Commun.* **116**, 489.
- Shen, K. M., A. Damascelli, D. H. Lu, N. P. Armitage, F. Ronning, D. L. Feng, C. Kim, Z. X. Shen, D. J. Singh, I. I. Mazin, S. Nakatsuji, Z. Q. Mao, Y. Maeno, T. Kimura, and Y. Tokura, 2001, *Phys. Rev. B* **64**, 180502.
- Shimizu, K., T. Kimura, S. Furomoto, K. Takeda, K. Kontani, Y. Onuki, and K. Amaya, 2001, *Nature (London)* **412**, 316.
- Shiraishi, J., and K. Maki, 1999, *J. Phys. IV* **9**, 293.
- Shirakawa, N., K. Murata, Y. Nishihara, S. Nishizaki, Y. Maeno, T. Fujita, J. G. Bednorz, F. Lichtenberg, and N. Hamada, 1995, *J. Phys. Soc. Jpn.* **64**, 1072.
- Shirakawa, N., K. Murata, S. Nishizaki, Y. Maeno, and T. Fujita, 1997, *Phys. Rev. B* **56**, 7890.
- Shivaram, B. S., Y. H. Jeong, T. F. Rosenbaum, and D. G. Hinks, 1986, *Phys. Rev. Lett.* **56**, 1078.
- Shoenberg, D., 1984, *Magnetic Oscillations in Metals* (Cambridge University, Cambridge, England).
- Shull, C. G., and F. A. Wedgwood, 1966, *Phys. Rev. Lett.* **16**, 513.
- Sidis, Y., M. Braden, P. Bourges, B. Hennion, W. Reichardt, Y. Maeno, and Y. Mori, 1999, *Phys. Rev. Lett.* **83**, 3320.
- Sigrist, M., 2000, *J. Phys. Soc. Jpn.* **69**, 1290.
- Sigrist, M., and D. F. Agterberg, 1999, *Prog. Theor. Phys.* **102**, 965.
- Sigrist, M., D. F. Agterberg, A. Furusaki, C. Honerkamp, K. K. Ng, T. M. Rice, and M. E. Zhitomirsky, 1999, *Physica C* **317-318**, 134.
- Sigrist, M., A. Furusaki, C. Honerkamp, M. Matsumoto, K. K. Ng, and Y. Okuno, 2000, *J. Phys. Soc. Jpn.* **69**, 127.
- Sigrist, M., and H. Monien, 2001, *J. Phys. Soc. Jpn.* **70**, 2409.
- Sigrist, M., and K. Ueda, 1991, *Rev. Mod. Phys.* **63**, 239.
- Sigrist, M., and M. E. Zhitomirsky, 1996, *J. Phys. Soc. Jpn.* **65**, 3425.
- Singh, D. J., 1995, *Phys. Rev. B* **52**, 1358.
- Suderow, H., H. Aubin, K. Behnia, and A. Huxley, 1997, *Phys. Lett. A* **234**, 64.
- Suderow, H., J. P. Brison, J. Flouquet, A. W. Tyler, and Y. Maeno, 1998, *J. Phys.: Condens. Matter* **10**, L597.
- Suderow, H., J. P. Brison, A. Huxley, and J. Flouquet, 1997, *J. Low Temp. Phys.* **108**, 11.
- Suderow, H., J. P. Brison, A. Huxley, and J. Flouquet, 1998, *Phys. Rev. Lett.* **80**, 165.
- Sumiyama, A., T. Endo, Y. Oda, Y. Yoshida, A. Mukai, A. Ono, and Y. Onuki, 2002, *Physica C* **367**, 129.
- Takigawa, M., P. C. Hammel, R. H. Heffner, and Z. Fisk, 1989, *Phys. Rev. B* **39**, 7371.
- Takigawa, M., M. Ichioka, K. Machida, and M. Sigrist, 2002, *Phys. Rev. B* **65**, 014508.
- Tanatar, M. A., S. Nagai, Z. Q. Mao, Y. Maeno, and T. Ishiguro, 2001, *Phys. Rev. B* **63**, 064505.
- Tanatar, M. A., M. Suzuki, S. Nagai, Z. Q. Mao, Y. Maeno, and T. Ishiguro, 2001, *Phys. Rev. Lett.* **86**, 2649.
- Tewordt, L., and D. Fay, 2001, *Phys. Rev. B* **64**, 024528.
- Tewordt, L., and D. Fay, 2002, *Phys. Rev. B* **65**, 104510.
- Tinkham, M., 1996, *Introduction to Superconductivity*, 2nd ed. (McGraw-Hill, Singapore).
- Tsuei, C. C., J. R. Kirtley, C. C. Chi, L. S. Yujahnes, A. Gupta, T. Shaw, J. Z. Sun, and M. B. Ketchen, 1994, *Phys. Rev. Lett.* **73**, 593.
- Tsuneto, T., 1998, *Superconductivity and Superfluidity* (Cambridge University, Cambridge, England).
- Tyler, A. W., A. P. Mackenzie, S. Nishizaki, and Y. Maeno, 1998, *Phys. Rev. B* **58**, R10 107.
- Udagawa, M., H. Hata, S. Nimori, T. Minami, N. Ogita, S. Sakita, F. Nakamura, T. Fujita, and Y. Maeno, 1998, *J. Phys. Soc. Jpn.* **67**, 2529.
- Vekhter, I., P. J. Hirschfeld, J. P. Carbotte, and E. J. Nicol, 1999, *Phys. Rev. B* **59**, R9023.
- Vogt, D., and D. J. Buttrey, 1995, *Phys. Rev. B* **52**, R9843.
- Vollhardt, D., and P. Wölfle, 1990, *The Superfluid Phases of ³He* (Taylor & Francis, London).
- Wada, M., H. Yaguchi, M. Yoshioka, Z. Q. Mao, and Y. Maeno, 2002, *J. Phys. Chem. Solids* (in press).
- Waldram, J. R., 1996, *Superconductivity of Metals and Cuprates* (Institute of Physics, University of Reading, Berkshire).
- Walker, M. B., M. F. Smith, and K. V. Samokhin, 2001, *Phys. Rev. B* **65**, 014517.
- Walz, L., and F. Lichtenberg, 1993, *Acta Crystallogr., Sect. C: Cryst. Struct. Commun.* **C49**, 1268.
- Wang, G. F., and K. Maki, 1999, *Europhys. Lett.* **45**, 71.
- Wheatley, J., 1975, *Rev. Mod. Phys.* **47**, 415.
- White, R. M., 1983, *Quantum Theory of Magnetism*, 2nd ed. (McGraw-Hill, New York).
- Wu, W. C., and R. Joynt, 2001, *Phys. Rev. B* **64**, 100507.
- Yaguchi, H., K. Deguchi, M. A. Tanatar, Y. Maeno, and T. Ishiguro, 2002, *J. Phys. Chem. Solids* **63**, 1007.
- Yamanaka, A., N. Asayama, M. Sasada, K. Inoue, M. Udagawa, S. Nishizaki, Y. Maeno, and T. Fujita, 1996, *Physica C* **263**, 516.
- Yamashiro, M., Y. Tanaka, and S. Kashiwaya, 1997, *Phys. Rev. B* **56**, 7847.
- Yamashiro, M., Y. Tanaka, and S. Kashiwaya, 1998b, *J. Phys. Chem. Solids* **59**, 2085.
- Yamashiro, M., Y. Tanaka, Y. Tanuma, and S. Kashiwaya, 1998a, *J. Phys. Soc. Jpn.* **67**, 3224.
- Yamashiro, M., Y. Tanaka, N. Yoshida, and S. Kashiwaya, 1999, *J. Phys. Soc. Jpn.* **68**, 2019.
- Yokoya, T., A. Chainani, T. Takahashi, H. Ding, J. C. Campuzano, H. Katayama-Yoshida, M. Kasai, and Y. Tokura, 1996b, *Phys. Rev. B* **54**, 13 311.

- Yokoya, T., A. Chainani, T. Takahashi, H. Katayama-Yoshida, M. Kasai, and Y. Tokura, 1996a, *Phys. Rev. Lett.* **76**, 3009.
- Yokoya, T., A. Chainani, T. Takahashi, H. Katayama Yoshida, M. Kasai, and Y. Tokura, 1997, *Phys. Rev. Lett.* **78**, 2272.
- Yoshida, K., 1997, Ph.D. thesis (Hiroshima University).
- Yoshida, K., Y. Maeno, S. Nishizaki, and T. Fujita, 1996a, *Physica C* **263**, 519.
- Yoshida, K., Y. Maeno, S. Nishizaki, and T. Fujita, 1996b, *J. Phys. Soc. Jpn.* **65**, 2220.
- Yoshida, Y., A. Mukai, R. Settai, K. Miyake, Y. Inada, Y. Onuki, K. Betsuyaku, H. Harima, T. D. Matsuda, Y. Aoki, and H. Sato, 1999, *J. Phys. Soc. Jpn.* **68**, 3041.
- Yoshida, Y., A. Mukai, R. Settai, Y. Onuki, and H. Takei, 1998, *J. Phys. Soc. Jpn.* **67**, 2551.
- Yoshida, K., F. Nakamura, T. Goto, T. Fujita, Y. Maeno, Y. Mori, and S. Nishizaki, 1998, *Phys. Rev. B* **58**, 15 062.
- Yoshida, Y., R. Settai, Y. Onuki, H. Takei, K. Betsuyaku, and H. Harima, 1998, *J. Phys. Soc. Jpn.* **67**, 1677.
- Yoshino, H., K. Murata, N. Shirakawa, Y. Nishihara, Y. Maeno, and T. Fujita, 1996, *J. Phys. Soc. Jpn.* **65**, 1548.
- Yosida, K., 1958, *Phys. Rev.* **110**, 769.
- Zhitomirsky, M. E., and T. M. Rice, 2001, *Phys. Rev. Lett.* **87**, 057001.
- Zhu, X., C. S. Ting, J. L. Shen, and Z. D. Wang, 1997, *Phys. Rev. B* **56**, 14 093.
- Ziman, J. M., 1960, *Electrons and Phonons* (Oxford University, New York). Reprinted in 2001, Oxford Classics Series.
- Ziman, J. M., 1972, *Principles of the Theory of Solids*, 2nd ed. (Cambridge University, Cambridge, England).